Efficient data collection through multi-path routing structures in wireless sensor networks

Luu, Van Hai

2012

Luu, V. H. (2012). Efficient data collection through multi-path routing structures in wireless sensor networks. Doctoral thesis, Nanyang Technological University, Singapore.

https://hdl.handle.net/10356/48202

https://doi.org/10.32657/10356/48202

Efficient Data Collection through Multi-path Routing Structures in Wireless Sensor Networks

Hai Van Luu

School of Computer Engineering

A thesis submitted to the Nanyang Technological University
in partial fulfillment of the requirements for the degree of
Doctor of Philosophy

February 2012

Abstract

In this thesis, we investigate data collection in wireless sensor networks through multi-path routing structures. We study methods to improve the robustness, energy efficiency and time efficiency of sensor data collection in error-prone communication environments.

First, we investigate the construction of a class of multi-path routing structures called *rings overlay* [NGSA04, CLKB04] for enhancing the robustness of sensor data collection. Rings overlay exploits the broadcast nature of wireless communication for transporting sensor data through multiple interleaving propagation paths to the base station. We propose a new distributed approach for organizing sensor nodes into different rings around the base station to form a rings overlay. The objective of our proposed approach is to assign sensor nodes to appropriate rings to let them benefit from multi-path routing as much as possible. The proposed ring assignment approach is fully distributed and does not require sensor nodes to have global knowledge about the entire network. We also design and analyze an enhanced scheme for relaying data to the base station from the sensor nodes next to the base station. The goal is to improve the resilience of these nodes to communication failures in data collection without requiring them to transmit their data multiple times. Experimental results show that compared with a baseline greedy construction approach and the original relay scheme, the proposed techniques of overlay construction and relay enhancement significantly improve the robustness and accuracy of sensor data collection through the rings overlay.

Next, we investigate the use of contention-free time division multiple access (TDMA) protocols for sensor data collection. To collect sensor data using TDMA

protocols, sensor nodes need to be assigned appropriate time slots for transmitting and receiving data. We design an efficient distributed scheduling algorithm for constructing TDMA schedules for sensor data collection through multi-path routing structures. The objective of our scheduling algorithm is to reduce both the message complexity and running time of the scheduling process as much as possible. We also develop a method for deriving a lower bound on the shortest possible length of the data collection schedule that can be built for a given routing structure. The lower bound estimation offers a method to evaluate the time efficiency of data collection schedules produced by scheduling algorithms. Experimental results show that our proposed scheduling algorithm substantially reduces the number of messages transmitted during the scheduling process and has much shorter running time compared to an existing algorithm. The length of the data collection schedule produced by our algorithm is normally within 1.5 times of the lower bound estimate across a wide range of network settings.

Finally, we propose a distributed method to construct multi-path routing structures for TDMA-based sensor data collection and develop an enhanced scheme for collecting sensor data. Our proposed method for constructing multi-path routing structures keeps the number of messages that each node transmits and receives in a round of data collection within a given limit in order to achieve a required level of energy consumption for communication. The enhanced scheme for data collection exploits overhearing to improve the robustness of data collection without sacrificing the latency of data collection and violating the required level of energy efficiency for communication. We analyze the control parameter setting in the enhanced data collection scheme for maximizing the benefits of overhearing. Experimental results show that our proposed methods achieve significantly better trade-offs among the robustness, latency and energy efficiency of data collection.

To my dear family

Acknowledgements

During nearly five years of my graduate study at Nanyang Technological University, many people kindly helped me to complete this thesis. First and foremost, I would like to thank my supervisor, Professor Xueyan Tang, for selecting me as a research student and guiding me through difficult stages of the graduate program. He inspired me to work on the research topic of efficient data collection in wireless sensor networks. He kept encouraging me to work hard on important aspects of sensor data collection from the beginning and throughout my study so that I could make research contributions in this thesis. To help improve the readability of my thesis, he gave me many expert advice to reorganize the presentation and development of the proposed methods in a concise, simple and intuitive way. In addition to the professional advice, he was always optimistic about the ultimate contributions that I could achieve in my study. Without the kindly support and encouragement of Professor Xueyan Tang, I would certainly never be able to write this thesis. I am grateful to Professor Lee Bu Sung, former associate chair of the School of Computer Engineering, for his help during my research. Many other magnificent professors at the School of Computer Engineering have influenced me in my graduate study and I wish I could live up to their standards.

I would like to express my deepest gratitude to my parents for their love and support. My parents are always the best and most important teachers I got in my life. They let me absorb important knowledge and get used to self-directed learning since I was just a very small kid. Working through many hard times with my parents gives me the strength and confidence to take more difficult challenges in my life. I owe my wife a lot for her genuine love and sympathy throughout the long years of my graduate study.

I would also like to thank the executives of the Parallel and Distributed Computing Center including Miss Ng-Goh Siew Lai and Mister Poliran Kenneth Caballes. Many other staffs I met at Nanyang Technological University never cease to help me and I am thankful for them. I was grateful to many new friends I have made at the School of Computer Engineering including, but not limited to, Liu Cheng, Li Zeng Xiang, Zhao Wenbo, Zhang Lu, and Zheng Hanying.

Contents

List of Tables

List of Figures

Chapter 1

Introduction

Recent advances in micro-electro-mechanical technology has enabled mass production of tiny sensor nodes with processing, sensing and wireless communication capabilities [HC02, NKA+05, PSC05, LSB08]. These sensor nodes are able to acquire information related to physical phenomena, manipulate the acquired data and then communicate with other sensor nodes or base stations through wireless media. Due to the low-cost and small size nature of wireless sensor nodes, their sensing, processing, communication and energy supply components are subject to capacity constraints. Thus, the capabilities of a single sensor node are rather limited compared to traditional wireless devices such as cellular phones or PDAs. Nevertheless, a group of wireless sensor nodes can collaborate with each other and form a wireless sensor network to accomplish complex data collection and processing tasks.

An essential advantage of wireless sensor networks is the simplicity and low cost of deployment. Tiny sensor nodes are usually just a few cubic centimeters in size [KKP00, KAH+04, PSC05] and can be easily deployed in different places. They can acquire and send sensing data to a base station without the need to install wired connections or other network infrastructures. Wireless sensor networks open opportunities for novel applications in agriculture, transportation and many other industries. Several useful applications of sensor networks have been studied for habitat monitoring [SOP+04, HBC+09], structure monitoring [XRC+04, PFKC08], health care [SGW01, GGW+06], environment monitoring

[HM06], surveillance [HKS+04], and object tracking [YS03, YG10].

1.1 Quality measurements of sensor data collection

Sensor data collection is an operation needed in many sensor network applications. Major quality measurements of sensor network applications on data collection normally include the energy efficiency, the time efficiency and the robustness against communication failures. These quality measurements heavily affect the lifetime of sensor networks, the time latency for collecting sensor data at the base station and the accuracy of the collected data. Thus, to realize the potentials of wireless sensor networks in a wide range of different applications, these quality measurements of sensor data collection must be carefully addressed. In this section, we elaborate these three quality measurements of sensor data collection and their relationships.

Energy efficiency of sensor data collection

Sensor nodes usually rely solely on their limited batteries for energy supply. Their batteries are inconvenient to replace or recharge in many situations. If sensor nodes are deployed in a harsh environment beyond the reach of network operators, it may even be infeasible to replace or recharge their batteries. Once their batteries are exhausted, sensor nodes cannot perform any operation such as acquiring data, receiving data from other nodes and transmitting data to the base station. Therefore, energy efficiency is an important quality measurement of the data collection process.

Communication is usually a dominant source of energy consumption for sensor nodes [NGSA04]. Transmitting data and receiving data both consume energy. The energy costs for transmitting and receiving one unit of data are similar. For example, popular low-power radio transceivers for sensor nodes such as the CC1100 or CC2500 RF transceivers consume about 60 mW when it is transmitting or receiving data [PHC04, MFHH03]. Thus, keeping the energy consumption for transmitting and receiving data as low as possible is a key to achieve energy

efficiency in sensor data collection.

Time efficiency of sensor data collection

The time efficiency of sensor data collection is also of primary importance in many sensor network applications due to the real time nature of monitoring applications especially in critical conditions. A significant amount of time latency in the data collection process is often caused by wireless communication among sensor nodes since their data transmission rate is limited [PHC04, MFHH03]. In general, the radio transceiver of a sensor node is able to receive or transmit only one message at a time. Thus, the time latency of sensor data collection would generally be shorter if the amount of data that sensor nodes transmit or receive is reduced. In addition, since low-power wireless communication among sensor nodes is highly susceptible to interference, the sensor nodes have to coordinate their transmissions to reduce collisions. The overhead cost of the coordination process among sensor nodes can be significant especially when the node density increases [DEA06]. Therefore, reducing the time for coordinating transmissions of sensor nodes would also help to reduce the latency of data collection.

Robustness of sensor data collection

Low-power wireless communication among sensor nodes is highly susceptible to failures [GKW+02, WTC03, ZG03, ZHKS04]. Each communication failure may drop the sensor data contained in the transmission and prevent it from reaching the base station. The accuracy of the collected data at the base station would be reduced greatly if a significant amount of sensor data is lost. Thus, the robustness against communication failures is also an essential quality measurement of the data collection process.

Coping with communication failures may require repeating the transmission of the same data multiple times among sensor nodes or transporting the same data along multiple propagation paths in parallel. Since performing more transmissions often introduces larger amounts of energy consumption and time latency, these methods may negatively affect the energy efficiency and time efficiency of the data collection process. Therefore, there is usually a trade-off between the robustness and the other two quality measurements of sensor data collection.

1.2 Thesis scope

In this thesis, we focus on collecting data acquired by sensor nodes in wireless sensor networks. Our objective is to develop new techniques for improving the robustness, energy efficiency and time efficiency of sensor data collection in error-prone communication environments.

First, we investigate a class of multi-path routing structures called *rings overlay* [NGSA04, CLKB04] that exploits the broadcast nature of wireless communication for transporting sensor data through multiple interleaving propagation paths to the base station. In the rings overlay, sensor data are successfully transported to the base station as long as any one propagation path is failure-free. Nevertheless, a rings overlay normally does not benefit all sensor nodes in the network. A casually constructed rings overlay may leave some nodes connected to the base station through a single propagation path only. In addition, each sensor node next to the base station inherently has only one single-hop propagation path to the base station in the rings overlay. All the above nodes do not enjoy the benefit of multi-path routing. The data acquired by these nodes remain to be transported by single-path routing that is highly susceptible to communication failures. The robustness of data collection through the rings overlay would be severely limited when there are a significant number of such nodes. To enhance the robustness of sensor data collection through the rings overlay, we aim to design a new approach for constructing the rings overlay to prevent sensor nodes from having only few propagation paths to the base station. The objective is to assign sensor nodes to appropriate rings to let them benefit from multi-path routing as much as possible. Then, we investigate an enhanced scheme for relaying data to the base station from the sensor nodes next to the base station. The goal is to improve the resilience of these nodes to communication failures in data collection without requiring them to transmit their data multiple times.

Next, we investigate the use of contention-free time division multiple access (TDMA) protocols for sensor data collection through multi-path routing structures. Our study is motivated by the fact that contention-based MAC protocols

for coordinating communication among sensor nodes often introduce much additional energy consumption and time latency due to control messages, idle listening and back off time [DEA06]. In contrast, contention-free TDMA protocols have the potential to improve the energy efficiency and reduce the time latency of data collection since communication among sensor nodes can proceed in synchronous time slots without contention time, collisions or idle listening [GDP05, MLW+09]. To collect sensor data using a TDMA protocol, sensor nodes need to be assigned appropriate time slots for transmitting and receiving data. We aim to design an efficient distributed scheduling algorithm for constructing TDMA schedules for wireless sensor data collection through multi-path routing structures. The objective of our scheduling algorithm is to reduce both the message complexity and running time of the scheduling process as much as possible.

Finally, we investigate a multi-path sensor data collection scheme that considers the energy efficiency for communication, the time latency and the robustness of data collection altogether. We study a distributed method to construct multi-path routing structures for TDMA-based sensor data collection. The construction method aims to keep the number of messages that each sensor node transmits and receives in a round of data collection within a given limit so as to achieve a required level of energy efficiency for communication. In addition, we investigate an enhanced scheme for data collection in which sensor nodes have opportunities to overhear data from their neighbors other than those in the multi-path routing structures constructed. The goal of the enhanced scheme is to improve the robustness of data collection without sacrificing the latency of data collection and violating the required level of energy efficiency.

1.3 Major contributions

The main contributions of the thesis are summarized as follows:

1. We propose a new distributed approach for organizing sensor nodes into different rings around the base station to form a rings overlay. The objective of the proposed approach is to assign sensor nodes to appropriate

rings to let as many nodes benefit from multi-path routing as possible. The proposed ring assignment approach is fully distributed and does not require sensor nodes to have global knowledge about the entire network. We also design and analyze an enhanced scheme for relaying data to the base station from the sensor nodes that are one hop away from the base station in the rings overlay. The goal is to improve the resilience of these nodes to communication failures without requiring them to transmit their data multiple times. Experimental results show that compared with a baseline greedy construction approach and the original relay scheme, the proposed techniques of overlay construction and relay enhancement significantly improve the robustness and accuracy of sensor data collection through the rings overlay.

2. We propose a distributed method for constructing multi-path routing structures for TDMA-based sensor data collection and develop an enhanced data collection scheme. In the multi-path routing structures constructed by our method, the number of messages that each node transmits and receives in a round of data collection is limited so as to achieve a required level of energy efficiency for communication. In the enhanced data collection scheme, sensor nodes exploit overhearing to increase the numbers of their data propagation paths to the base station and improve the robustness of data collection without sacrificing the latency of data collection and violating the required level of energy efficiency. We analyze the control parameter setting in the enhanced data collection scheme for maximizing the benefits of overhearing. Experimental results show that our proposed methods achieve significantly better trade-offs among the robustness, latency and energy efficiency of data collection.

3. We propose an efficient distributed scheduling algorithm for TDMA-based sensor data collection through multi-path routing structures. We also develop a method for deriving a lower bound on the shortest possible length

of the data collection schedule that can be built for a given routing structure. The lower bound estimation offers a method to evaluate the time efficiency of data collection schedules produced by scheduling algorithms. Experimental results show that our proposed scheduling algorithm greatly reduces the number of messages transmitted in the scheduling process and has much shorter running time as compared to an existing algorithm. The length of the data collection schedule produced by our algorithm is normally within 1.5 times of the lower bound estimate across a wide range of network settings.

1.4 Outline of the thesis

The rest of the thesis is organized as follows. Chapter 2 reviews the related work on sensor data collection. Chapter 3 presents and evaluates our proposed techniques for organizing sensor nodes into different rings around the base station and the enhanced relay scheme to improve the robustness of sensor data collection. The next two chapters focus on TDMA-based sensor data collection through multi-path routing structures. Chapter 4 presents an efficient distributed scheduling algorithm for TDMA-based sensor data collection through multi-path routing structures. Chapter 5 investigates the construction of multi-path routing structures for TDMA-based sensor data collection and an enhanced scheme for collecting sensor data. Chapter 5 is presented after Chapter 4 because the techniques and experiments described in Chapter 5 have some dependency on the scheduling algorithm of Chapter 4. Finally, Chapter 6 summarizes the research contributions and concludes the thesis.

Chapter 2

Background and related work

In this chapter, we review the existing literature related to various aspects of data collection in wireless sensor networks. Wireless communication failures among sensor nodes and existing methods to overcome communication failures are discussed in Section 2.1. In Section 2.2, we discuss the routing methods for sensor data collection. In Section 2.4, we summarize in-network data processing and aggregation techniques for conserving energy in sensor data collection. Section 2.5 discusses several MAC protocols for wireless sensor networks. Scheduling algorithms for sensor data collection are discussed in Section 2.6.

2.1 Communication failures among sensor nodes

A popular transmission medium for wireless communication among sensor nodes is radio wave [HC02,NKA+05,PSC05,LSB08]. Due to the strict energy constraint, sensor nodes are often equipped with low-power radio transceivers. These low-power transceivers are highly susceptible to collisions, interference and noise. Thus, radio communication among sensor nodes frequently suffers from packet losses [GKW+02, WTC03, ZG03, ZHKS04]. Figure 2.1, which is taken from an empirical study [ZG03], shows the packet reception rates at different distances between a transmitter and a receiver. As seen from these results, the packet reception rates are relatively high within a certain distance threshold. Beyond the distance threshold, the packet reception rate drops rapidly with increasing

transmission distance.

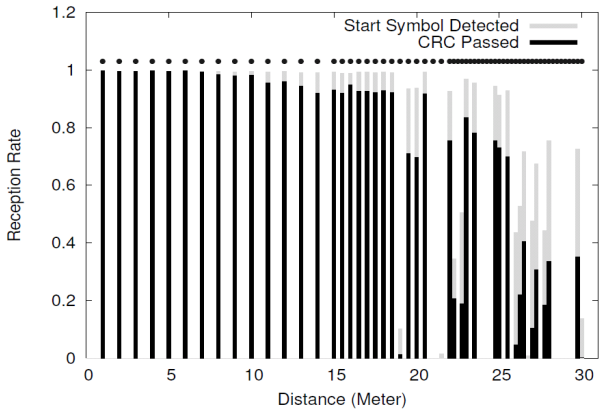

Figure 2.1: Packet reception rates at different distances of transmission [ZG03].

The packet reception rate not only depends on the distance of transmission but also depends on the communication environment. Figure 2.2, which is also taken from [ZG03], shows the average packet loss rates among sensor nodes deployed in three different communication environments. In Figure 2.2, the In Door curve represents the average packet loss rate among sensor nodes deployed inside a building, the Out Door curve represents the loss rate resulting from a car park deployment, and the Habitat curve represents the loss rate resulting from a natural park deployment. Each point (x, y) on these curves means that y proportion of the communication links experience a loss rate of at least x percent. These empirical results show that the packet loss rates can be quite different in different communication environments. For example, in the building deployment, nearly 53% of all the communication links experience a loss probability greater than 10%, and 40% of all the communication links experience a loss probability of at least 30%. In the natural park deployment, 35% of all the communication links experience a loss probability greater than 10%, and 24% of all the communication links experience a loss probability of at least 30%.

The high loss rates of low-power radio communication among sensor nodes significantly affect the proportion of sensor data that can be successfully transported through multi-hop propagation paths. Figure 2.3, which is taken from [YZLZ05], shows the multi-hop loss rates at different hop-distances in which the packet

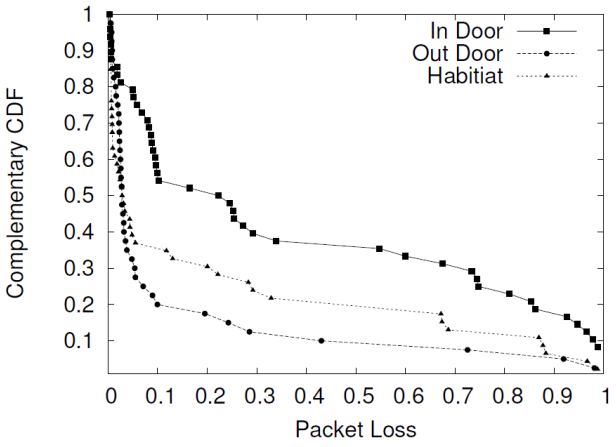

Figure 2.2: Average packet loss rates in different communication environments [ZG03].

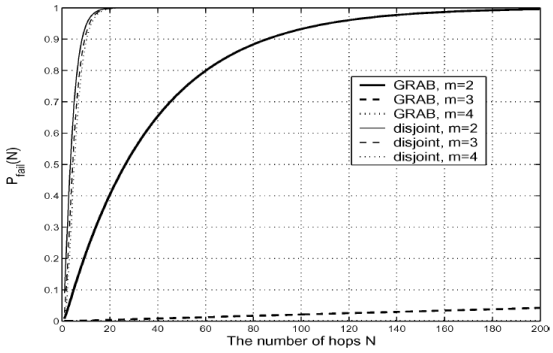

Figure 2.3: The probability that a packet fails to reach hop N as a function of hop number N when the packet loss rate of one-hop transmission is 30% [YZLZ05].

loss rate of one-hop transmission is kept at 30%. The GRAB curves represent the probability that a packet fails to reach hop N in a mesh network, and the disjoint curves represent the probability that a packet fails to reach hop N in a path-disjoint network. It can be seen that, more than 90% of packets would fail to reach the destination after 10 hops even though every packet is transmitted through 4 disjoint paths. The above studies show that data collection in large-scale sensor networks would be severely affected by high probabilities of communication failures among sensor nodes.

One approach to overcome communication failures among sensor nodes is to improve the packet reception rate of every individual link along the propagation

paths from source nodes to destination nodes. Forward error correction codes have been used in sensor networks [ASSC02, JE06] to recover the packets received with a few error bits. In this approach, redundant information is sent together with sensor data from the senders and this information would be used to correct possible errors in the data received at the receivers. Several forward error correction codes such as SECDEC and Manchester code have been proposed to correct single-bit or double-bit errors in the packets received. The overhead of these encoding schemes is quite significant in that the amount of redundant information to be transmitted together with the data would increase the size of transmitted packets significantly [JE06].

In radio communication, the packet reception rate is strongly related to the received signal, interference and noise strength [LZZ+06, SKH04]. To measure the quality of received signal compared to interference and noise, the ratio of the signal strength over the interference and noise strength (SINR) is used. A higher SINR at the receiver indicates a better quality of the received radio signal. Several studies [SKH04, LZZ+06] have proposed to increase the transmission power level at the transmitters to improve the SINR at the receivers and hence improve the packet reception rate. Nevertheless, a higher power level for transmitting data produces a stronger signal strength and hence the number of transmissions that can proceed in parallel without collisions would decrease. As a result, increasing the transmission power level may affect both the energy efficiency and time efficiency of data collection.

The packet reception rate can also be improved by using reliable transport protocols in which additional control messages and retransmissions are used to ensure data delivery. Stann and Heidemann [SH03] proposed a reliable transport protocol using negative acknowledgements called RMST (Reliable Multi-Segment Transport). Specifically, a receiver can send a negative acknowledgement to a sender to request for the retransmission of a certain data packet if the receiver does not receive the data packet within a timeout period. Wan *et al.* [WCK02] proposed another reliable transport protocol using negative acknowledgements called PSFQ (Pump Slowly, Fetch Quickly). In the PSFQ protocol, a negative

acknowledgement can be sent by a receiver when it receives a data packet with a higher sequence number than expected. Instead of using negative acknowledgements, Luo and Wu [LW03] proposed to used positive acknowledgements from the receivers to improve the reliability of multicast transmissions. To avoid using acknowledgements explicitly, Cao *et al.* [CHF+06] proposed to let the sender overhear the transmissions from the receiver to its downstream nodes and use them as implicit acknowledgements. Liu *et al.* [LRC+08] pointed out that relying solely on implicit acknowledgements may significantly increase duplicate data reception and hence they proposed another transport protocol using both implicit and explicit acknowledgements. Due to the transmission and reception of acknowledgements and data retransmissions, the above reliable transport protocols usually incur significant overhead costs of time latency and energy consumption. Thus, they would generally compromise the energy efficiency and time efficiency of sensor data collection.

Another approach to deal with communication failures in sensor data collection is to transport data through multiple propagation paths from source nodes to destination nodes. This approach will be discussed in the next section that reviews different routing methods for sensor networks.

2.2 Routing methods for sensor networks

2.2.1 Single path routing methods

An simple routing method for sensor networks is the traditional gossip-based method [KW07]. In this method, a sensor node randomly chooses one of its neighbors to transmit its data to. The receiving node, in turn, transmits the received data to one of its neighbors in a similar manner. In the traditional gossip-based routing method, each sensor node transmits its data to only one of its neighbors. Thus, sensor data has only one propagation path to the destination node, limiting the robustness of data delivery. Moreover, the traditional gossip-based routing method may waste a significant amount of energy since the number of hops used to deliver the data to the destination node is likely to be much higher

than the length of the shortest propagation path from the source node to the destination node. This also increases the time latency of data delivery. To reduce the hop number of data delivery in the traditional gossip-based routing method, Dimakis *et al.* [DSW06] proposed a geographical gossip-based routing method in which the location information of sensor nodes is used for choosing the next gossip neighbor that is closer to the destination node. While this method reduces the hop number of data delivery, it requires some special geographical localization processes or complex location systems that may not always be available for sensor nodes with limited capabilities.

Opportunistic routing [BM04,HZ09] is also a routing method for data delivery from a source node to a destination node. In this method, when a node transmits its data, the downstream nodes hearing the transmission can elect the best one to forward the data to the destination node. In this way, a good propagation path from the source node to the destination node can be established on the fly. However, opportunistic routing methods often incur a significant amount of time and energy overheads for electing the best node at each hop to forward each message.

Directed diffusion [IGE+03] is another routing method that construct the data propagation path from a source node to a destination node for data collection. When a destination node wants to collect data, it floods an interest-description message describing the data that it is interested in over the network (see Figure 2.4(a)). During the propagation of the interest-description message, sensor nodes record the nodes from which they receive the interest-description message so that they can forward the data back to the destination node later. These recorded paths are referred to as the interest gradients (see Figure 2.4(b)). A sensor node having matching data reports to the destination node through the interest gradients to identify itself as a source node. Then, among the interest gradients, the destination node selects one path with good performance in terms of energy efficiency, time latency, or other quality measurements for collecting data from the source node (see Figure 2.4(c)).

Tree-based routing is a popular routing method for collecting data acquired

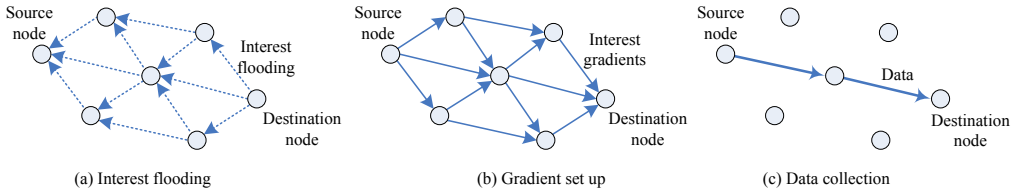

Figure 2.4: A simplified example of the directed diffusion routing method [IGE+03].

from many sensor nodes to a base station. Madden *et al.* [MFHH05, MFHH02] proposed to construct a routing tree rooted at the base station to collect data from sensor nodes. To construct the routing tree, the base station first sets its level to 0 and broadcasts a message including its identifier and its level number to other nodes within its communication range. On receiving a message, if a sensor node has not been assigned to any level, it sets its level to the level number contained in the message plus one and selects the sending node of the message as its parent. Then, the receiving node broadcasts a message with its own identifier and level number. The routing tree construction completes when all nodes are assigned levels and have selected their parents. In data collection, each sensor node first receives data from all of its children and then transmits the received data together with its own acquired data to its parent. Some other studies have developed different methods for constructing tree-based routing structures to enhance the energy efficiency or the time efficiency of the data collection process. Ding *et al.* [DCX03] developed a tree structure rooted at the base station based on the residual energy of sensor nodes. In this approach, sensor nodes with lower residual energy normally determine their level numbers and broadcast their messages after sensor nodes with higher residual energy. As a result, the nodes with lower residual energy would have higher chances to become leaf nodes in the routing tree, thereby conserving their energy in data collection since leaf nodes do not have to receive data from any other nodes in data collection. Dasgupta *et al.* [DKN03] presented another heuristic algorithm for constructing tree-based routing structures for a number of data collection rounds so as to maximize the minimum residual energy of sensor nodes after each round. Cheng *et al.* [CLJ06] investigated the construction of tree-based routing structures for time-constrained

data collection by limiting the maximum node degree and the height of the routing tree. Hu *et al.* [HYJ06] and Choi *et al.* [CLL+06] proposed other heuristic algorithms to construct tree-based routing structures such that the total energy cost for collecting sensor data is minimized and the latency of data collection is bounded by predetermined values.

Lindsey and Raghavendra [LR02] proposed a chain-based routing method for collecting data acquired from many sensor nodes to a base station called PEGASIS (Power-Efficient Gathering in Sensor Information Systems). The chain construction starts with the node furthest from the base station and inserts one node into the chain at a time. Each new node selected to be inserted into the chain is the node closest to the last node that has been added into the chain. When the chain construction completes, a node is elected as the chain leader. Sensor nodes forward their acquired data towards the chain leader through their neighbors along the chain structure. Then, the chain leader sends its locally acquired data together with data received from other nodes directly to the base station.

Heinzelman *et al.* [HCB02] proposed a cluster-based routing method, called LEACH (Low-Energy Adaptive Clustering Hierarchy), to collect sensor data to a base station. In this routing method, sensor nodes are organized into clusters in a distributed manner. Each sensor node elects itself to be a cluster head by a probability that is calculated according to the node density. Then, the cluster heads send advertisement messages to invite other nodes to join their clusters. A sensor node selects its cluster based on the signal strength of the advertisement messages it receives. In data collection, the sensor nodes in a cluster report their data directly to the cluster head and the cluster heads forward their locally acquired data together with the received data directly to the base station. In this routing method, the cluster heads have to receive data from all the nodes in their clusters. In addition, due to the possibly long distances from the cluster heads to the base station, they may need to use higher power levels for transmitting data to the base station. Therefore, in general, cluster heads would consume much more energy than other sensor nodes in the network. Several variants of the

cluster-based routing method have been investigated. Yao *et al.* [YG02, YG03] proposed to use additional metrics to elect the cluster heads and the nodes in a cluster can be multiple hops away from the cluster head. Patterm *et al.* [PKG04] proposed another cluster-based routing method in which the cluster heads can forward data through multi-hop paths to the base station.

2.2.2 Multi-path routing methods

In all the above routing methods for data collection, each piece of sensor data is transported to the base station through a single propagation path only. However, single-path routing methods are highly susceptible to communication failures in that each failure results in the loss of data acquired from one or a group of sensor nodes. To cope with communication failures in data delivery, several multi-path routing methods have been proposed. Ganesan *et al.* [GGSE01] proposed to construct a set of disjoint alternative paths together with a primary data propagation path from a source node to a destination node. In data collection, the source node sends data to the destination node through the primary path. In addition, the source node also sends keep-alive messages through the alternative paths to the destination node at low rate for maintaining these alternative paths. If the primary path fails to deliver data to the destination node due to some failures, the destination node can select one of the alternative paths as the new primary path for data delivery. Ye *et al.* [YZLZ05] proposed to create a mesh of interleaved paths from a source node to a destination node and forward data through these paths in parallel. Chatzigiannakis *et al.* [CDNS06] proposed a probabilistic broadcasting method to transmit data from a source node to a destination node through multiple propagation paths. Each sensor node rebroadcasts its received data with a probability calculated based on the angle between the line from the node to the data's source and the line from the node to the data's destination. Thus, the data received at a sensor node is more likely to be rebroadcast if the receiving node is closer to the line from the data's source to the data's destination. Lou and Kwon [LK06] proposed to split data into multiple shares using a secret sharing method and transport each share along multiple disjoint

paths to the destination in parallel to improve the robustness of data delivery. In addition, the security of data delivery is also improved in the sense that the data would not be compromised even if some data delivery paths are compromised.

The above multi-path approaches have focused on transporting data from one source node to one destination node. Seah and Tan [ST06] proposed a multi-path routing method for collecting data from sensor nodes to a number of base stations in underwater sensor networks. A separate routing structure rooted at each base station is constructed to collect data from sensor nodes. In data collection, a sensor node can forward its data in parallel to a number of base stations with short hop-distances away. The base stations are assumed to be connected via high speed links and have sufficient energy resources. Data from a sensor node is considered to be delivered successfully to all the base stations if it is successfully received at one of them. To improve the robustness of data collection from the entire network to a base station, Nath *et al.* proposed a class of multi-path routing structures called rings overlay [NGSA04]. Rings overlay is a class of multi-path routing structures that makes use of the broadcast nature of wireless communication to increase the number of propagation paths from the sensor nodes to the base station. In the rings overlay, sensor nodes are conceptually organized into different rings around the base station with increasing hop-distance to it. Data collection is carried out by level-by-level propagation and aggregation. The sensor nodes in the outermost ring first broadcast their locally acquired data. The sensor nodes in the next inner ring receive the data and aggregate the received data with their own acquired data. Then, these nodes broadcast the aggregated data to the nodes in the further inner ring. This process continues until the aggregated data reach the base station. Manjhi *et al.* [MNG05] proposed to use the rings overlay routing structure and the tree-based routing structure in different regions of a sensor network. The rings overlay routing structure is used to transport data aggregated from many sensor nodes or in the high loss rate region to improve the robustness of data collection. The tree-based routing structure is used to transport data in the low loss rate region.

The advantage of the rings overlay is that each piece of data would be forwarded to the base station through multiple propagation paths while the number of messages generated during the data collection process remains the same as that of the tree-based routing structure. Nevertheless, a casually constructed rings overlay may leave some sensor nodes still having a single or few propagation paths to the base station, and all the nodes in the ring next to the base station inherently have only one single-hop propagation path to the base station. Thus, these nodes are still susceptible to communication failures. In this thesis, we shall present new approaches for constructing the rings overlay routing structure and carrying out data collection to remedy these problems and improve the robustness of sensor data collection.

2.3 Data collection in sensor networks

Collecting data acquired from sensor nodes to a base station is a basic operation in many sensor network applications. Existing data collection methods in sensor networks can be roughly classified into two groups, i.e., non-aggregate data collection and aggregate data collection.

Non-aggregate sensor data collection methods [PH08, CDHH06, GZH08] focus on collecting individual data acquired by sensor nodes to the base station. Chu *et al.* [CDHH06] considered a non-aggregate data collection method that guarantees a fix error bound on the collected data. To reduce the network traffic and energy consumption of data collection, every sensor node maintains a prediction model and only forwards the acquired data to the base station if the predicted data is beyond the required error bound. Paradis and Han [PH08] proposed another non-aggregate sensor data collection method in which sensor nodes periodically acquire data and forward their data to a base station. Data acquired by multiple nodes are put together in a packet to reduce the number of packet transmissions and the latency of data collection. Gandham *et al.* [GZH08] developed a scheduling algorithm to minimize the latency of non-aggregate data collection through a tree-based routing structure.

Aggregate sensor data collection methods [NGSA04,CLKB04,MFHH02,SBAS04, LR02, HCB00] focus on computing or monitoring the summaries (e.g., sum, average and median) of the data acquired from sensor nodes instead of collecting individual sensor data. During the aggregate data collection process, sensor nodes can prune excessive data received from other nodes before forwarding data to the base station in order to conserve their limited energy resources and prolong the network lifetime. Madden *et al.* [MFHH02] proposed a data aggregation method for tree-base routing structures. Lindsey and Raghavendra [LR02] investigated a data aggregation method for a chain-based routing structure. Heinzelman *et al.* [HCB00] considered another data aggregation method for a cluster-based routing structure. All the above sensor data collection methods are developed for single-path routing structures. Nath *et al.* [NGSA04] developed a data aggregation method for a multi-path routing structure to improve the robustness of data collection. In this thesis, we focus on improving the quality measurements of aggregate sensor data collection from the entire network to a base station through multi-path routing structures in an error-prone wireless communication environment.

2.4 In-network data aggregation

As discuss in Chapter 1, energy efficiency is a major quality measurement of sensor data collection since sensor nodes are usually equipped with limited batteries and it is not feasible to replace or recharge their batteries in many situations. Wireless communication is usually the dominant source of energy consumption for sensor nodes [BCL03, NGSA04, DEO09]. Thus, an important approach to reduce the energy consumption of sensor nodes and prolong the network lifetime is to reduce the amount of network traffic in data collection. In many sensor network applications, data acquired by sensor nodes can be processed and aggregated before sending to the base station to reduce the network traffic. In-network data aggregation techniques have been proposed to deal with the distributed processing of data within the network.

Madden *et al.* [MFHH02] proposed aggregation techniques for calculating simple aggregates such as min, max, sum, count and average. For example, to collect the average value of the data acquired by sensor nodes at the base station through a tree-based routing structure, each sensor node can send two values to its parent in the routing tree: one value represents the number of nodes in the subtree rooted at the node, and one value represents the sum of its locally acquired data and all the data acquired by its descendants. In this way, every sensor node would need to send only one message containing two aggregated values to its parent regardless of its location in the routing tree. On receiving the aggregated values, the base station can compute the average value of sensor data by dividing the sum by the number of sensor nodes. Shrivastava *et al.* [SBAS04] developed another aggregation technique for calculating median and quantile aggregates. The proposed aggregation technique makes use of a special data structure called quantile digest that can represent the distribution of sensor data with a certain degree of approximation. Using the quantile digest, the distribution of a large amount of raw sensor data can be summarized in a single message that has much smaller size compared to the total size of the raw data. The quantile digests produced by different sensor nodes are aggregated along their propagation to the base station. The above aggregation techniques can significantly reduce the network traffic in data collection. However, they are sensitive to data duplication in that the aggregated result produced at the base station would be changed if some sensor data are accounted for more than once in the data aggregation process. Thus, these aggregation techniques are only suitable for data collection through single-path routing structures where each piece of data is sent to the base station through only one propagation path without duplication.

In multi-path routing structures, each node could have multiple interleaving propagation paths to the base station. Thus, in the data aggregation process, a sensor node may receive and have to aggregate the same piece of data more than once in an arbitrary order. Order- and duplicate-insensitive data representations and aggregation techniques have been developed to deal with data duplication and maintain the accuracy of aggregated results [NGSA04, DGGR04]. Nath *et*

al. [NGSA04] proposed a digest-based representation of aggregated data called synopsis. A synopsis is basically a bitmap of certain length. Each piece of sensor data is mapped to one or multiple bits in the bitmap through a hash function. To incorporate a piece of sensor data into the synopsis, its mapped bits would be set to 1. Initially, every node creates a bitmap that incorporates its locally acquired data. During in-network data aggregation, an intermediate node combines the bitmaps received from its children together with the bitmap of its locally acquired data by using the logical bit-wise OR function to produce a new aggregated bitmap. In this way, duplicate data received from different children are naturally suppressed. The synopsis representation is order- and duplicate-insensitive in that it is independent of the order in which sensor data are aggregated and how many times the same data are aggregated. After the base station receives the aggregated bitmaps, it is able to produce a variety of aggregation results of sensor data from the bitmaps.

2.5 MAC protocols for sensor networks

In this section, we shall discuss various Medium Access Control (MAC) protocols for sensor networks and their potential usage in sensor data collection.

2.5.1 Contention-based MAC protocols

In contention-based MAC protocols for sensor networks, all sensor nodes contend for the same communication channel to coordinate their transmissions. A basic contention-based protocol is the Carrier Sensed Multiple Access (CSMA) protocol which has two variants: persistent CSMA protocol [Sto05, HSC06], and non-persistent CSMA protocol [TJB04, DEA06]. In the persistent CSMA protocol, when a sensor node wants to transmit data, it first listens to the communication channel to check whether the channel is idle. If the channel is found idle, the node performs its transmission. Otherwise, if the channel is found busy, the sensor node keeps listening to the channel and transmits its data immediately when the channel becomes idle. In the non-persistent CSMA protocol, the node also

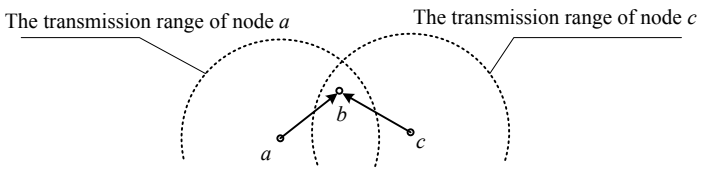

Figure 2.5: The hidden terminal problem of the CSMA protocol.

performs its transmission if the channel is found idle. However, if the channel is found busy, the sensor node waits for some random period before checking the channel again. The CSMA protocol is able to reduce collisions among sensor nodes since the contention process described above does not allow two neighboring nodes to perform data transmissions concurrently. However, the CSMA protocol cannot completely avoid collisions because two sensor nodes that are not neighbors of each other may still collide with each other in their transmissions. For example, in Figure 2.5, node b is located within the transmission ranges of both nodes a and c while nodes a and c are not within the transmission ranges of each other. During the time when node b is receiving data from node c, node a may also want to transmit data to node b. Since node a is beyond the transmission range of node c, a would consider that the channel is idle and transmit data to b straightaway. Thus, the transmissions from a and c would collide at node b. As a result, both the transmissions from nodes a and c to node b would fail. This issue is known as the hidden terminal problem of the CSMA protocol [Sto05].

Besides the hidden terminal problem, the CSMA protocol may also result in inefficient utilization of the communication channel. For example, in Figure 2.6, nodes a and c are both located within the transmission range of node b, while node d is outside the transmission range of node b. When node b is transmitting data to node a, node c may want to transmit data to node d. Since node c is within the transmission range of node b, c would consider that the channel is busy and it has to defer its transmission until the transmission of node b completes. In fact, the transmission from node c to node d can proceed in parallel with the transmission from node b to node a without any collision because both the receiving nodes a and d would only hear the transmission from one transmitter. This

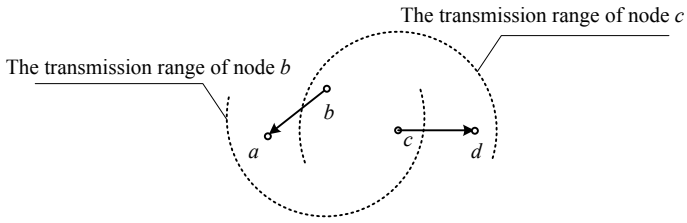

Figure 2.6: The exposed terminal problem of the CSMA protocol.

issue is known as the exposed terminal problem of the CSMA protocol [Sto05]. Several techniques were proposed to remedy the hidden terminal and exposed terminal problems by using addition handshaking messages between transmitters and receivers at the cost of higher energy consumption and time latency [Sto05].

Keeping the radio transceivers on all the time in the CSMA protocol would result in significant energy waste. To conserve energy, Ye *et al.* [YHE02] proposed a S-MAC protocol. In this protocol, the radio transceivers of sensor nodes are kept off most of the time and are only periodically turned on for short periods. In the short periods when the radio transceivers are awake, sensor nodes can contend for the communication channel and transmit data or receive data from other nodes following the traditional CSMA protocol. In order for the sensor nodes within the communication ranges of each other to communicate, their wake-up periods need to be synchronized. In this way, the S-MAC protocol can reduce idle listening and hence the energy consumption of sensor nodes. However, S-MAC introduces extra latency to every transmission because sensor nodes have to wait for their wake-up periods in order to receive or transmit data. This extra latency would add up and become significant for data collection through multiple hops especially in large-scale sensor networks.

El-Hoiydi *et al.* [EHD04] proposed another MAC protocol for reducing idle listening time, called WiseMAC, which is based on the non-persistent CSMA protocol with preamble sampling technique. Like the S-MAC protocol, in the WiseMAC protocol, sensor nodes turn on their radio periodically for short periods to sample the channel. However, in the WiseMAC protocol, the schedules of sensor nodes are independent. To alert the receivers, a wake-up preamble is transmitted in front of every data packet. When a node wakes up and finds that

the medium is busy, it continues to listen until it receives a data packet or until the medium becomes idle. Although the WiseMAC protocol can effectively reduce idle listening time, the protocol still suffers from the hidden terminal problem since WiseMAC is based on the non-persistent CMSA protocol.

2.5.2 Contention-free MAC protocols

Contention-free MAC protocols allow sensor nodes to share the communication channel by partitioning the channel along either the time domain (Time Division multiple Access), frequency domain (Frequency Division Multiple Access) or code domain (Code Division Multiple Access) [MEB06].

Frequency Division Multiple Access (FDMA) protocols [MLG06] divide the frequency domain into multiple ranges and assigns them to sensor nodes. The sensor nodes assigned different frequency ranges would be able to perform transmissions simultaneously without collisions. However, the hardware components for switching among different radio frequencies are complex and hard to be embedded into sensor nodes. Thus, FDMA protocols have limited usage in sensor networks. Code Division Multiple Access (CDMA) protocols [LBPJ04] employ spread-spectrum technologies and special coding schemes where each sensor node is assigned a code for separating its transmissions with other simultaneous transmissions using coding theory. CDMA protocols avoid the collisions at the cost of heavy computational processing, large amounts of memory and complex radio transceivers at sensor nodes. Therefore, CDMA protocols also have limited usage in sensor networks.

Time Division Multiple Access (TDMA) protocols [AYY02,PC01] divide time into slots and assign time slots to the sensor nodes for transmitting and receiving data. The sensor nodes turn on their radio transceivers only in the time slots when they need to transmit or receive data. Otherwise, the sensor nodes can turn off their radio transceivers to conserve energy. To avoid collisions, only the transmissions that do not interfere with each other are assigned to proceed in the same time slot.

Some sensor node products support TDMA-based protocols. TELOSB [Cro09b]

and MICAz motes [Cro09a] use the IEEE 802.15.4 protocol which has a "guarantee time slots" service in which time slots are assigned to sensor nodes for their transmissions. BTNode [BTn07] supports the Bluetooth protocol which is also a TDMA communication paradigm.

In the next section, we shall discuss some TDMA scheduling algorithms for assigning time slots to sensor nodes for transmitting and receiving data.

2.6 TDMA scheduling for sensor networks

In an early work, Ramaswami and Parhi [RP89] presented a centralized algorithm and a distributed algorithm for scheduling broadcast transmissions so as to maximize the number of nodes broadcasting data to their neighbors in each time slot. Rajendran *et al.* [ROGLA06] proposed a scheduling method for sensor networks in which the slot number and the identification of each node are used to calculate a priority for the node to transmit data to its neighbors in that time slot. A node transmits its data in a time slot if it has the highest priority for that time slot compared to its two-hop neighbors to avoid collisions with other transmissions.

Early work of link scheduling in wireless sensor networks has focused on building schedules for every pair of neighboring nodes to communicate once. Gandham *et al.* [GDP05] introduced a distributed link scheduling algorithm that consists of two phases. The first phase is to find a valid edge coloring of all links using $(\Delta + 1)$ colors, where Δ is the maximum degree of the nodes in the network. Then, the transmission direction of each link is determined in the second phase to construct a collision-free schedule. It was proved that reversing the transmission directions of all links results in another collision-free schedule. Thus, two-way communications among nodes are supported with at most $2(\Delta+1)$ time slots. Cheng and Yin [CY07] built a directed graph to represent the network and proposed a scheduling algorithm that assigns time slots to directed edges directly. Ma *et al.* [MLW+09] introduced link scheduling algorithms that assign consecutive time slots to the links destined at the same node. The resultant link

schedule guarantees that every node switches to the listening mode only once for receiving data from all its neighbors. However, the above studies did not consider in-network data aggregation in scheduling.

To facilitate in-network data aggregation, the child nodes have to be scheduled for transmission before their parent nodes in the routing structure. In this way, sensor nodes can aggregate data received from their children before transmitting the data to their parents. Wu *et al.* [WLX06] proposed a distributed scheduling algorithm to assign time slots to the links of a tree-based routing structure rooted at the base station. The proposed distributed scheduling algorithm is executed at every sensor node following four constraints: neighboring nodes must have different transmission slots; nodes that have common parents must have different transmission slots; the children of a node must have different transmission slots from all the neighbors of the node; and the transmission slots of a parent node must be later than its children in each round of data collection. The first three constraints are used to avoid collisions during sensor data collection. The last constraint is used to guarantee that the parent node is able to perform data aggregation on its own acquired data and the data received from its children. Based on these four constraints, possible transmission slots of each sensor node are calculated and sent to their parent nodes. The parent nodes make final assignments of transmission slots to their children and inform the children of the schedules. While this algorithm guarantees that there is no collision in data collection, it may suffer from the exposed terminal problem [Sto05] since it requires each sensor node to have a transmission slot different from those of all the nodes within its communication range.

Paradis and Han [PH08] also considered the link scheduling problem for collecting data from sensor nodes to a base station through a tree-based routing structure. This study exploited in-network processing for collecting raw sensor data readings. It was assumed that each packet transmitted can accommodate a certain number of sensor readings. A two-phase algorithm called TIGRA was proposed to schedule links for data collection. The objective of TIGRA is to put as many raw data readings as possible into each packet in order to reduce

the number of packets transmitted and hence reduce the energy consumption of sensor nodes in data collection. The scheduling problem was formulated as a graph coloring problem in which two nodes must be assigned different time slots for their transmissions if the parent of one node is within the transmission range of the other node. A negotiation-based heuristic was used to solve the scheduling problem. TIGRA provides a collision-free schedule for sensor data collection and energy consumption is optimized by grouping raw data readings together in the packets transmitted. However, since no data aggregation is exploited, the energy consumption of the nodes closer to the base station would normally be much higher than that of the nodes further away from the base station because the nodes closer to the base station would have to forward many data packets from their descendants to the base station. As a result, the sensor nodes closer to the base station would deplete their energy sources more rapidly than other nodes.

Many aggregation scheduling algorithms employ a simple greedy strategy to select the transmission slot of a sensor node as the earliest collision-free time slot after the transmission slots of all the children of the node [CHZ05, HWV+07, YLL09, LGP10]. Chen *et al.* [CHZ05] designed an approximation scheduling algorithm for data collection and aggregation through a tree-based routing structure. It was also shown that the scheduling problem for data aggregation with minimum latency through tree-based routing structures is NP-hard. Huang *et al.* [HWV+07] proposed a scheduling algorithm for data collection through an improved tree structure with a latency bound of $23R + \Delta - 18$, where R is the network radius and Δ is the maximum degree of sensor nodes in the network. Wan *et al.* [WSW+09] further improved the tree structure for data collection and provided scheduling algorithms with lower latency bounds. All the above scheduling algorithms are centralized in nature. Yu *et al.* [YLL09] developed a distributed scheduling algorithm for data collection and aggregation through tree-based routing structures and proposed a new tree structure to further improve the latency bound. The same scheduling algorithm was also used by Li *et al.* in [LGP10]. Xu *et al.* [XWM+09] designed a scheduling algorithm for tree-based routing structures in which the communication range and the interference range

of sensor nodes are assumed to be different. However, none of the above work has considered scheduling data collection through multi-path routing structures.

In this thesis, we shall present an efficient distributed algorithm for constructing data collection schedules for multi-path routing structures. We shall also present new methods for multi-path TDMA-based sensor data collection that consider the energy efficiency, the time latency and the robustness of data collection altogether.

Chapter 3

A robust multi-path routing structure

As discussed in Chapters 1 and 2, wireless communication among sensor nodes is prone to failures. Hence, dealing with wireless communication failures is an important problem that needs to be addressed for supporting a wide variety of sensor network applications. One approach to address wireless communication failures in sensor data collection is to use multi-path routing structures. In this chapter, we investigate the construction of a class of multi-path routing structures in sensor networks called *rings overlay* for enhancing the robustness of sensor data collection. Rings overlay [NGSA04, CLKB04] exploits the broadcast nature of wireless communication to cope with communication failures.

A rings overlay conceptually organizes sensor nodes into a set of rings around the base station with increasing hop counts to it. For each node, all of its neighbors in the next inner ring are known as its *parents*. Sensor data are collected through level-by-level propagation from the outermost ring to the base station. For example, Figure 3.1 shows a rings overlay consisting of three rings R_1, R_2 and R_3. To collect data, node f in ring R_3 first broadcasts its data to its parents d and g in ring R_2. Then, nodes d and g aggregate their data with the data received from f, and broadcast to their parents in ring R_1. Meanwhile, nodes a and c in ring R_2 also broadcast their data to their parents in ring R_1. Finally, the nodes in ring R_1 aggregate their data with the data received from their children,

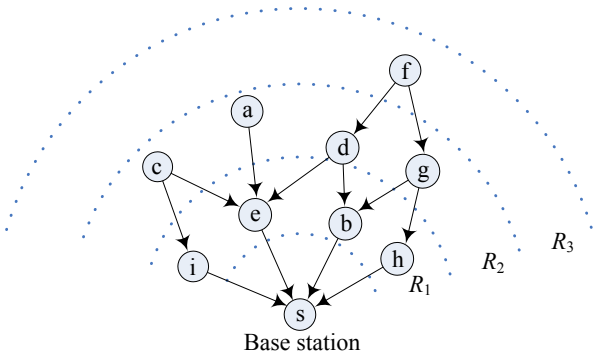

Figure 3.1: An example rings overlay.

and broadcast the aggregated data to the base station s.

By exploiting the broadcast nature of wireless communication, the rings overlay enables sensor data transportation through multiple interleaving paths from sensor nodes to the base station. Thus, the data are successfully transported to the base station as long as any one of these propagation paths is failure-free. Nevertheless, a rings overlay normally does not benefit all sensor nodes in the network. First, a casually constructed rings overlay may leave some nodes connected to the base station through a single propagation path only. In Figure 3.1, for instance, node a has only one propagation path $a \rightarrow e \rightarrow s$ to the base station. Second, each node in the ring next to the base station (e.g., nodes b, e, h and i in ring R_1 of Figure 3.1) inherently has only one single-hop propagation path to the base station. All the above nodes do not enjoy the benefit of multi-path routing. The data acquired by these nodes remain to be transported by single-path routing that is highly susceptible to communication failures. The robustness of data collection through the rings overlay would be severely limited when there are a significant number of such nodes.

In this chapter, we first develop a new approach for constructing the rings overlay to prevent sensor nodes from having only few propagation paths to the base station. The objective is to assign sensor nodes to appropriate rings to let them benefit from multi-path routing as much as possible. The proposed construction approach is fully distributed and only requires sensor nodes to have local neighborhood information. Then, we design and analyze an enhanced scheme for

relaying data to the base station from the sensor nodes in the ring next to the base station. The goal is to improve the resilience of these nodes to communication failures in data collection without requiring them to transmit their data multiple times. A wide range of experiments are conducted to evaluate the proposed techniques. Experimental results show that compared with a baseline greedy construction approach and the original relay scheme, the proposed techniques of overlay construction and relay enhancement substantially improve the robustness of sensor data collection through the rings overlay.

The remainder of this chapter is organized as follows. Section 3.1 introduces how data are collected and aggregated through the rings overlay as preliminaries. Section 3.2 presents the proposed approach for constructing the rings overlay. The enhanced relay scheme for data collection is elaborated in Section 3.3. The experimental evaluation is described in Section 3.4. Finally, Section 3.5 summarizes the chapter.

3.1 Preliminaries

We consider a wireless sensor network in which sensor nodes periodically sample local phenomena such as temperature and humidity, and report their acquired data to a base station. A rings overlay in the sensor network conceptually organizes the sensor nodes into a set of rings $R_1, R_2, ...$ around the base station. For each node v in a ring R_i, all nodes in the next inner ring R_{i-1} that are within v's radio transmission range are called v's *parents*.

To collect sensor data at the base station, sensor nodes are loosely time synchronized to propagate data level-by-level [NGSA04]. The nodes in each ring R_i listen to the transmissions of the nodes in ring R_{i+1}, aggregate their locally acquired data with the data received from their children and then broadcast the aggregated data to their parents in ring R_{i-1}. This propagation and aggregation process continues until the base station receives the aggregated data from the nodes in ring R_1. As shown in Figure 3.2, a round of data collection proceeds in M time frames if the rings overlay has M rings $R_1, R_2, ..., R_M$. Each node turns

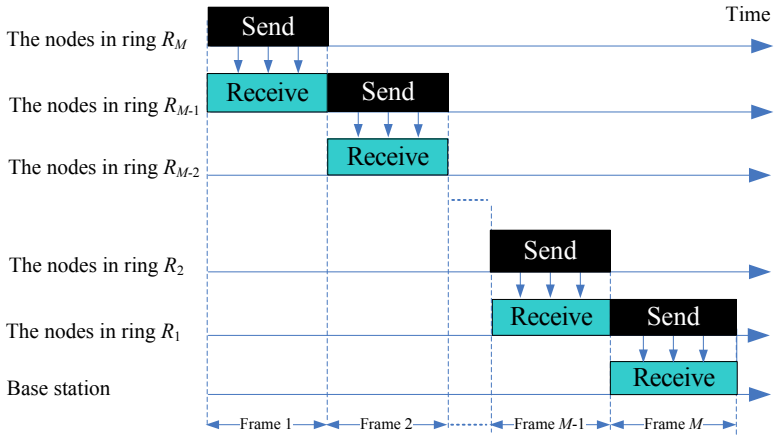

Figure 3.2: Sending and receiving schedules of sensor nodes in data collection through rings overlay.

on its radio for two time frames: one frame for sending data to its parents and one frame for receiving data from its children. A simple time synchronization protocol similar to that used by TinyDB [MFHH05, GKS03] can be employed to let sensor nodes agree on a global time base that allows them to wake up and transmit or receive data following the schedules based on their levels as shown in Figure 3.2.[1] The length of the time frame can be determined a priori based on the density of node deployment so that the nodes get enough time to broadcast their data once in the frame [NGSA04]. Successive rounds of data collection may be carried out in either a sequential or pipelined manner.

In general, the aggregated data broadcast by the nodes of inner rings include larger amount of raw sensor data than the aggregated data broadcast by the nodes of outer rings. To prevent the size of aggregated data from growing steadily in the propagation process, digest-based representations of aggregated data such as sketches [CLKB04] and synopses [NGSA04] have been developed to compactly summarize sensor data during in-network aggregation. These representations allow the aggregated data to maintain constant and small size as they are propagated toward the base station. As a result, the size of the aggregated data transmitted by each node to its parents is the same, irrespective of

[1]This protocol achieves a typical time synchronization error of about 10ms [MFHH05]. In general, such imprecision in time synchronization can be tolerated in data collection by letting the receivers turn on their radios several milliseconds before their receiving frames and keep awake till several milliseconds after their receiving frames.

its ring index and the rings overlay structure. In addition, these representations are order- and duplicate-insensitive in that they are independent of the order in which sensor data are aggregated and how many times the same data are aggregated. These features enable the base station to produce a variety of aggregation results with the aggregated data received. The data acquired by a sensor node are accounted for at the base station in a round of data collection if there exists at least one failure-free propagation path from the node to the base station. To facilitate presentation, we shall refer to the probability for the local data acquired by a sensor node to be successfully delivered to the base station as the *success ratio* of the sensor node. Note that the success ratios of different sensor nodes are inter-related because the nodes of inner rings relay the data acquired by the nodes of outer rings in the data collection process.

3.2 Assigning sensor nodes to rings

3.2.1 Related work: Baseline greedy approach

A rings overlay is built by assigning sensor nodes to rings based on their hop counts to the base station. In a simple approach for rings overlay construction [NGSA04, CLKB04], a message is flooded over the entire network from the base station and sensor nodes are assigned to rings in a greedy manner. Specifically, the base station starts by broadcasting a message with label 0, and any node receiving this message is assigned to ring R_1. Then, each node in ring R_1 broadcasts a message with label 1. Any node receiving a label-1 message is assigned to ring R_2, and so on. In general, a sensor node is assigned to ring R_{i+1} if it first receives a message with label i. The construction process completes when all sensor nodes are assigned to rings. The rings overlay shown in Figure 3.1 is in fact constructed by this greedy approach. In this example, node a is assigned to ring R_2 since node a first receives a label-1 message from node e. Thus, node a has only a single data propagation path to the base station: $a \rightarrow e \rightarrow s$. Therefore, the success ratio of node a is limited since the data acquired by node a would be successfully delivered to the base station only if both transmissions $a \rightarrow e$ and

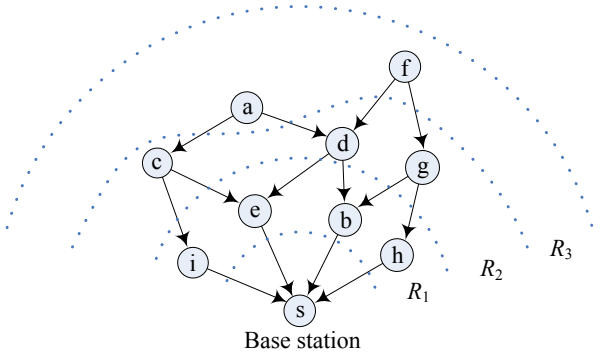

Figure 3.3: A rings overlay that increases the number of propagation paths from node a to the base station.

$e \rightarrow s$ succeed.

3.2.2 Threshold-based approach

To prevent sensor nodes from having only one propagation path to the base station, an intuitive strategy is to avoid them from having only a single parent in the rings overlay. Consider node a in the network of Figure 3.1. If node a is assigned to ring R_3 as shown in Figure 3.3, node a may have two parents c and d if a is within the radio ranges of c and d, which would increase the number of propagation paths from node a to the base station, thereby improving a's success ratio. Thus, the general idea of our new approach is to create opportunities for the nodes first receiving label-i messages to be assigned to ring R_{i+2} instead of ring R_{i+1} if such assignments increase their number of parents. To do so, the nodes that first receive a label-i message continue to listen for more messages. A threshold T is employed to guide the assignment of the nodes to rings. If a node is able to receive T or more label-i messages, the node is assigned to ring R_{i+1} and then, the node broadcasts a label-$(i+1)$ message. A node receiving less than T label-i messages keeps listening for these label-$(i+1)$ messages. If the node receives more label-$(i+1)$ messages than label-i messages, the node is assigned to ring R_{i+2}. Otherwise, it is assigned to ring R_{i+1}.

To implement the above strategy, our threshold-based construction approach works in phases. Phase 1 starts by the base station broadcasting a message with

label 0. Any node receiving this message is assigned to ring R_1 immediately. Each subsequent phase i finalizes the set of sensor nodes in ring R_i. Specifically, in phase i, all nodes in ring R_{i-1} would have broadcast label-$(i-1)$ messages since ring R_{i-1} has been finalized by the end of phase $i-1$. All unassigned nodes that receive these label-$(i-1)$ messages would be assigned to rings by the end of phase i. Among these unassigned nodes, the nodes receiving at least T label-$(i-1)$ messages are assigned to ring R_i immediately, where T is the threshold employed in overlay construction. Then, these newly assigned nodes in ring R_i broadcast label-i messages. The unassigned nodes receiving less than T label-$(i-1)$ messages keep listening for these label-i messages until the end of phase i. Each of these nodes compares the number of label-$(i-1)$ messages with the number of label-i messages it receives. If more label-i messages are received than label-$(i-1)$ messages, the node is assigned to ring R_{i+1}. Otherwise, the node is assigned to ring R_i.

Figure 3.3 shows an example execution of the threshold-based construction approach with threshold $T = 2$ on the network of Figure 3.1. In this example, in phase 2, nodes c and d each receives two label-1 messages from the nodes in ring R_1, reaching the threshold. Therefore, nodes c and d are assigned to ring R_2 and they broadcast label-2 messages. Meanwhile, node a receives only one label-1 message from node e in ring R_1, which is less than the threshold. So, node a keeps listening. By the end of phase 2, node a receives the two label-2 messages broadcast by nodes c and d, so node a is assigned to ring R_3. As a result, node a has two parents c and d in ring R_2. Since nodes c and d each has two parents in ring R_1, node a has a total of 4 propagation paths to the base station. Recall that the rings overlay constructed by the greedy approach in Figure 3.1 provides node a with only a single data propagation path to the base station. Therefore, the rings overlay constructed by the threshold-based approach would increase node a's success ratio significantly.

In rings overlay construction, sensor nodes do not need to explicitly identify or keep track of their children since their relationships are implicitly resolved by the ring indexes. The ring assignment algorithm executed by each node in the

threshold-based construction approach is summarized in Algorithm 1. Denote by n the number of sensor nodes in the network. In the threshold-based overlay construction, each node broadcasts one message as soon as it is assigned to a ring. Thus, the total number of broadcast messages, including the broadcast message from the base station, is $n + 1$. This message complexity is the same as that of the baseline greedy construction approach in which each node also broadcasts one message when it is assigned to a ring. Since the overlay construction process is executed only once prior to the start of data collection, the associated traffic and energy overhead, amortized over network lifetime, is minimal. In the data collection process, sensor nodes listen to the data transmissions from all of their children simply by following their sending and receiving schedules according to their ring indexes as shown in Figure 3.2.

We remark that in our proposed threshold-based approach for overlay construction, a sensor node receives label messages in at most two phases before it is assigned to a ring. After being assigned to a ring, a node may receive label messages in other phases but this does not affect its ring assignment. If a node first receives a label-i message, it will be assigned to a ring immediately if $i = 0$ or by the end of phase $i + 1$ (according to lines 3 and 9 of Algorithm 1). A label-i message can be broadcast in phase i by the nodes receiving at least T label-$(i - 1)$ messages and assigned to ring R_i. Otherwise, a label-i message can be broadcast in phase $i + 1$ by other nodes assigned to ring R_i. However, label-i messages cannot be broadcast before phase i or after phase $i + 1$ (according to lines 5, 14, 20 and 23 of Algorithm 1). Thus a sensor node can only receive label messages in at most two phases before it is assigned to a ring.

The energy consumption of sensor nodes in data collection includes the energy costs for transmitting data and receiving data. In a round of data collection through rings overlays, each node transmits data only once irrespective of the rings overlay structure. Therefore, the same number of transmissions occur in data collection via the rings overlays constructed by the threshold-based and greedy approaches. To receive data, the nodes in these rings overlays also remain awake for the same amount of time (i.e., one time frame) in a round of data

Algorithm 1: Ring assignment algorithm executed by each node in the threshold-based approach for overlay construction

```
1  wait until a message is received;
2  let i be the label of the received message;
3  if i = 0 then
4  |  assign the local node to ring R_1;
5  |  broadcast a label-1 message in phase 2;
6  else
7  |  set label-i message counter c_i = 1;
8  |  set label-(i + 1) message counter c_{i+1} = 0;
9  |  while phase i + 1 has not ended do
10 |  |  if a label-i message is received then
11 |  |  |  set c_i = c_i + 1;
12 |  |  if c_i ≥ T then
13 |  |  |  assign the local node to ring R_{i+1};
14 |  |  |  broadcast a label-(i + 1) message in phase i + 1;
15 |  |  |  return;
16 |  |  if a label-(i + 1) message is received then
17 |  |  |  let c_{i+1} = c_{i+1} + 1;
18 |  if c_i ≥ c_{i+1} then
19 |  |  assign the local node to ring R_{i+1};
20 |  |  broadcast a label-(i + 1) message in phase i + 2;
21 |  else
22 |  |  assign the local node to ring R_{i+2};
23 |  |  broadcast a label-(i + 2) message in phase i + 2;
24 return;
```

collection. The largest child numbers of sensor nodes in the threshold-based rings overlay are likely to be smaller than those in the greedy rings overlay. This is because in a rings overlay, the nodes having the largest numbers of children are generally those located close to the outer boundary of their rings. In the greedy construction approach, when such a node broadcasts a message, all unassigned nodes receiving the message become its children. Nevertheless, in the threshold-based construction approach, not every unassigned node receiving the message would be assigned to the immediate outer ring. Some of them may be assigned to the next outer ring if they receive more higher-label messages. Thus, in the threshold-based rings overlay, the largest child numbers of the nodes are likely to be smaller (as shall be shown by experimental results in Section 3.4). As a result, the numbers of transmissions received by these nodes in data collection also tend to be smaller.

3.2.3 Setting threshold values

The threshold value T is important to determining how sensor nodes are assigned to rings in our proposed approach. On one hand, when $T = 1$, each sensor node would be assigned to a ring immediately when it receives the first message in overlay construction. Thus, the threshold-based approach degenerates to the baseline greedy approach described in Section 3.2.1. On the other hand, when T is larger than the maximum number of neighbors of the sensor nodes, no node would receive at least T messages with the same label so that the rings overlay constructed would also be the same as that produced by the greedy approach. It is intuitive that an effective threshold value should be set proportional to the node density.

Assume that all sensor nodes have the same transmission range and let r be their transmission range. Consider a sensor node v that has a communication range represented by a circular disk of radius r and centered at v. This communication range normally includes nodes in the same ring as node v as well as in the inner and outer rings than v in a rings overlay. Since the nodes belonging to the same ring must be within the transmission ranges of the nodes in the immediate

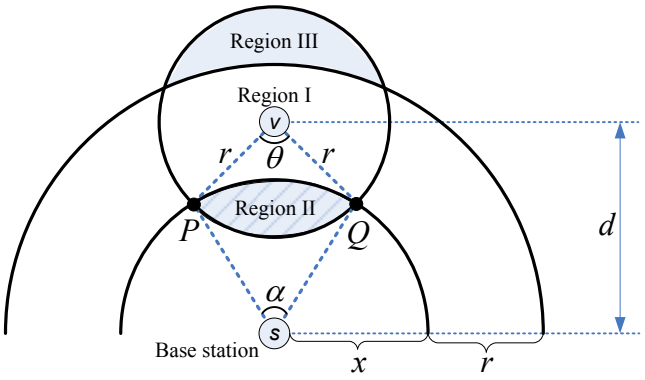

Figure 3.4: Estimating the expected number of parents for node v.

inner ring, the width of a ring would not exceed r. For simplicity of the analysis, we suppose that the width of the ring containing node v is r. As shown in Figure 3.4, we divide v's communication range by a ring-shaped strip of width r centered at the base station s. The strip partitions the communication range into three regions: one region containing node v (region I in Figure 3.4), one region closer to the base station than v (region II), and one region further away from the base station than v (region III). We approximate the set of nodes in the same ring as v by the nodes in region I, and approximate the set of v's parents in the next inner ring by the nodes in region II. Then, the expected number of parents for node v is given by the expected area of region II times the node density.

Denote by d the distance from node v to the base station s, and denote by x the inner radius of the ring-shaped strip containing node v (see Figure 3.4). It is obvious that $(d - r) \leq x \leq d$. Let P and Q be the intersection points of the inner strip boundary and the boundary of v's communication range. Region II is the intersection area of sectors vPQ and sPQ. Let θ be the angle of sector vPQ, and α be the angle of sector sPQ. The areas of sectors vPQ and sPQ are $\frac{1}{2}\theta r^2$ and $\frac{1}{2}\alpha x^2$ respectively, and the areas of triangles $\triangle vPQ$ and $\triangle sPQ$ are $\frac{1}{2}r^2 \sin\theta$ and $\frac{1}{2}x^2 \sin\alpha$ respectively. Therefore, the area of region II is given by

$$\left(\frac{1}{2}\theta r^2 - \frac{1}{2}r^2 \sin\theta\right) + \left(\frac{1}{2}\alpha x^2 - \frac{1}{2}x^2 \sin\alpha\right).$$

Considering triangle $\triangle vsQ$, we have

$$\cos\frac{\theta}{2} = \cos\widehat{svQ} = \frac{r^2 + d^2 - x^2}{2rd},$$

and

$$\cos\frac{\alpha}{2} = \cos\widehat{vsQ} = \frac{x^2 + d^2 - r^2}{2xd}.$$

Since the inner radius x of the ring-shaped strip containing node v can be any value between $(d-r)$ and d, the expected area of region II for a node v that has distance d to the base station is given by

$$\begin{aligned}
A(d) &= \frac{1}{r}\int_{d-r}^{d}\left(\frac{1}{2}\theta r^2 - \frac{1}{2}r^2\sin\theta + \frac{1}{2}\alpha x^2 - \frac{1}{2}x^2\sin\alpha\right)dx \\
&= \frac{1}{r}\int_{d-r}^{d}\left(r^2\arccos\frac{r^2+d^2-x^2}{2rd} - r^2\sin\frac{\theta}{2}\cos\frac{\theta}{2}\right)dx \\
&\quad + \frac{1}{r}\int_{d-r}^{d}\left(x^2\arccos\frac{x^2+d^2-r^2}{2xd} - x^2\sin\frac{\alpha}{2}\cos\frac{\alpha}{2}\right)dx \\
&= \frac{1}{r}\int_{d-r}^{d}\left(r^2\arccos\frac{r^2+d^2-x^2}{2rd}\right)dx \\
&\quad - \frac{1}{r}\int_{d-r}^{d}\left(r^2\cdot\frac{r^2+d^2-x^2}{2rd}\cdot\frac{\sqrt{4r^2d^2-(r^2+d^2-x^2)^2}}{2rd}\right)dx \\
&\quad + \frac{1}{r}\int_{d-r}^{d}\left(x^2\arccos\frac{x^2+d^2-r^2}{2xd}\right)dx \\
&\quad - \frac{1}{r}\int_{d-r}^{d}\left(x^2\cdot\frac{x^2+d^2-r^2}{2xd}\cdot\frac{\sqrt{4x^2d^2-(x^2+d^2-r^2)^2}}{2xd}\right)dx \\
&= \int_{d-r}^{d}\left(r\cdot\arccos\frac{r^2+d^2-x^2}{2rd} + \frac{x^2}{r}\arccos\frac{x^2+d^2-r^2}{2xd}\right)dx \\
&\quad - \frac{1}{2r}\int_{d-r}^{d}\sqrt{2r^2d^2+2r^2x^2+2x^2d^2-x^4-r^4-d^4}\,dx.
\end{aligned}$$

It has been shown that the above integrals are incomplete elliptic integrals which cannot be expressed by elementary functions [AS72]. Thus, we use the trapezoidal sum method [WR67] to numerically calculate an approximation of region II's area and plot $A(d)$ as a function of d in Figure 3.5. As can be seen, the curve of $A(d)$ flattens as d increases. Denote by ρ the node density in the communication range of node v. The expected number of nodes in region II is

then given by $A(d) \cdot \rho$.

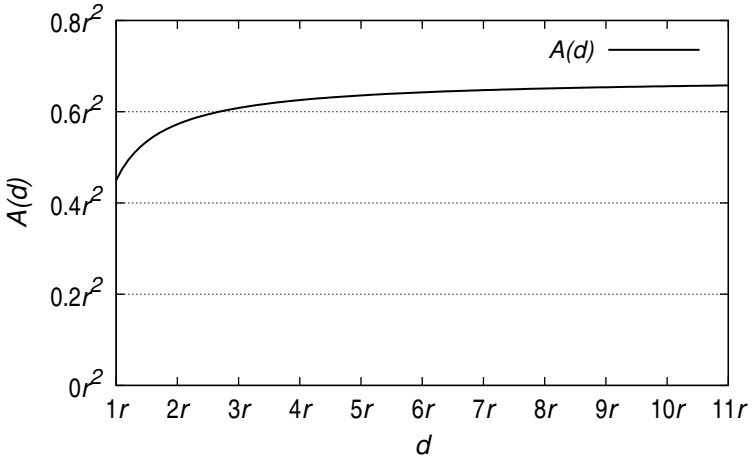

Figure 3.5: Area $A(d)$ of region II as a function of distance d.

To apply the analytical result to the threshold-based construction approach, we propose two methods as follows. The first method sets a uniform threshold at all nodes in the network for constructing the rings overlay. We shall call it *the global threshold-based approach* (GT). In large networks, the distance between most sensor nodes and the base station is much longer than the transmission range r. When $d \gg r$, and hence $x \gg r$, both α and $\sin\alpha$ approach 0. Therefore, as shown in Figure 3.5, $A(d)$ is approximated by

$$\begin{aligned} A(d) &\approx \frac{1}{r}\int_{d-r}^{d}\left(\frac{1}{2}\theta r^2 - \frac{1}{2}r^2\sin\theta\right)\,dx \\ &= \int_{d-r}^{d}\left(\frac{1}{2}\theta r - \frac{1}{2}r\cdot\sin\theta\right)\,dx \\ &= \int_{d-r}^{d}\left(r\cdot\arccos\frac{d-x}{r} - \frac{d-x}{r}\sqrt{r^2-(d-x)^2}\right)\,dx \\ &= \frac{2}{3}r^2. \end{aligned}$$

The node density ρ, on the other hand, can be estimated by dividing the total number of sensor nodes by the area of the sensing field. The analytical threshold value for the global threshold-based approach is then given by $\frac{2}{3}r^2\rho$.

In practice, the exact number of sensor nodes may not be known a priori. In this case, the node density has to be estimated on the fly. Moreover, it is

also possible for the node density to differ at different parts of the sensing field due to reasons such as inadequate control in sensor deployment or node failures. This motivates us to design a method for each sensor node to calculate its own threshold value based on local estimates of node density ρ and area $A(d)$. We shall call it *the localized threshold-based approach* (LT). In the localized approach, each sensor node estimates the local node density ρ_l as the number of neighbors in its communication range normalized by the area of its communication range. To do so, each node broadcasts a message to all neighbors in its communication range and calculates the number of neighbors by counting the number of broadcast messages received. To estimate localized $A(d)$, we make use of the messages sent in overlay construction to approximately estimate the distance between sensor nodes and the base station. Recall that messages sent in overlay construction are labelled with the ring index of the sending node. Thus, if the first message received by a sensor node in overlay construction is labelled with i, the shortest path from the sensor node to the base station is at most $i+1$ hops. So, we approximate the distance from the node to the base station by $\left(i + \frac{1}{2}\right) r$. Integrating the above estimates, the threshold value for a sensor node is set to $A\left(\left(i + \frac{1}{2}\right) r\right) \cdot \rho_l$ in the localized threshold-based approach. The localized threshold setting does not require sensor nodes to have global knowledge about the node density. Different sensor nodes may use different threshold values for overlay construction.

3.2.4 Coping with communication failures in assigning sensor nodes to rings

The communication among sensor nodes is subject to failures not only in the data collection process from sensor nodes to the base station but in overlay construction as well. Due to communication failures, some sensor nodes may not receive any message in overlay construction and thus would not be assigned to any ring. Hence, the rings overlay constructed might not span all sensor nodes in the network, thereby preventing the base station from collecting data from all sensor nodes.

As elaborated in Section 2.1, the failure rates of single-hop communication

among sensor nodes can be reduced using methods such as forward error correction codes [ASSC02, JE06], transmission power control [SKH04, LZZ+06], and reliable transport protocols [SH03, WCK02, LW03, CHF+06]. Forward error correction methods send redundant information together with sensor data from the senders and this information would be used to correct possible errors in the data received at the receivers. These encoding schemes usually require a significant amount of redundant information to be transmitted together with the data. Transmission power control methods can improve the signal to interference and noise ratio at the receivers and hence improve the success rates of communication links. However, adjusting the transmission power levels of sensor nodes is usually a costly process. The failure rates of single-hop links can also be improved by using reliable transport protocols in which additional control messages and retransmissions are used to ensure data delivery. This method usually incurs an overhead cost due to the transmission and reception of control messages and data retransmissions.

To reduce the impact of communication failures and control the overhead cost incurred in overlay construction, we propose to exploit a simple strategy that repeats the messages broadcast in rings overlay construction for a number of times. Accordingly, each sensor node should set its threshold value to the expected number of parents from which it successfully receives messages in overlay construction. This can be done by adjusting the threshold calculation. In the global threshold-based approach, the threshold value can be scaled by an estimated probability that a node successfully receives at least one of the duplicate messages broadcast by a neighbor. In the localized threshold-based approach, the same duplicate transmission can be employed when sensor nodes broadcast to their neighbors for estimating the local node density. The local node density is then calculated based on the number of neighbors from which broadcast messages are successfully received.

3.3 Relay enhancement for data collection

3.3.1 Enhanced relay scheme

In the original relay scheme described in Section 3.1, the nodes in the ring next to the base station (i.e., ring R_1) transmit their data directly to the base station only once. A possible approach for improving the success ratios of the nodes in ring R_1 is to create additional time frames in a round of data collection for these nodes to repeatedly transmit their data to the base station [NGSA04]. This approach, however, implies that the nodes in ring R_1 have to turn on their radios for more time frames than the nodes in other rings. As a result, their batteries would be depleted more rapidly than others. When the nodes in ring R_1 run out of energy, none of the nodes in any other rings can transport their data to the base station. Therefore, the network lifetime would be reduced remarkably. In this section, we present an enhanced relay scheme to improve the success ratios of the nodes in ring R_1 without requiring them to transmit their data multiple times in a round of data collection.

A round of data collection in our enhanced relay scheme proceeds in $M + 1$ time frames, where M is the number of rings in the overlay. Figure 3.6 shows the sending and receiving schedules for the sensor nodes of different rings. In each frame i of the enhanced relay scheme where $1 \leq i \leq M - 2$, the nodes in rings R_{M-i+1} still broadcast data to their parents in ring R_{M-i} and the nodes in ring R_{M-i} wake up to receive the data, similar to the original relay scheme. The last three frames $M - 1$, M and $M + 1$ of the enhanced relay scheme are different from the original relay scheme. Specifically, the nodes in ring R_1 are partitioned into two proportions β and $(1 - \beta)$, where $0 < \beta < 1$. In frame $M - 1$, the nodes in the β proportion of ring R_1 wake up to receive the data sent by the nodes in ring R_2. Then, these nodes aggregate the received data with the locally acquired data and broadcast the aggregated data in frame M to the base station as well as the nodes in the $(1 - \beta)$ proportion of ring R_1. The purpose is to create multiple propagation paths from the nodes in the β proportion to the base station through the nodes in the $(1 - \beta)$ proportion of ring R_1. The

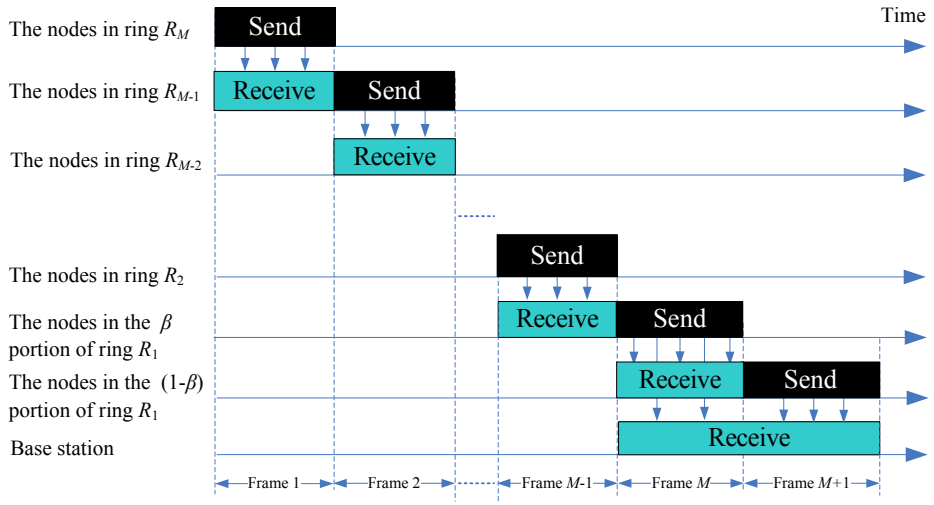

Figure 3.6: Sending and receiving schedules of sensor nodes in the enhanced relay scheme.

nodes in the $(1-\beta)$ proportion of ring R_1 turn off their radios in frame $M-1$ and do not listen to the transmissions of the nodes in ring R_2. In frame M, they wake up to receive the data sent by the nodes in the β proportion of ring R_1. Finally, the nodes in the $(1-\beta)$ proportion of ring R_1 aggregate their locally acquired data with the data received from the nodes in the β proportion of ring R_1 and send the resultant aggregated data to the base station in frame $M+1$. In this enhanced relay scheme, each sensor node in ring R_1 still turns on its radio for only two time frames in a round of data collection: one frame for receiving data and one frame for sending data, similar to the nodes in all the other rings. Since each node in ring R_1 still transmits data only once in each round of data collection, the enhanced relay scheme keeps the same number of transmissions as the original relay scheme. The enhanced relay scheme can be applied to the nodes in ring R_1 of the rings overlays constructed by both the greedy approach and the threshold-based approaches.

Figure 3.7 illustrates the enhanced relay scheme with the example network of Figure 3.1. Suppose that among the nodes in ring R_1 of this network, nodes e, h are in the β proportion and nodes b, i are in the $(1-\beta)$ proportion. In the enhanced relay scheme, in addition to transmitting its data to the base station s, node e also transmits its data to nodes b and i. Similarly, node h also transmits

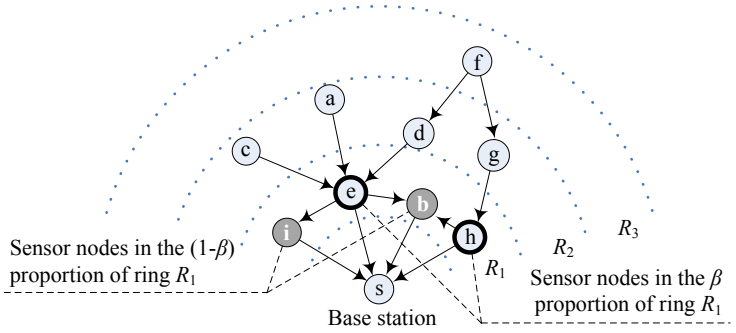

Figure 3.7: An example of relay enhancement.

its data to node b in addition to the base station s. As a result, nodes e and h in the β proportion have two and one additional data propagation paths to the base station respectively, besides the direct single-hop path to the base station. Thus, the success ratios of nodes e and h would increase.

As seen from Figure 3.7, while the enhanced relay scheme creates multiple propagation paths for the nodes in the β proportion of ring R_1, the nodes in the $(1-\beta)$ proportion of ring R_1 continue to have a single propagation path to the base station. In fact, the nodes in the $(1-\beta)$ proportion would never benefit from multi-path routing if the partitioning of the nodes in ring R_1 is fixed. In order to benefit all nodes in ring R_1, the nodes in the β and $(1-\beta)$ proportions are rotated by letting each node randomly determine whether it is in the β or $(1-\beta)$ proportion in every round of data collection. Specifically, each node in ring R_1 autonomously assigns itself to the β proportion with β probability and to the $(1-\beta)$ proportion with $(1-\beta)$ probability. In this way, the partitioning of the nodes in ring R_1 is done in a *fully distributed* manner without any communication among the nodes.

Figure 3.7 also shows that in addition to the nodes in ring R_1, the enhanced relay scheme also affects the transportation of data acquired by the nodes in ring R_2. On one hand, the nodes in the $(1-\beta)$ proportion of ring R_1 turn off their radios when the nodes in the β proportion of ring R_1 listen to the transmissions of the nodes in ring R_2. Hence, compared to the original relay scheme, the enhanced relay scheme reduces the number of parents in ring R_1 that listen for

the transmissions from the nodes in ring R_2. On the other hand, the nodes in the β proportion of ring R_1 now have multiple propagation paths to the base station. These nodes would have higher chances of relaying the data received from the nodes in ring R_2 to the base station, compared to the original relay scheme.

To better understand the enhanced relay scheme, we develop an analytical model to examine the impact of β value on the robustness of data collection.

3.3.2 Analyzing the enhanced relay scheme

Assume that the communication range of a node v is a circular disk of radius r and centered at v, where r is the transmission range of sensor nodes. Suppose that any node that can communicate directly with the base station (i.e., within transmission range r from the base station) is assigned to ring R_1. Denote the circular disk of radius r and centered at the base station by S. Assume that sensor nodes are uniformly distributed in S. Then, for any node v in ring R_1 or R_2, the number of its neighbors in ring R_1 is proportional to the overlapping area between its communication range and S. If v itself is in ring R_1 (v is inside S, see Figure 3.8(a)), the minimum possible overlapping area is $2 \cdot \left(\frac{\pi r^2}{3} - \frac{\sqrt{3}r^2}{4}\right)$. This happens when v approaches the boundary of S as shown in Figure 3.8(b). Thus, for the nodes in ring R_1, their minimum number of neighbors in R_1 is given by the number of nodes in an area of $2 \cdot \left(\frac{\pi r^2}{3} - \frac{\sqrt{3}r^2}{4}\right)$, which we shall denote by u. If node v is in ring R_2 (v is outside S, see Figure 3.8(c)), the maximum possible overlapping area is also $2 \cdot \left(\frac{\pi r^2}{3} - \frac{\sqrt{3}r^2}{4}\right)$. This again happens when v approaches the boundary of S as shown in Figure 3.8(d). Therefore, for any node in ring R_2, its number of parents in ring R_1 cannot exceed u. Denote by l the link loss rate. Our analysis is carried out based on β, u and l.

First, we analyze the improvement of the enhanced relay scheme in the success ratios of the nodes in ring R_1. In the enhanced relay scheme, each node in the $(1-\beta)$ proportion of ring R_1 has one single-hop propagation path to the base station. Hence, its success ratio is $1-l$. Each node in the β proportion of ring R_1, besides sending data to the base station directly, also sends data to its neighbors in the $(1-\beta)$ proportion of R_1. Since the node has a minimum of u neighbors in

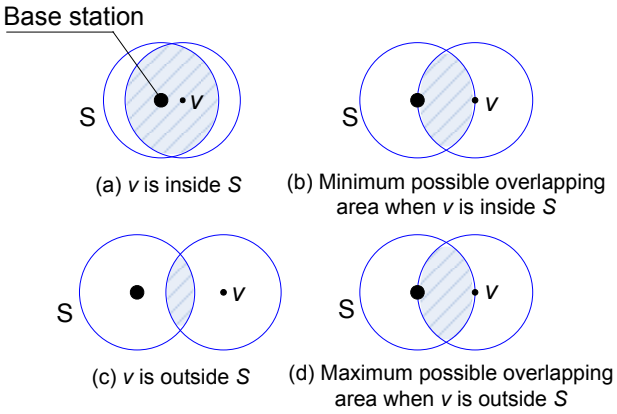

Figure 3.8: Overlapping area between the communication range of a node v and the circle S of radius r and centered at the base station.

ring R_1, there are at least $(1-\beta)\cdot u$ neighbors in the $(1-\beta)$ proportion of R_1. Therefore, the node has one single-hop propagation path and at least $(1-\beta)\cdot u$ two-hop propagation paths to the base station. The loss rate of the single-hop path is l, and the loss rate of each two-hop path is $1-(1-l)^2 = 2l-l^2$. Since all these paths are disjoint, the success ratio of a node in the β proportion of ring R_1 is at least $1-l(2l-l^2)^{(1-\beta)u}$. Due to rotation, each node in ring R_1 has β probability to be in the β proportion and $(1-\beta)$ probability to be in the $(1-\beta)$ proportion in any round of data collection. Therefore, the expected success ratio of the nodes in ring R_1 is given by

$$(1-l)\cdot(1-\beta) + \left(1-l(2l-l^2)^{(1-\beta)u}\right)\cdot\beta.$$

Figure 3.9 plots the analytical results for the expected success ratio of the nodes in ring R_1 at link loss rates 30%, 50% and 80%. We vary β from 1 down to 0.1 to compare our enhanced relay scheme ($0<\beta<1$) against the original relay scheme ($\beta=1$)[2], and vary u to explore a variety of node density. As can be seen, the success ratio of the nodes in ring R_1 at $\beta=1$ is lower than that at any β value between 0 and 1. This is because our enhanced relay scheme makes the nodes in the β proportion benefit from multi-path routing which improves their success ratios. At link loss rates 30% and 50%, the success ratio of the nodes in

[2]When $\beta=1$, the enhanced relay scheme degenerates to the original relay scheme.

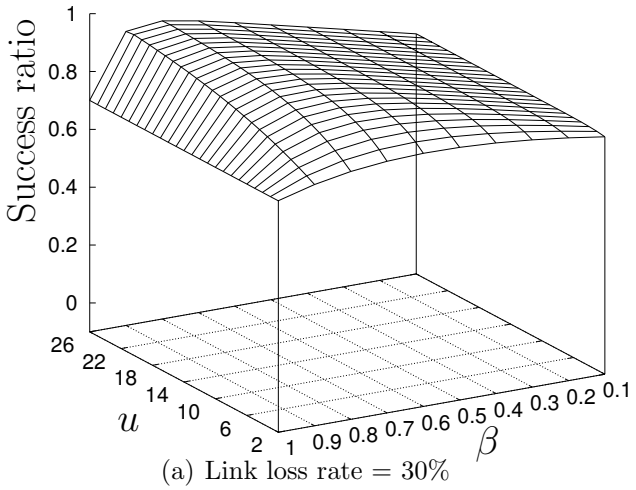

(a) Link loss rate = 30%

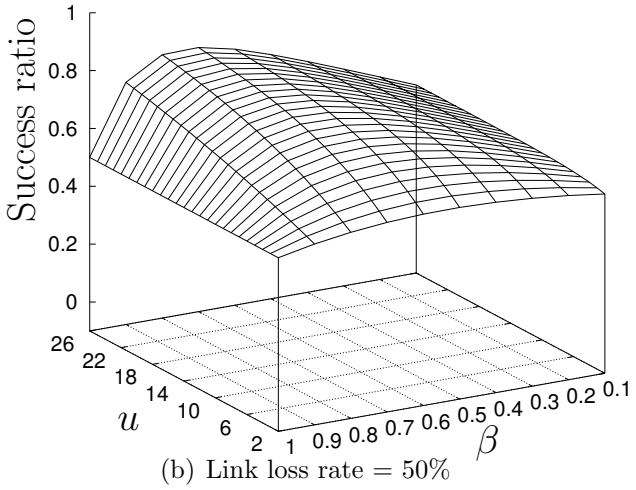

(b) Link loss rate = 50%

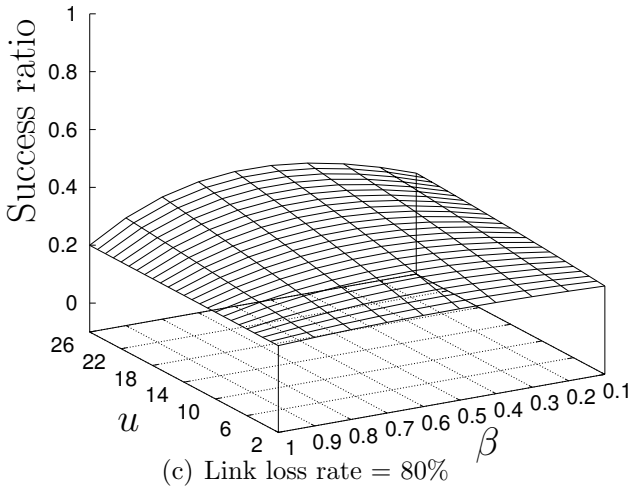

(c) Link loss rate = 80%

Figure 3.9: Analytical results on the expected success ratio of the sensor nodes in ring R_1.

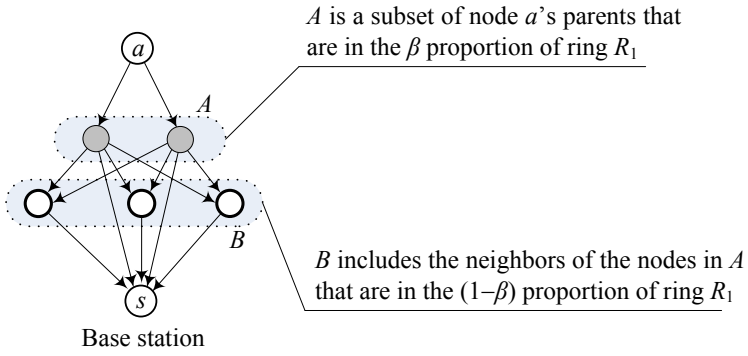

Figure 3.10: Analytical model for the nodes in ring R_2 in the enhanced relay scheme.

ring R_1 increases rapidly when β decreases from 1 to around 0.8, below which the success ratio gradually goes down with decreasing β value. The performance trend is similar for the link loss rate of 80% except that the peak success ratio is reached at β value around 0.7. These trends demonstrate two impacts of β value: first, the $(1-\beta)$ proportion of ring R_1 expands with decreasing β value so that each node in the β proportion of ring R_1 benefits more significantly from multi-path routing; second, the β proportion of ring R_1 shrinks with decreasing β value so that fewer nodes benefit from multi-path routing. At large β values, the first impact dominates whereas at small β values, the second impact dominates. The results in Figure 3.9 indicate that the enhanced relay scheme always improves the expected success ratio of the nodes in ring R_1 compared to the original relay scheme. Setting $\beta = 0.8$ achieves near optimal success ratios for the nodes in ring R_1 across wide ranges of node density and link loss rate.

Now, we analyze the success ratios of the nodes in ring R_2 under the enhanced relay scheme. As shown in Figure 3.10, let a be a node in ring R_2 that have t parents in ring R_1, where $0 < t \leq u$. Among these parents, a subset of $\beta \cdot t$ nodes are expected to be in the β proportion of ring R_1 and hence listen to the transmissions of node a in the enhanced relay scheme. Denote this subset of $\beta \cdot t$ nodes by A. Then, the probability for node a's data to be successfully delivered

to exactly m nodes in A is given by

$$P(m) = \binom{m}{\beta \cdot t} \cdot (1-l)^m \cdot l^{\beta \cdot t - m}.$$

In the enhanced relay scheme, the nodes in A send data to the base station directly as well as to the nodes in the $(1-\beta)$ proportion of ring R_1. If m nodes in A receive the data sent by node a, the probability for node a's data to be successfully delivered from these nodes to the base station directly is $1-l^m$. On the other hand, each node in A has at least $(1-\beta) \cdot u$ neighbors in the $(1-\beta)$ proportion of ring R_1. We conservatively assume that all nodes in A have a common set of $(1-\beta) \cdot u$ neighbors in the $(1-\beta)$ proportion of R_1. Denote this set of $(1-\beta) \cdot u$ nodes by B. If m nodes in A receive the data sent by node a and broadcast data to the nodes in B, the probability for each node in B to successfully receive node a's data is $1-l^m$. Note that the nodes in B send data to the base station directly. Therefore, the probability for node a's data to be delivered to the base station through any given node in B is $(1-l^m) \cdot (1-l)$. Since there are $(1-\beta) \cdot u$ nodes in B, the probability for node a's data to be successfully delivered to the base station through the nodes in B is

$$\begin{aligned} & 1-(1-(1-l^m) \cdot (1-l))^{(1-\beta) \cdot u} \\ =& 1-(l+l^m-l^{m+1})^{(1-\beta) \cdot u}. \end{aligned}$$

Taking into account the probability for node a's data to be delivered from the nodes in A to the base station directly, if m nodes in A receive the data sent by node a, the probability for node a's data to be successfully delivered to the base station is

$$1-l^m \cdot (l+l^m-l^{m+1})^{(1-\beta) \cdot u}.$$

Considering all possible m values, the expected success ratio of node a is given by

$$\sum_{m=1}^{\beta \cdot t} P(m) \cdot \left(1-l^m \cdot (l+l^m-l^{m+1})^{(1-\beta) \cdot u}\right).$$

Figure 3.11 plots the analytical results for the expected success ratio of a

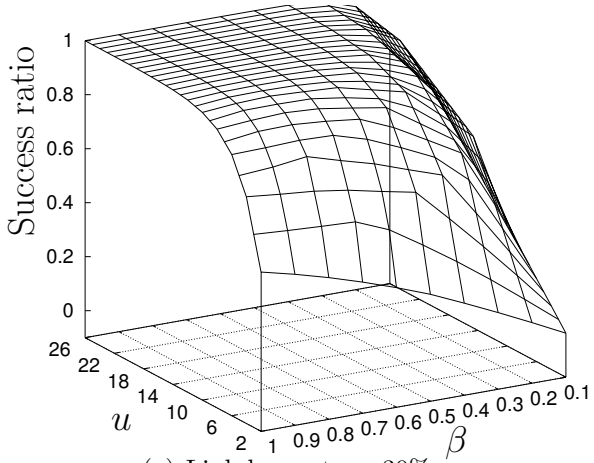

(a) Link loss rate = 30%

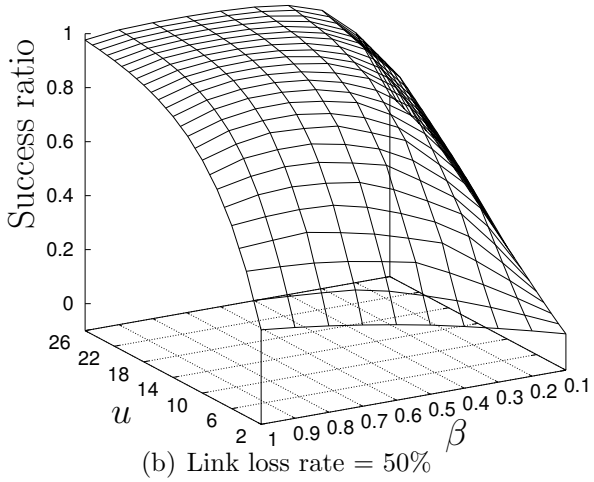

(b) Link loss rate = 50%

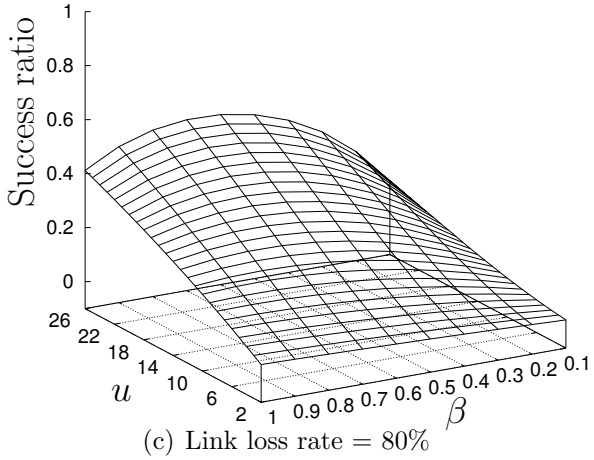

(c) Link loss rate = 80%

Figure 3.11: Analytical results on the expected success ratio of a sensor node in ring R_2 that has $t = 0.5 \cdot u$ parents in ring R_1.

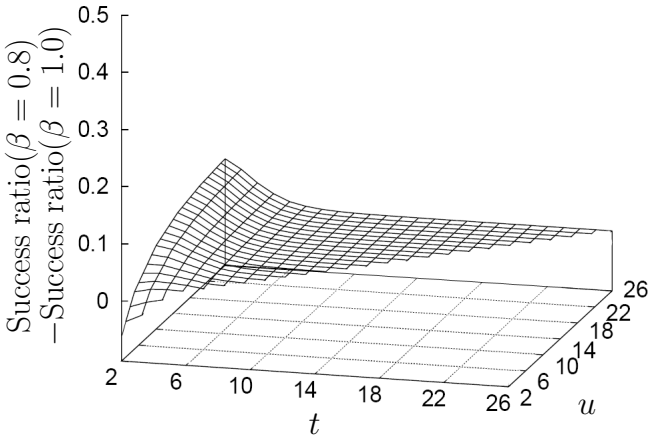

(a) Link loss rate = 30%

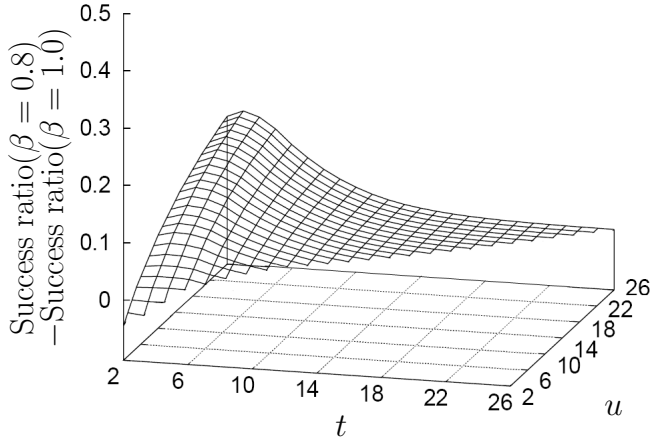

(b) Link loss rate = 50%

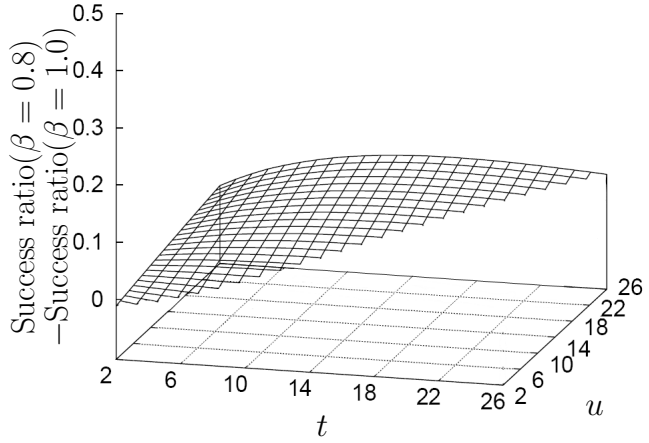

(c) Link loss rate = 80%

Figure 3.12: Difference between the expected success ratio of a sensor node in ring R_2 at $\beta = 1.0$ and $\beta = 0.8$.

node in ring R_2 that has $t = 0.5 \cdot u$ parents in ring R_1 at link loss rates 30%, 50% and 80%. It is seen that when β decreases from 1 to 0.8, the enhanced relay scheme generally improves the success ratio of the node in ring R_2 compared to the original relay scheme. This is because if the node in ring R_2 has more than a handful number of parents ($u > 4$ and hence $t > 2$), in the enhanced relay scheme with $\beta = 0.8$, there are still a significant number of sensor nodes in the β proportion of ring R_1 listening to the transmissions of the node in ring R_2. Since the enhanced relay scheme increases the success ratios of the nodes in the β proportion of ring R_1, the success ratio of the node in ring R_2 also improves. If the sensor node in ring R_2 has very few parents ($u \leq 4$ and hence $t \leq 2$), the enhanced relay scheme with $\beta = 0.8$ may slightly reduce the success ratio of the node in ring R_2, but the reduction is marginal even in the worst case as seen from Figure 3.11. When β continues to decrease from 0.8 to 0.1, the success ratio of the node in ring R_2 goes down steadily due to fewer parents in ring R_1. To further investigate, we compute the difference between the success ratios of a node in ring R_2 at $\beta = 0.8$ and $\beta = 1$ for a wide range combinations of t and u values. Figure 3.12 plots the results at link loss rates 30%, 50% and 80%. As seen from these figures, the success ratio at $\beta = 0.8$ is almost always higher than that at $\beta = 1$ and the improvement is more substantial when $t \ll u$, i.e., the node in ring R_2 has much smaller number of parents than the number of neighbors that the nodes in ring R_1 have. The results in Figures 3.11 and 3.12 show that the enhanced relay scheme with $\beta = 0.8$ almost always improves the expected success ratio of the nodes in ring R_2 compared to the original relay scheme over wide ranges of node density and link loss rate.

We remark that the success ratios of sensor nodes in different rings are inter-related because the nodes of inner rings relay the data acquired by the nodes of outer rings in data collection. Since the enhanced relay scheme improves the success ratios of the nodes in rings R_1 and R_2, it is expected to improve the success ratios of the nodes in other outer rings as well. This shall be verified by the experimental results in Section 3.4.3.

3.4 Performance evaluation

3.4.1 Experimental setup

Simulation experiments were conducted to evaluate our proposed techniques for enhancing the robustness of sensor data collection through the rings overlay. We implemented the proposed techniques using the Prowler simulator [IfSIS, SVML03]. Prowler is a generic wireless sensor network simulator targeted at the Berkeley MICA motes running TinyOS [HSW+00]. Its MAC layer consists of a simple Carrier Sense Multiple Access (CSMA) protocol. In this protocol, a node that has a packet to transmit waits for a random period before polling the channel. If the channel is found idle, the node transmits the packet. If the channel is found busy, the node waits for a random back-off interval before polling the channel again. Communication among sensor nodes in the construction process of rings overlays as well as in the data collection process is carried out using the default CSMA protocol in Prowler.

The radio propagation model in Prowler incorporates the signal attenuation, the fading effect and the time-varying nature of the signal strength. In particular, the received signal strength at a receiving node is calculated by the following probabilistic function:

$$P_{rx}(d) = \frac{P_{tx}}{1 + d^{\eta}}(1 + \alpha(d))(1 + \lambda(t)),$$

where P_{tx} is the transmitting power of a transmitter, d is the distance from the transmitter to the receiving node, η is the attenuation parameter, $\alpha(d)$ and $\lambda(t)$ are random variables of normal distributions $N(0, \sigma_\alpha)$ and $N(0, \sigma_\lambda)$, respectively. We use the default settings in the Prowler simulator for these parameters: $P_{tx} = 1.0$, $\eta = 2.2$, $\sigma_\alpha = 0.45$, $\sigma_\lambda = 0.02$.

When a node receives a signal from a transmitter, the signal strength from all other transmitters in the network is used to evaluate the signal to interference and noise ratio (SINR) at the receiving node. SINR indicates how obtrusive the noise and interference are. In the Prowler simulator, a transmission is receivable

if the SINR is above a default threshold value of 2.0. Under the above model, the transmission range of sensor nodes is about 30 m. The successful bit reception rate is calculated based on the SINR using the analytical model for MICA motes in [ZK04]. Specifically, the bit reception rate is given by:

$$1 - \frac{1}{2} e^{-\frac{\gamma}{2}\frac{1}{0.64}},$$

where γ is the SINR. The packet reception rate is then estimated based on the bit reception rate according to the model presented in [ZK04].

Both square sensing fields and rectangular sensing fields were employed in our experiments. Sensor nodes were deployed at random in the field and the base station was placed at the center of the field. In the default settings, 400 sensor nodes were deployed in a square field of 150 m $\times$ 150 m or in a rectangular field of 75 m $\times$ 300 m. Besides the default settings, we also vary the sensing field size and node density over wide ranges in Sections 3.4.4 and 3.4.5 respectively to investigate their impacts on our proposed approaches. In both overlay construction and data collection, message losses were randomly determined based on the packet reception rates calculated.

In overlay construction, we employed duplicate message transmission as described in Section 3.2.4 to cope with communication failures: each message was broadcast twice. We note that the number of message duplications in overlay construction can be adjusted by the users to adapt with different network conditions. For example, if the failure rate of communication links among sensor nodes is very high, the users can set the number of duplicate messages in overlay construction to larger values to ensure that sensor nodes are assigned to rings. On constructing the rings overlay, we simulated 1000 rounds of data collection. For simplicity, we assumed that the sizes of the aggregated data transmitted by sensor nodes to their parents in a round of data collection fit into one packet by means of digest-based representations [NGSA04, CLKB04]. The robustness of data collection was measured by the mean proportion of nodes whose acquired data reach the base station in a round of data collection. For each experimental setting, we plot the average results of 40 randomly generated node placements

Table 3.1: Simulation parameter settings.

Parameter	Value
Transmitting power level P_{tx}	1.0
Attenuation parameter η	2.2
Variance parameter σ_α	0.45
Variance parameter σ_λ	0.02
SINR threshold for reception	2.0
Energy consumption for transmitting one byte	0.025 mJ
Energy consumption for receiving one byte	0.019 mJ

and the 99% confidence interval of the results. We also compared the energy consumption of sensor nodes in data collection through different rings overlays. We focused on the energy consumption of transmitting and receiving data as the energy cost of computation at sensor nodes is insignificant compared to that of wireless communication [NGSA04]. The energy consumption was modeled according to power measurements of MICA motes reported in [PHC04]. Specifically, the energy consumed by a sensor node for transmitting and receiving one byte is 0.025mJ and 0.019mJ, respectively. Table 3.1 summarizes the parameter settings used in our experiments.

3.4.2 Performance of threshold-based approaches

Figure 3.13 shows the robustness of data collection resulting from different overlay construction approaches and different sensing fields. Here, Greedy represents the baseline greedy approach [NGSA04, CLKB04], GT(x) represents the global threshold-based approach setting a uniform threshold value x at all sensor nodes, and LT represents the localized threshold-based approach.

As seen from Figure 3.13(a), for a square sensing field of 150 m $\times$ 150 m, the greedy approach leads to robustness of only 63%. The robustness resulting from the global threshold-based approach increases rapidly with the threshold value up to 3 and the robustness reaches 93% at the threshold value of 3. Figure 3.13(b) shows similar performance trends for a rectangular sensing field of 75 m $\times$ 300 m. The robustness resulting from the greedy approach is merely 58%

while the robustness resulting from the global threshold-based approach increases with the threshold value up to 3 where the robustness reaches 92%. This shows the effectiveness of guiding overlay construction with a threshold on the number of parents for each node. The robustness of the global threshold-based approach gradually decreases with increasing threshold value beyond 3. This is because at a large threshold value T, sensor nodes are less likely to receive at least T messages with the same label from their neighbors during overlay construction. This reduces the chance for the nodes first receiving a label-i message to receive T label-i messages so as to be assigned to ring R_{i+1} immediately and broadcast label-$(i+1)$ messages. So, it in turn reduces the number of label-$(i+1)$ messages that can be received by the nodes receiving less than T label-i messages. Therefore, the nodes first receiving label-i messages are less likely to be assigned to ring R_{i+2} and more likely to be assigned to ring R_{i+1} eventually. As a result, the threshold-based approach with large threshold values has less impact on the rings overlay constructed. Note that compared to the baseline greedy approach, the global threshold-based approach can only improve the robustness of data collection, irrespective of the threshold value used.

In addition to the aforementioned default packet loss model that is derived from the bit reception rate, we also tested a simpler loss model that assigns the same loss probability to every receivable transmission. Similar performance trends are also observed from Figures 3.14(a) and 3.14(b) under the simple loss model with different loss probabilities. The global threshold-based approach is able to substantially improve the robustness of data collection over the baseline greedy approach. Based on the analysis in Sections 3.2.3 and 3.2.4, the analytical threshold value is $\frac{2}{3}r^2\rho$ scaled by the expected probability p that a node successfully receives at least one of the duplicate messages broadcast by a neighbor. Due to the irregularity nature of the radio propagation model in the Prowler simulator, the transmission range of sensor nodes is not a perfect circular disk and the packet reception rate may not be the same along all transmission directions. Figure 3.15 shows the mean packet reception rate as a function of transmission

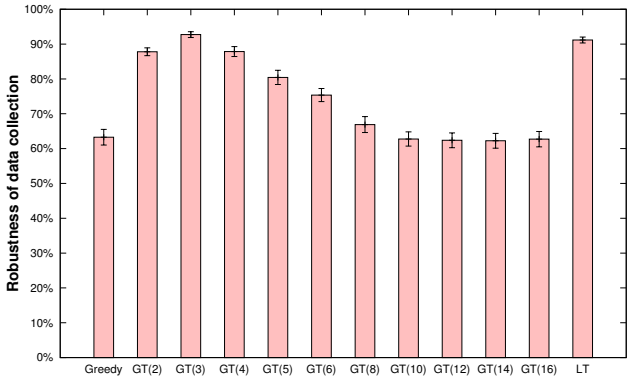

(a) Square sensing field

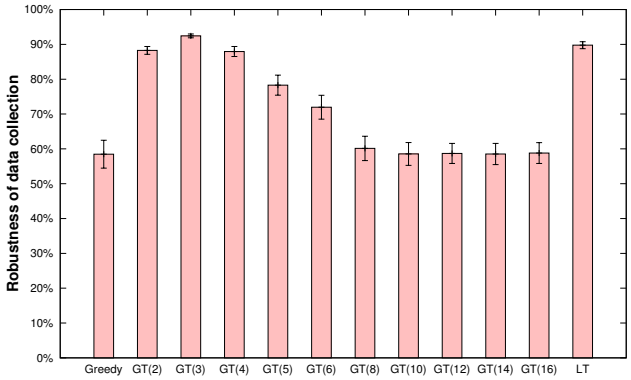

(b) Rectangular sensing field

Figure 3.13: Robustness of data collection for different overlay construction approaches under the default loss model. Error bars indicate the 99% confidence intervals of the results.

distance under the default packet loss model and the simple loss model following the radio propagation model in the Prowler simulator. As can be seen, the packet reception rate gradually reduces when the transmission distance increases. Based on the results shown in Figure 3.15, if a neighbor broadcasts a message twice, p can be approximated by $\sum_{i=1}^{30}(1-l_i^2)\cdot\frac{\pi\cdot i^2-\pi\cdot(i-1)^2}{\pi\cdot 30^2}$, where l_i is the mean loss rate at transmission distance i meters. Under the default loss model, p is 0.29. Under the simple loss model with loss probabilities 30%, 50% and 80%, p are 0.40, 0.32 and 0.14, respectively. Therefore, the analytical threshold value is about $\frac{2}{3}r^2\rho\cdot 0.29 \approx 3.1$ under the default loss model, and the analytical threshold values are $4.3, 3.4$, and 1.6 under the simple loss model with loss probabilities $30\%, 50\%$ and 80% respectively. They are very close to the experimental optimal

threshold values shown in Figures 3.13 and 3.14. This validates our analysis of threshold setting.

Figures 3.13 and 3.14 also show that the localized threshold-based approach outperforms the baseline greedy approach significantly. The robustness of the localized threshold-based approach is close to the highest achievable robustness of the global threshold-based approach. It demonstrates that the localized threshold-based approach is effective in setting threshold values in a distributed manner without a prior knowledge of node density and link loss rate.

To examine the impact of overlay construction on the accuracy of data collected at the base station, we implemented two types of synopsis representation to summarize sensor data in in-network aggregation for collecting COUNT and SUM aggregates at the base station [NGSA04]. Each synopsis representation consists of twenty 32-bit synopses which takes around 14 bytes after compression [NGSA04]. In our experiments, the default message payload size was set at 29 bytes following that in TinyOS [LLH02]. Thus, the synopsis representation fits into one message. The data acquired by the sensor nodes were randomly assigned from a uniform distribution between 1 and 100. For each round of data collection, let A be the aggregate computed from the synopsis representation received at the base station and E be the exact aggregate computed using raw sensor data acquired by all nodes. Then, the relative error is given by $e = \frac{|A-E|}{E}$. To measure the accuracy of data collection, we computed the mean and root mean square (RMS) of the relative errors over the 1000 rounds of data collection simulated.

Table 3.2 shows the accuracy of different data collection approaches for the default square sensing field of 150 m $\times$ 150 m under the default loss model. As can be seen, the threshold-based approaches are able to reduce mean and RMS errors of data collection by about half compared to the baseline greedy approach. In addition, we also computed the approximation error of synopsis representation, which refers to the relative error of the aggregate computed from the synopsis representation that incorporates raw sensor data acquired by all nodes. Approximation error represents a lower bound on the error of synopsis-based data collection (i.e., the relative error in the absence of communication failures). Table

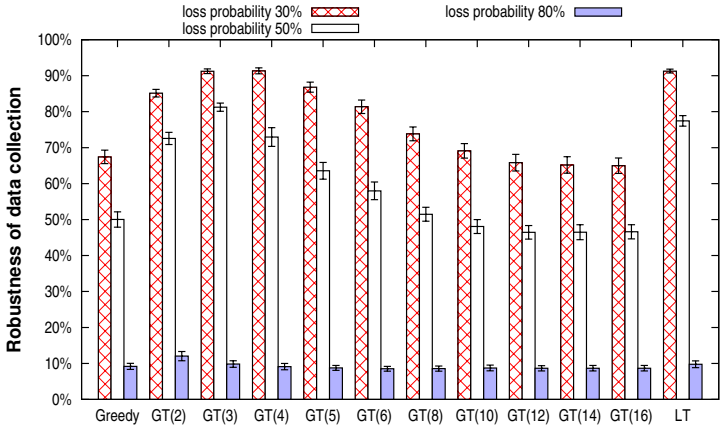

(a) Square sensing field

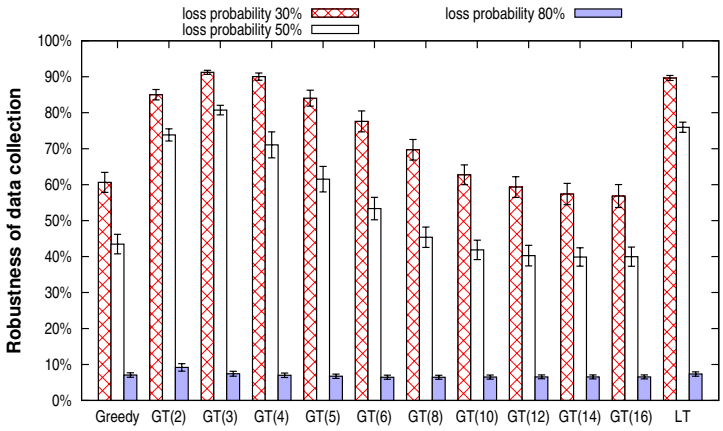

(b) Rectangular sensing field

Figure 3.14: Robustness of data collection for different overlay construction approaches under the simple loss model. Error bars indicate the 99% confidence intervals of the results.

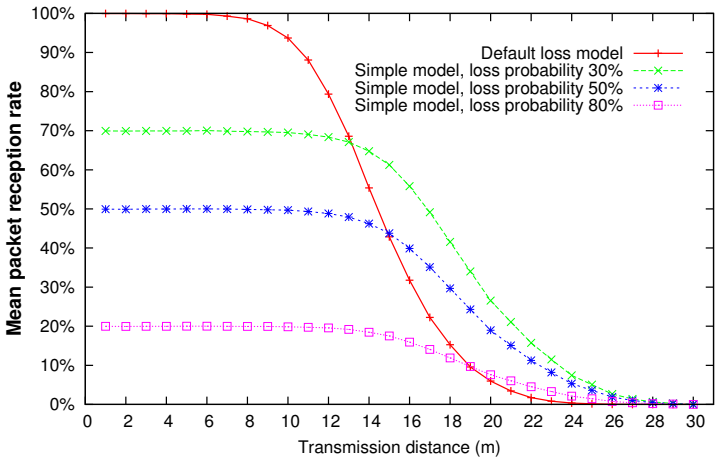

Figure 3.15: Mean packet reception rate under the default loss model and the simple loss model.

Table 3.2: Accuracy of data collection through rings overlays in the default square sensing field.

		Mean Error		RMS Error	
Approach	Robustness	COUNT	SUM	COUNT	SUM
Greedy	63%	0.362	0.335	0.383	0.359
LT	91%	0.151	0.140	0.182	0.175
GT(3)[3]	93%	0.146	0.139	0.178	0.174
Approximation error of synopsis representation	100%	0.141	0.138	0.171	0.169

3.2 shows that the relative errors resulting from the threshold-based approaches are very close to the lower bound. Similar performance trends also are observed from the results for the default rectangular sensing field as shown in Table 3.3.

Table 3.4 shows the 95th percentile of the child numbers of sensor nodes in different rings overlays for the default square sensing field. As explained in Section 3.2.2, the largest child numbers of sensor nodes resulting from the threshold-based construction approaches tend to be smaller than those of the greedy construction approach. Note that each node transmits data only once in a round of data collection, irrespective of the rings overlay structure. Therefore, as shown in Table 3.4, the threshold-based approaches reduce the total transmitting and receiving

[3]As presented earlier, 3 is the analytical threshold value of the global threshold-based approach for this experimental setting.

Table 3.3: Accuracy of data collection through rings overlays in the default rectangular sensing field.

		Mean Error		RMS Error	
Approach	Robustness	COUNT	SUM	COUNT	SUM
Greedy	58%	0.413	0.387	0.431	0.409
LT	90%	0.166	0.152	0.198	0.184
GT(3)	92%	0.146	0.138	0.177	0.174
Approximation error of synopsis representation	100%	0.141	0.138	0.171	0.169

Table 3.4: Energy consumption of data collection through rings overlays in the default square sensing field.

Approach	95th percentile of the child numbers of sensor nodes	Total transmitting and receiving energy consumption of the node with the 95th percentile child number per round of data collection (mJ)
Greedy	16.5	18.96
GT(3)	14.0	16.30
LT	13.0	15.23

energy consumption of the nodes with largest child numbers in data collection. The performance trends for the default rectangular sensing field are similar as shown in Table 3.5.

3.4.3 Performance of relay enhancement for data collection

To investigate the performance of relay enhancement, we varied its algorithm parameter β from 0 to 1 in the experiments. Figures 3.16(a) and 3.16(b) show the performance results for applying relay enhancement to rings overlays constructed by the global threshold-based approach (with the analytical threshold value) and the localized threshold-based approach in the default square sensing field, respectively. In these figures, the mean success ratios of the nodes in ring R_1, ring R_2 and other outer rings are plotted separately. The success ratio of each node was measured by the proportion of rounds in which the local data acquired by the

Table 3.5: Energy consumption of data collection through rings overlays in the default rectangular sensing field.

Approach	95th percentile of the child numbers of sensor nodes	Total transmitting and receiving energy consumption of the node with the 95th percentile child number per round of data collection (mJ)
Greedy	15.6	17.99
GT(3)	13.4	15.66
LT	12.5	14.7

node were successfully delivered to the base station among the 1000 rounds of data collection simulated. We report in Figure 3.16 only the experimental results for the default square sensing field as the performance trends for the rectangular sensing field are similar.

When $\beta = 1$, the enhanced relay scheme degenerates to the original relay scheme in which the nodes in ring R_1 do not benefit from multi-path routing. Thus, the success ratios of the nodes in ring R_1 are limited. As seen from Figures 3.16(a) and 3.16(b), when β decreases from 1 to 0.8, the mean success ratio of the nodes in ring R_1 improves substantially from about 72% to over 86%. When β continues to decrease below 0.7, the mean success ratio gradually decreases with β. When $\beta = 0$, again, none of the nodes in ring R_1 benefits from multi-path routing. Therefore, the success ratios of the nodes in ring R_1 are the same at $\beta = 0$ and $\beta = 1$.

For the nodes in ring R_2, their mean success ratio improves slightly when β decreases from 1 to 0.8. When β is below 0.8, the mean success ratio gradually decreases with β. When $\beta = 0$, none of the nodes in ring R_1 listen to the transmissions of the nodes in ring R_2. Thus, the success ratios of the nodes in ring R_2 and hence any outer ring further away from the base station become 0. Figures 3.16(a) and 3.16(b) also show that the success ratios of the nodes in rings other than R_1 and R_2 are hardly affected by β value unless β is small (below 0.4). This is because these nodes normally have multiple ancestors in ring R_2, so they are not significantly affected by the enhanced relay scheme.

The performance results shown in Figures 3.16(a) and 3.16(b) verify that the

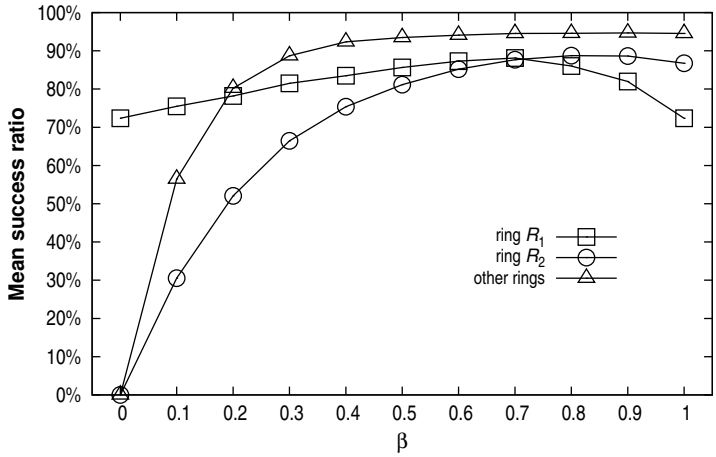

(a) Global threshold-based approach GT(3)

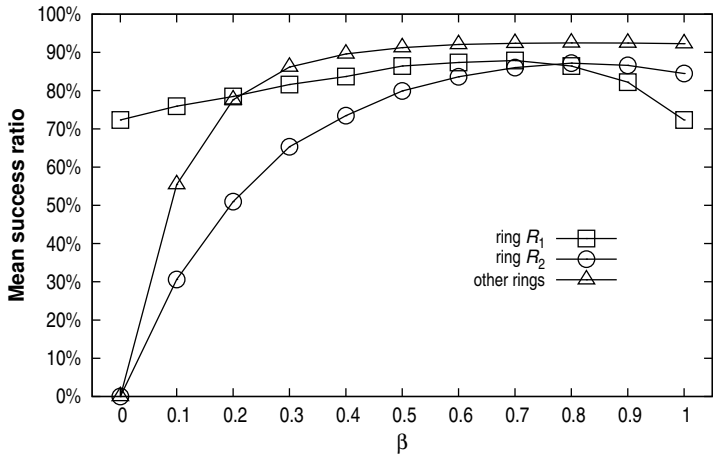

(b) Localized threshold-based approach LT

Figure 3.16: Performance of relay enhancement with different β values on the rings overlays constructed by the threshold-based approaches in the default square sensing field.

Table 3.6: Performance of relay enhancement with $\beta = 0.8$.

Approach	Robustness	Standard deviation of success ratios
GT(3)	93%	0.17
GT(3) + Relay Enhancement	94%	0.15
LT	91%	0.20
LT + Relay Enhancement	92%	0.18

Table 3.7: Energy consumption in relay enhancement with $\beta = 0.8$.

Approach	Mean number of transmissions that R_1 nodes listens to	Total transmitting and receiving energy consumption per R_1 node per round of data collection (mJ)
GT(3)	10.2	12.57
GT(3) + Relay Enhancement	10.1	12.46
LT	10.2	12.57
LT + Relay Enhancement	10.1	12.46

enhanced relay scheme with $\beta = 0.8$ improves the success ratios of the nodes in rings R_1 and R_2. Such improvement allows the data acquired by these nodes to have much fairer chances to contribute to the aggregates collected by the base station compared to the data acquired by other nodes. Table 3.6 summarizes the robustness of data collection and the standard deviation of the success ratios of individual sensor nodes for different approaches. It can be seen that relay enhancement not only improves the robustness of data collection, but also reduces the standard deviation of nodes' success ratios. Table 3.7 shows the mean number of transmissions that a node in ring R_1 listens to in the original and enhanced relay schemes. As can be seen, the number remains similar in the two relay schemes. Note that in the enhanced relay scheme, each node in ring R_1 still transmits data only once in a round of data collection. Thus, the enhanced relay scheme keeps the energy consumption of the nodes in ring R_1 for transmitting and receiving data in data collection similar to that in the original relay scheme.

3.4.4 Impact of network size

To examine the impact of network size, we kept the average node density at 4/225 node per square meter and varied the sensing field size. Square sensing field size was increased from 50 m × 50 m to 500 m × 500 m, and rectangular sensing field size was increased from 75 m × 100 m to 75 m × 1900 m. We evaluated the robustness of data collection through rings overlays constructed by the baseline greedy approach, the global threshold-based approach (with

the analytical threshold value), the localized threshold-based approach, and the threshold-based approaches integrated with relay enhancement. In addition, two tree-based approaches are also included for comparison: the standard TAG approach [MFHH02] that uses tree-based routing structures, and a modified TAG approach (called TAG4) that repeatedly transmits each message four times in data collection to improve robustness. Figures 3.17(a) and 3.17(b) show the performance results of different data collection approaches in different sensing fields.

As seen from Figure 3.17(a), in a sensing field of 50 m $\times$ 50 m, most nodes are within two hops from the base station, so the threshold-based approaches perform similarly to the greedy approach. When the size of the sensing field increases, the robustness resulting from the greedy construction approach decreases steadily. This indicates that in larger networks, the greedy construction approach leads to a higher proportion of sensor nodes having few propagation paths to the base station. In contrast, the robustness resulting from the threshold-based construction approaches remain quite stable with increasing size of sensing field. This implies that even sensor nodes far away from the base station in large networks have sufficient numbers of propagation paths to the base station when the threshold-based construction approaches are used. Therefore, the threshold-based approaches substantially outperform the greedy approach in term of robustness. Moreover, the proposed relay enhancement further improves the robustness of data collection through rings overlays constructed by the threshold-based approaches. The improvement is generally more significant for smaller networks in which a higher proportion of sensor nodes are in ring R_1. Figure 3.17(b) shows that when the rectangular sensing field stretches from 75 m $\times$ 100 m to 75 m $\times$ 1900 m, the robustness resulting from the threshold-based approaches is quite stable, but the robustness resulting from the greedy approach decreases rapidly. Similar to the performance trends observed in Figure 3.17(a), the threshold-based approaches consistently outperform the greedy construction approach over different network sizes.

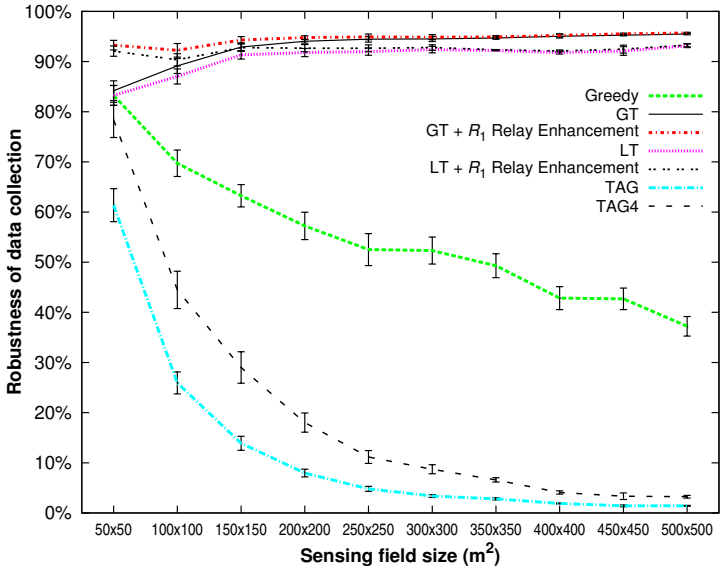

(a) Square sensing fields

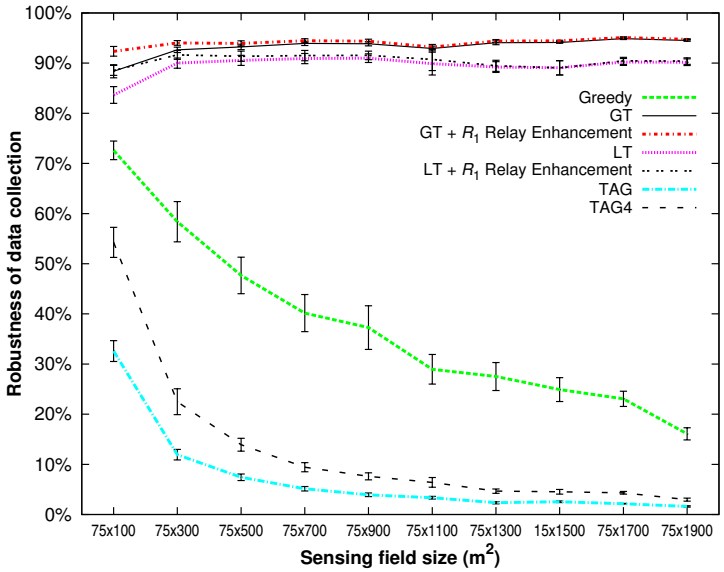

(b) Rectangular sensing fields

Figure 3.17: Robustness of data collection for different sizes of sensing field. Error bars indicate the 99% confidence intervals of the results.

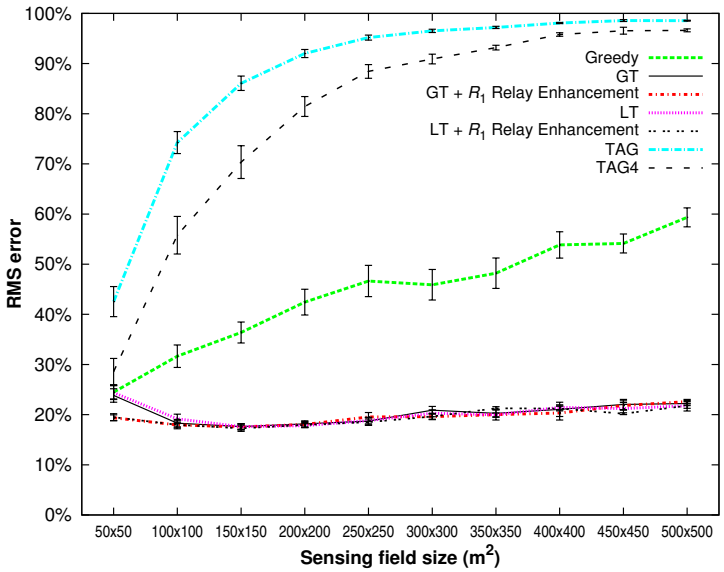

(a) Square sensing fields

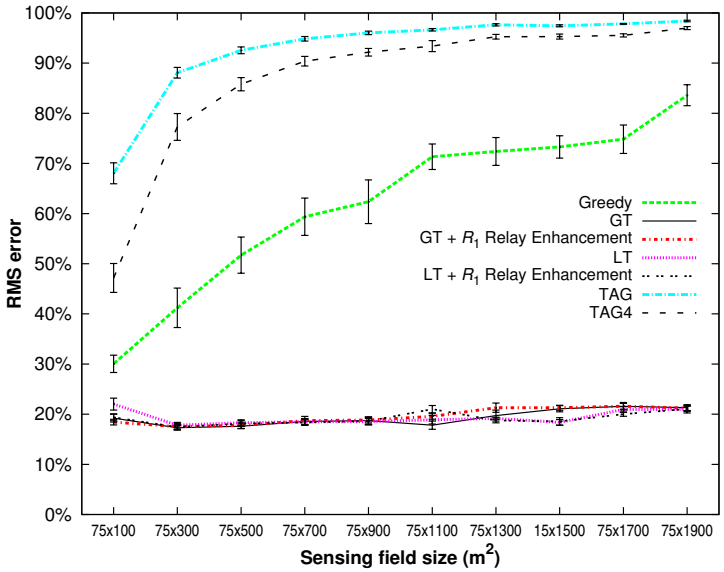

(b) Rectangular sensing fields

Figure 3.18: RMS errors of collecting SUM aggregates for different sizes of sensing field. Error bars indicate the 99% confidence intervals of the results.

The standard TAG approach is the least robust against communication failures among all approaches tested. This is because in tree-based routing structures, each transmission failure drops the data acquired by sensor nodes in an entire subtree. As a result, only a small fraction of sensor data reach the base station. The robustness of TAG decreases rapidly with increasing size of sensing field. The TAG4 approach considerably improves the robustness of data collection over TAG, but it is still far worse than any approach that uses rings overlays except for very small networks in which the routing tree has just few levels. Note that the improved robustness of TAG4 is achieved at the cost of letting all sensor nodes repeat their transmissions by four times.

Figure 3.18(a) shows the RMS errors of collecting SUM aggregates for different data collection approaches in square sensing fields. Following the performance trends of robustness, the RMS errors of data collection through rings overlays are almost always significantly lower than those of tree-based data collection. Among all approaches tested, threshold-based overlay construction integrated with relay enhancement produces the best accuracy of data collection throughout a wide range of network size. Similar performance trends are also observed in Figure 3.18(b) for rectangular sensing fields.

3.4.5 Impact of node density

To examine the impact of node density, we varied the number of nodes in the network from 200 to 900 while keeping the square sensing field at 150 m $\times$ 150 m and the rectangular sensing field at 75 m $\times$ 300 m. Figures 3.19(a) and 3.19(b) show the performance results of different data collection approaches in different sensing fields.

As expected, the robustness of data collection through rings overlays increases with node density due to increasing number of propagation paths in the rings overlay. When the network is sparse, the robustness improves rapidly with more nodes deployed. When the network becomes sufficiently dense, most nodes have many propagation paths to the base station. Thus, further increasing node density does not improve the robustness of data collection significantly. Both Figures

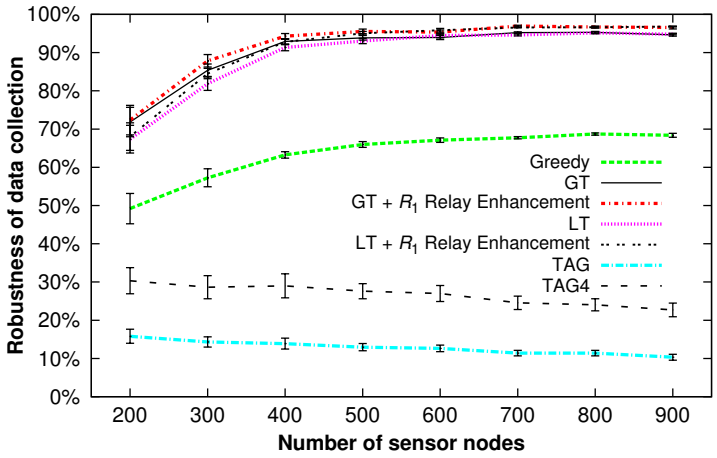

(a) Square sensing field

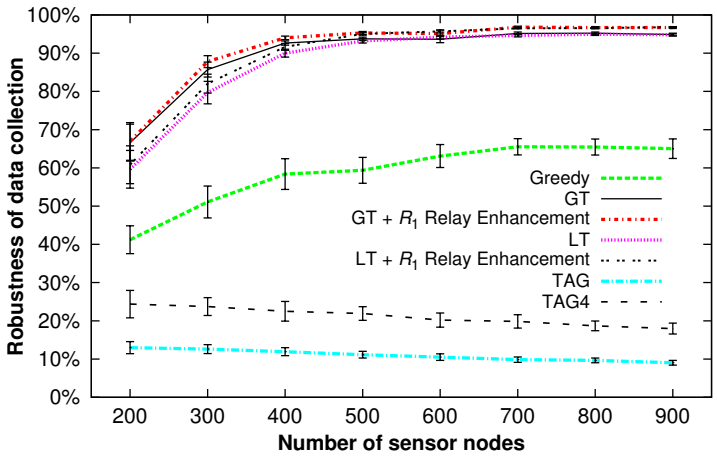

(b) Rectangular sensing field

Figure 3.19: Robustness of data collection for different node densities. Error bars indicate the 99% confidence intervals of the results.

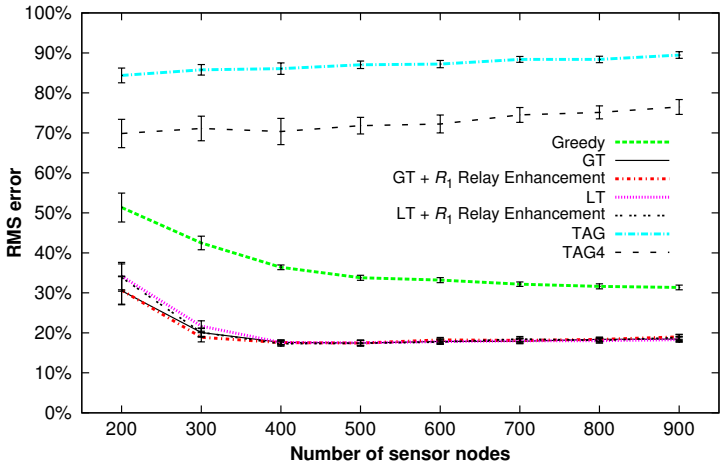

(a) Square sensing field

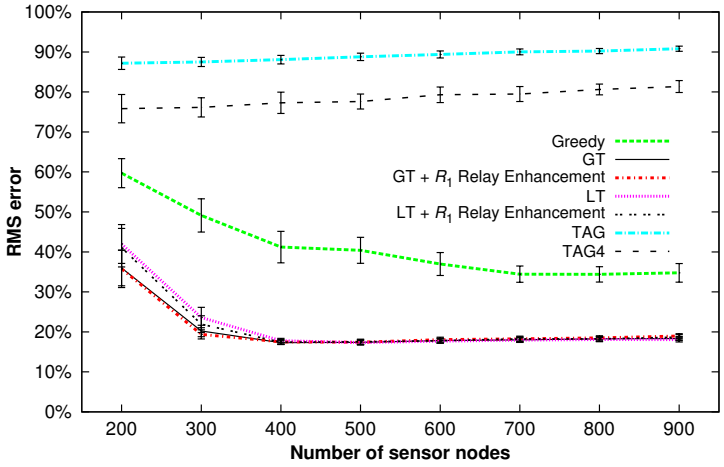

(b) Rectangular sensing field

Figure 3.20: RMS errors of collecting SUM aggregates for different node densities. Error bars indicate the 99% confidence intervals of the results.

3.19(a) and 3.19(b) show that the threshold-based approaches lead to substantially higher robustness of data collection than the baseline greedy approach even if the network is very dense. The proposed relay enhancement further improves the robustness on top of the threshold-based approaches. The robustness of tree-based approaches, on the other hand, is mainly determined by the height of the routing tree. Given the size of sensing field, the tree height is largely independent of node density. As a result, TAG and TAG4 are not able to take advantage of higher node density to improve the robustness of data collection.

Figures 3.20(a) and 3.20(b) show the RMS errors of collecting SUM aggregates for different data collection approaches. The performance trends of RMS error are consistent with those of robustness. Rings overlays result in much more accurate data collection than tree-based routing structures. Threshold-based approaches for overlay construction greatly reduce the RMS errors of data collection compared to the baseline greedy approach over a wide range of node density.

3.5 Summary

In this chapter, we have presented two new techniques for improving the robustness of sensor data collection through the rings overlay: a distributed approach for constructing the rings overlay, and an enhanced relay scheme for data collection. The proposed construction approach is guided by a threshold on the number of parents for each node in order to prevent sensor nodes from having few propagation paths to the base station in the rings overlay. We have analyzed the threshold setting and developed a localized method for sensor nodes to calculate their threshold values based on local neighborhood information. The enhanced relay scheme allows the sensor nodes in the ring next to the base station to benefit from multi-path routing without requiring these sensor nodes to repeat their data transmissions. Experimental results show that the proposed approach for overlay construction and the enhanced relay scheme significantly improve the robustness and accuracy of sensor data collection through the rings overlay.

Chapter 4

Efficient data collection scheduling

In Chapter 3, we have focused on improving the robustness of data collection in wireless sensor networks by exploiting the broadcast nature of wireless communication to transport sensor data through multiple propagation paths toward the base station. Besides the robustness against communication failures, both energy efficiency and time efficiency are also of primary importance in sensor data collection due to the limited energy supplies of sensor nodes and the real-time nature of sensor network applications. As discussed in Chapter 2, the energy efficiency and time efficiency of sensor data collection are heavily dependent on MAC layer protocols used to carry out wireless communication among sensor nodes. Contention-based MAC protocols for coordinating communication among sensor nodes often introduce significant amounts of energy cost and time latency due to control messages, idle listening and back off periods [DEA06]. In contrast, contention-free time division multiple access (TDMA) protocols have the potential to reduce the energy consumption and the latency of sensor data collection since communication among sensor nodes can proceed in synchronous time slots without contention, collisions or idle listening [GDP05, MLW+09].

To collect sensor data using a TDMA protocol, sensor nodes need to be assigned appropriate time slots for transmitting and receiving data prior to the data collection process. Recently, there have been several studies on TDMA scheduling

for sensor data collection through single-path routing structures [YLL09,LGP10]. Nevertheless, as discussed in Chapter 3, single-path routing structures are highly susceptible to communication failures since a failure would result in the loss of data acquired by sensor nodes in an entire subtree. Little work has studied TDMA scheduling for sensor data collection through multi-path routing structures.

In this chapter, we design a distributed scheduling algorithm for constructing TDMA schedules for sensor data collection through multi-path routing structures. The objective of our scheduling algorithm is to reduce both the message complexity and running time of the scheduling process as much as possible. Experimental results confirm that our proposed algorithm significantly reduces the number of messages transmitted during the scheduling process and the running time compared to existing scheduling algorithms. Our proposed scheduling algorithm is generic and is applicable to any single-path and multi-path routing structures. In addition, we develop a method for deriving a lower bound on the shortest possible latency of data collection through a given routing structure. The lower bound latency estimation offers a practical method to evaluate the efficiency of data collection schedules produced by scheduling algorithms.

The remainder of this chapter is organized as follows. Section 4.1 introduces some preliminaries on collecting sensor data through multi-path routing structures and the requirements of a valid schedule for data collection. Our distributed scheduling algorithm for data collection is described in Section 4.2 and the lower bound latency analysis is presented in Section 4.3. Experimental evaluation is described in Section 4.4. Finally, Section 4.5 summarizes the chapter.

4.1 Preliminaries

As in Chapter 3, we consider a wireless sensor network consisting of a set of sensor nodes and a base station. The sensor nodes periodically sample local phenomena such as temperature and humidity, and report their acquired data to the base station through a multi-path routing structure using a TDMA MAC protocol. Conceptually, the multi-path routing structure is a directed acyclic

graph rooted at the base station, in which each node has multiple *parents* and multiple *children*, and each edge represents a communication link from one child node to one parent node. The nodes within the communication range of a sensor node, including its parents and its children, are called the *neighbors* of the node. For ease of presentation, we shall refer to the nodes within the communication range of a sensor node that are neither its parents nor its children as the *plain neighbors* of the node.

We assume that in each round of data collection, the aggregated result of the data acquired by all sensor nodes is to be collected at the base station as in Chapter 3. To do so, each node first receives data from all of its children and aggregates the received data with its own locally acquired data. After that, the node transmits the aggregated data to all of its parents by broadcast. This propagation and aggregation process starts from the nodes with no children in the multi-path routing structure and proceeds until the base station receives data from all of its children. As described in Chapter 3, digest-based representations of aggregated data [CLKB04, NGSA04] can be used to compactly summarize sensor data during in-network aggregation and let the aggregated data maintain constant and small size as they are propagated toward the base station. Thus, we assume that the sizes of the messages transmitted by all sensor nodes to their parents are the same, irrespective of the routing structure.

During the data collection process with TDMA, time is divided into slots and the duration of a time slot allows a sensor node to transmit exactly one message to its parents by broadcast. To construct a TDMA schedule for data collection, each sensor node needs to be assigned with one time slot for transmitting its aggregated data to its parents and a set of time slots for receiving data from its children. The length of a schedule indicates the *latency of data collection*.

Due to interference, each sensor node can only successfully receive a message without collisions if there is exactly one node within its communication range performing data transmission at a time [WLX06, GDP05, GZH06, YLL09, LGP10]. If transmission slots are assigned to sensor nodes such that parent nodes can

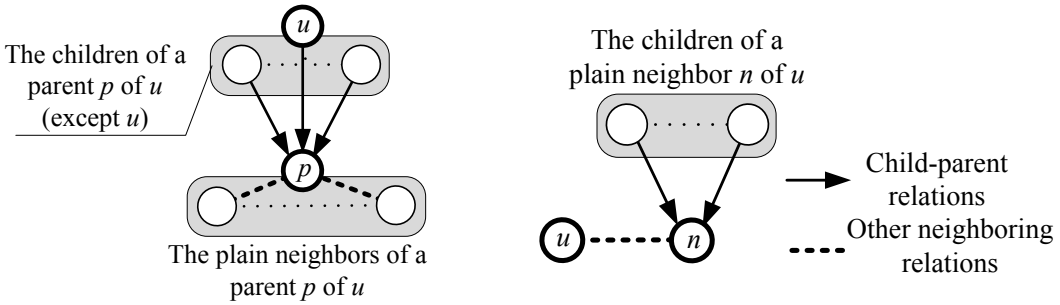

(a) Node u conflicts with all the children and plain neighbors of its parent p.

(b) Node u conflicts with all the children of its plain neighbor n.

Figure 4.1: Conflicting nodes of a node u.

receive data from all of their children without collisions, then the corresponding data collection schedule is considered as a *valid* schedule. In a multi-path routing structure, two sensor nodes are called *conflicting* with each other if any parent of either node is within the communication range of the other so that their transmissions would collide at that parent. Specifically, for each sensor node, all the children and plain neighbors of its parents conflict with the node due to collisions at the node's parents (see Figure 4.1(a)). In addition, all the children of a node's plain neighbors conflict with the node due to collisions at these plain neighbors (see Figure 4.1(b)). Thus, a node's *conflicting set* includes all children and all plain neighbors of the node's parents, and all children of the node's plain neighbors. In a valid data collection schedule, each node must be assigned a transmission slot different from those of all nodes in its conflicting set. In addition, to allow for in-network data aggregation, the transmission slot of each node must be scheduled after the transmission slots of all of its children.

4.2 Constructing data collection schedules

In this section, we present a distributed algorithm to efficiently construct a valid schedule for data collection through a multi-path routing structure. In our algorithm, each sensor node selects its own transmission slot in a distributed manner. For ease of presentation, we shall refer to sensor nodes that have selected their

transmission slots as *scheduled nodes* and those that are yet to select their transmission slots as *unscheduled nodes*. When a node selects its transmission slot, we say that the node *makes its schedule*. A sensor node is ready to make its schedule when it knows the transmission slots of all of its children. Thus, parent nodes always make their schedules after their children do. This is to ensure that each parent node will select a transmission time slot later than those of all of its children in order to facilitate in-network aggregation.

In our algorithm, each node u maintains two sets of transmission slots of other nodes: $\mathcal{R}(u)$ records the transmission slots of its children; and $\mathcal{L}(u)$ records the transmission slots of other nodes conflicting with it. Upon learning the transmission slots of all of its children in $\mathcal{R}(u)$, node u employs a simple greedy strategy to select its transmission slot $\mathcal{S}[u]$ as the earliest time slot that is later than all the slots in $\mathcal{R}(u)$ and different from all the slots in $\mathcal{L}(u)$. After node u makes its schedule, all of its parents and other nodes conflicting with u are informed of u's transmission slot $\mathcal{S}[u]$.

It is important to remark that the above greedy slot assignment strategy only guarantees that when a sensor node u makes its schedule, its selected transmission slot $\mathcal{S}[u]$ is different from all transmission slots recorded in $\mathcal{L}(u)$ at that time. This does not necessarily guarantee that at the end of the scheduling process, $\mathcal{S}[u]$ is different from the transmission slots of all the nodes conflicting with u. In fact, if two nodes conflicting with each other make their schedules at the same time, they may not know the slot assignment of each other immediately due to the latency of message exchange between them. As a result, they may select the same time slot for their transmissions which would cause collisions in data collection. Therefore, to guarantee that the produced schedule is valid, when a sensor node is choosing its transmission slot, it is imperative to prevent all the nodes conflicting with it from selecting their transmission slots concurrently.

4.2.1 Related work

Most of the existing TDMA scheduling algorithms are centralized and sequential in nature [WLX06, HCB00, CHZ05, HWV+07, WSW+09]. To assure that conflicting nodes do not make their schedules concurrently, a distributed coordination scheme among conflicting nodes has been presented in [YLL09]. In this scheme, when a sensor node is ready to make its schedule, it asks for permissions from all the unscheduled nodes conflicting with it by sending requests to them and waiting for their responses. The responses can be either permissions or denials. If the node receives denial responses from some unscheduled nodes conflicting with it, it has to wait until these nodes have made their schedules and then it asks for permissions from the rest of the unscheduled conflicting nodes again. A sensor node completes the above coordination process and makes its schedule only when it receives permissions from all the unscheduled nodes conflicting with it. As a result, this coordination scheme may incur significant overheads for the communication between conflicting nodes. In contrast to the above coordination scheme, we propose to resolve the relative scheduling order among conflicting nodes prior to the scheduling process so that conflicting nodes do not need to compete with each other when making their schedules. With a predetermined scheduling order, sensor nodes simply wait for their turns to make their schedules and then inform their conflicting nodes about their transmission slots. In the following, Section 4.2.2 elaborates how to resolve the scheduling order for sensor nodes, and Section 4.2.3 presents our distributed scheduling algorithm.

4.2.2 Scheduling order for sensor nodes

We determine the scheduling order of sensor nodes by exploiting the topology of the routing structure. Since the routing structure is a directed acyclic graph, every sensor node has a number of cycle-free data propagation paths to the base station. Each of these data propagation paths has a finite hop-length. We define the maximum hop-length of all data propagation paths of a sensor node as its *rank*. It is obvious that the rank of a node is always lower than the ranks of all

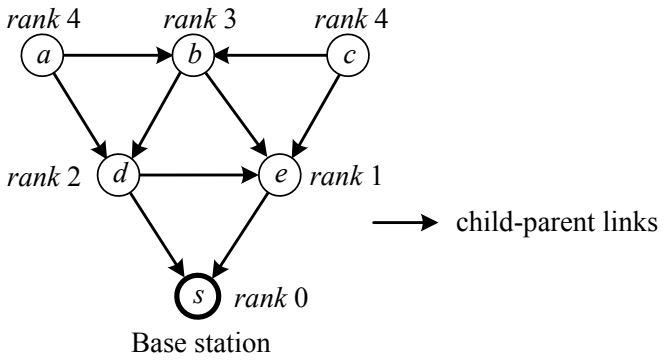

Figure 4.2: The ranks of sensor nodes in a sample multi-path routing structure.

of its children by at least 1. In our scheduling order, we let the nodes having higher ranks to make their schedules before the nodes having lower ranks so as to ensure that child nodes make their schedules before their parents do. This also resolves the scheduling order of conflicting nodes having different ranks. The scheduling order of conflicting nodes having the same ranks is resolved by their identifiers. The nodes with greater identifiers are to make their schedules before their conflicting nodes having smaller identifiers.

The ranks of sensor nodes are computed in a distributed manner as follows. First, the base station sets its rank to 0 and broadcasts a rank message containing its rank and its identifier to all the nodes within its communication range. When a sensor node has received all of its parents' ranks, it picks the maximum rank m received from its parents and sets its rank to $m + 1$. Then, the node broadcasts a rank message containing its rank and its identifier to all the nodes within its communication range.

Figure 4.2 shows an example multi-path routing structure and the ranks of sensor nodes computed using the above method. In this figure, solid arrows represent the communication links from children to parents in the routing structure. In this example, node e has only one parent that is the base station s at rank 0, so e is assigned rank 1. Node d has two parents including the base station s at rank 0 and node e at rank 1, so d is assigned rank 2. Similarly, node b has two parents including node e at rank 1 and node d at rank 2, so b is assigned rank 3. Node c has two parents e and b at ranks 1 and 3 respectively, so c is assigned rank 4. Node a has two parents d and b at ranks 2 and 3 respectively, so a is

assigned rank 4.

In addition to computing its rank, each sensor node u also needs to initialize a conflicting list $\mathcal{W}(u)$. The function of the conflicting list $\mathcal{W}(u)$ is to record the ranks and the identifiers of all unscheduled nodes conflicting with u so as to allow node u to determine its turn to make schedule in the scheduling process. Initially, $\mathcal{W}(u)$ should consist of all children and plain neighbors of u's parents and all children of u's plain neighbors. To initialize conflicting lists, when a parent node receives rank messages from its children, the parent node records their ranks and identifiers in its child list, and when a node receives rank messages from its plain neighbors, the node records their ranks and identifiers in its plain neighbor list. After a node gets the ranks of all of its children and plain neighbors, it broadcasts a message containing its own identifier, its child list and its plain neighbor list to all the nodes within its communication range. A node u initializes its conflicting list $\mathcal{W}(u)$ by combining the child lists received from its plain neighbors with the child lists and the plain neighbor lists received from its parents. When node u completes initializing its conflicting list $\mathcal{W}(u)$, it proceeds to execute the scheduling process as described in the next section.

4.2.3 Distributed scheduling algorithm

In the scheduling process, the nodes recorded in the conflicting list $\mathcal{W}(u)$ of each node u are gradually removed from the list when they have made their schedules. Each node u assigns its transmission slot when all of u's children have made their schedules and u has the highest rank compared to all nodes in $\mathcal{W}(u)$ and has the greatest identifier compared to all nodes in $\mathcal{W}(u)$ having the same rank as u. After a node u makes its schedule, its parents and the unscheduled nodes conflicting with it are informed of u's transmission slot through three types of messages: report-transmit (RT), interfere-through-parent (ITP) and interfere-through-neighbor (ITN). These messages have the form of $\langle t, s, u, \mathcal{S}[u] \rangle$ where t is the type of the message (t's value is either RT, ITP or ITN), s is the identifier of the message sender, u is node u's identifier, and $\mathcal{S}[u]$ is the transmission slot assigned to u. The RT message is sent by node u to its neighbors, ITP messages

are sent by u's parents to their children and plain neighbors, and ITN messages are sent by u's plain neighbors to their children.

After making its schedule, node u broadcasts a message $\langle \text{RT}, u, u, \mathcal{S}[u] \rangle$ to all the nodes within its communication range. When a parent p of u receives the message $\langle \text{RT}, u, u, \mathcal{S}[u] \rangle$, node p records $\mathcal{S}[u]$ as a transmission slot of its children in set $\mathcal{R}(p)$. Then, node p broadcasts a message $\langle \text{ITP}, p, u, \mathcal{S}[u] \rangle$ to all the nodes within its communication range. When a child or a plain neighbor v of p receives the message $\langle \text{ITP}, p, u, \mathcal{S}[u] \rangle$, node v records $\mathcal{S}[u]$ as a transmission slot of its conflicting nodes in set $\mathcal{L}(v)$ if node v has not yet made its schedule. Then, node v removes u from its conflicting list $\mathcal{W}(v)$ since node u has made its schedule. On the other hand, when an unscheduled plain neighbor w of u receives the message $\langle \text{RT}, u, u, \mathcal{S}[u] \rangle$, node w broadcasts a message $\langle \text{ITN}, w, u, \mathcal{S}[u] \rangle$ to all the nodes within its communication range. When a child node v of w receives the message $\langle \text{ITN}, w, u, \mathcal{S}[u] \rangle$, node v records $\mathcal{S}[u]$ as a transmission slot of its conflicting nodes in set $\mathcal{L}(v)$ if node v has not made its schedule. Then, node v removes u from its conflicting list $\mathcal{W}(v)$.

The pseudo code of our distributed scheduling algorithm is summarized in Algorithm 2. The correctness of our distributed scheduling algorithm is proved by the following theorem.

Theorem 1. *Algorithm 2 produces a valid TDMA schedule for data collection.*

Proof. First, we shall prove that all sensor nodes shall be scheduled following Algorithm 2. Assume on the contrary that there exist some nodes which are never scheduled. Among all these unscheduled nodes, there must be one or more nodes which have the highest rank. Let k be this highest rank. Since the ranks of child nodes are always greater than the ranks of their parents, the children of these unscheduled nodes with rank k must have been scheduled. Among these unscheduled nodes having rank k, let x be the node having the greatest identifier. Initially, $\mathcal{W}(x)$ contains all the nodes conflicting with node x. During the scheduling process, when other nodes conflicting with x makes their schedules, they are removed from $\mathcal{W}(x)$. Therefore, if x has the greatest identifier among all unscheduled nodes having rank k, x must also be the node having the greatest

Algorithm 2: Distributed scheduling algorithm executed at a sensor node u.

```
1  R(u), L(u) ← ∅;
2  while u has not made its schedule do
3      let msg be a message u receives;
4      switch msg do
5          case ⟨RT, v, v, S[v]⟩, where v is a child of u:
6              R(u) ← R(u) ∪ {S[v]};
7              broadcast a message ⟨ITP, u, v, S[v]⟩ to all nodes within u's
               communication range;
8          case ⟨RT, v, v, S[v]⟩, where v is a plain neighbor of u:
9              broadcast a message ⟨ITN, u, v, S[v]⟩ to all nodes within u's
               communication range;
10         case ⟨ITP, w, v, S[v]⟩, where w is a parent or plain neighbor of u:
11             L(u) ← L(u) ∪ {S[v]};
12             remove v from W(u);
13         case ⟨ITN, w, v, S[v]⟩, where w is a parent of u:
14             L(u) ← L(u) ∪ {S[v]};
15             remove v from W(u);
16     if all the children of u have made their schedules and u has the highest
       rank compared to all nodes in W(u) and u has the greatest identifier
       compared to all nodes in W(u) having the same rank as u then
17         if R(u) = ∅ then
18             S[u] ← 0;
19         else
20             S[u] ← max_{s∈R(u)} s + 1;
21         while L(u) contains a slot equal to S[u] do
22             S[u] ← S[u] + 1;
23         broadcast a message ⟨RT, u, u, S[u]⟩ to all nodes within u's
           communication range.
```

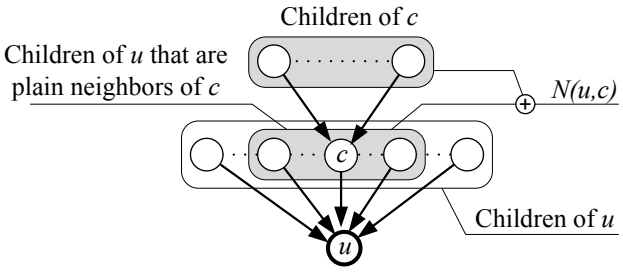

Figure 4.3: Analyzing the earliest possible transmission slot of node u.

identifier among the nodes having rank k in $\mathcal{W}(x)$. Thus, node x satisfies all the conditions in line 16 of Algorithm 2 and should proceed to make its schedule. This contradicts to the assumption that node x is never scheduled. Hence, it follows that all nodes shall be scheduled following Algorithm 2.

In addition, it is guaranteed that conflicting nodes never make their schedules at the same time due to the conditions in line 16 of Algorithm 2. As a result, when a node u selects its transmission slot as the earliest time slot that is later than the transmission slots of its children in set $\mathcal{R}(u)$ and different from the transmission slots of its conflicting nodes in set $\mathcal{L}(u)$ (lines 17 to 22 of Algorithm 2), it is guaranteed that there is no collision at u's parents. It follows that Algorithm 2 always produces valid schedules for data collection. □

In our proposed scheduling algorithm, we assume symmetric communication links among sensor nodes. Nevertheless, our scheduling algorithm would not suffer from asymmetric communication due to existing reliable transport protocols that are capable of overcoming the impact of asymmetric wireless communication links in sensor networks [LRC+08, TW07]. Using such transport protocols, our scheduling algorithm would still be able to produce collision-free data collection schedules even in the case that some communication links among sensor nodes are asymmetric.

4.3 Lower bound latency analysis

In this section, we present a method to estimate a lower bound on the shortest possible length of the data collection schedule that can be built for a given routing structure. Our estimation method calculates the earliest possible transmission slot of every sensor node based on its descendants that conflict with each other.

Consider a sensor node u and its descendants as shown in Figure 4.3. All the children of u conflict with each other. Thus, they must have different transmission slots in a valid data collection schedule. In addition, u's transmission slot must be later than all of its children's transmission slots. Let $c_1, c_2, \ldots, c_l$ be the list of u's children, where l is the number of u's children, and let $E(c_i)$ be the earliest possible transmission slot of c_i. Without loss of generality, assume that $E(c_1) \geq E(c_2) \geq \ldots \geq E(c_l)$. Let $E(u)$ be the earliest possible transmission slot of node u. Since the transmission slots of u's children are different from each other, $E(u)$ must be at least $\max\{E(c_1)+1, E(c_2)+2, \ldots, E(c_l)+l\}$.

The above estimation method can be extended to include some of u's grandchildren in the calculation as follows. Let c be a child of u. Denote by $N(u,c)$ the set of u's children which are also c's plain neighbors, plus c and all of c's children as shown in Figure 4.3. Note that every child of u that is also a plain neighbor of c conflicts with all of c's children. In addition, all of c's children conflict with each other. Therefore, all the nodes in $N(u,c)$ conflict with each other and must have different transmission slots in a valid data collection schedule. Since all of these nodes are u's descendants, their transmission slots must all be earlier than u's transmission slot. Thus, the earliest possible transmission slot of u can be derived from the earliest possible transmission slots of the nodes in $N(u,c)$ in a similar manner as described above.

We further generalize the estimation method to include other descendants of node u in estimating u's earliest possible transmission slot. Let $d_1, d_2, d_3, \ldots$ be the list of all u's descendants in descending order of their estimated earliest possible transmission slots, i.e., $E(d_1) \geq E(d_2) \geq E(d_3) \geq \ldots$. Starting from d_1, we scan all the descendants in the list to construct a subset $N(u)$ of u's descendants such that all nodes in $N(u)$ must have different transmission slots

Algorithm 3: Estimating a lower bound on the latency of data collection.

```
1  foreach node u do
2      if node u has no children in the routing structure then
3          E(u) ← 0;
4  while there exist some nodes v whose earliest possible transmission slots
     E(v) are not calculated do
5      pick a node u whose E(u) is not calculated but for every descendant
       node c of u, E(c) is already calculated;
6      let d_1, d_2, d_3, ... be the list of all u's descendants such that
       E(d_1) ≥ E(d_2) ≥ E(d_3) ≥ ...;
7      let N(u) ← {d_1};
8      foreach i > 1 do
9          if d_i conflicts with or is a descendant of all the existing nodes in
           N(u) then
10             N(u) ← N(u) ∪ {d_i};
11     let d_{i_1}, d_{i_2}, d_{i_3}, ..., d_{i_|N(u)|} be the list of nodes in the constructed set
       N(u) where i_1 ≤ i_2 ≤ i_3 ≤ ... ≤ i_|N(u)|;
12     E(u) ← max{E(d_{i_1}) + 1, E(d_{i_2}) + 2, ..., E(d_{i_|N(u)|}) + |N(u)|};
13 return E(s) where s is the base station;
```

from each other in a valid data collection schedule. Specifically, each node d_i ($i \geq 1$) is added to $N(u)$ if d_i conflicts with or is a descendant of all the existing nodes in $N(u)$. As a result, all the nodes in the constructed set $N(u)$ must have different transmission slots in a valid data collection schedule. Since $N(u)$ is a subset of u's descendants, u's transmission slot must be later than the transmission slots of all nodes in $N(u)$. Let $d_{i_1}, d_{i_2}, d_{i_3}, \ldots, d_{i_{|N(u)|}}$ be the list of nodes in the constructed set $N(u)$ where $i_1 \leq i_2 \leq i_3 \leq \ldots \leq i_{|N(u)|}$. Then, $E(u)$ must be greater than or equal to $\max\left\{E(d_{i_1}) + 1, E(d_{i_2}) + 2, \ldots, E(d_{i_{|N(u)|}}) + |N(u)|\right\}$.

Algorithm 3 shows the pseudo code of our algorithm for estimating a lower bound on the latency of data collection for a given routing structure.

The algorithm starts by setting the nodes having no children in the routing structure with the earliest possible transmission slot 0. Then, the earliest possible

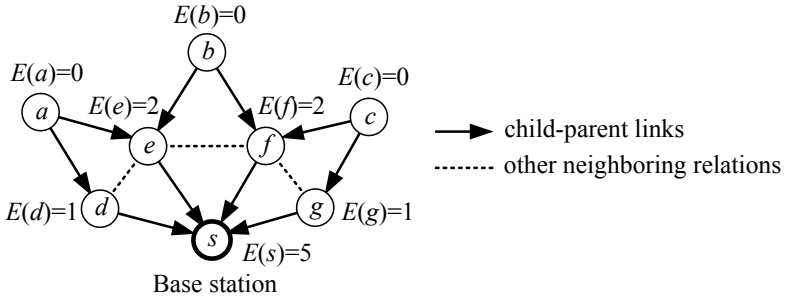

Figure 4.4: The earliest possible transmission slots of sensor nodes in a sample routing structure.

transmission slots of other nodes are calculated in a topological order based on the generalized estimation method discussed above. When the calculation completes, the base station's earliest possible transmission slot represents the earliest possible time for the base station to receive data from all of its children and it is used as the lower bound estimation on the latency of data collection.

Figure 4.4 shows an example routing structure and the earliest possible transmission slots of sensor nodes calculated using the above algorithm. In this figure, solid arrows represent the communication links from children to parents and dotted lines represent other neighboring relations among sensor nodes in the routing structure. In this example, nodes a, b and c do not have any children so their earliest possible transmission slots are set to 0. Node d has only one descendant a whose earliest possible transmission slot is 0, so the earliest possible transmission slot of d is 1. Similarly, node g has only one descendant c whose earliest possible transmission slot is 0, so the earliest possible transmission slot of g is 1. Node e has two descendants a and b and they conflict with each other (since they are e's children), so both a and b are added to the set $N(e)$. Nodes a and b have the same earliest possible transmission slot 0, so e's earliest possible transmission slot is calculated as $E(e) = \max\{0+1, 0+2\} = 2$. Similarly, node f has two conflicting descendants b and c that both have the same earliest possible transmission slot 0. So f's earliest possible transmission slot is 2. As a result, the descendants of the base station s in descending order of their estimated earliest possible transmission slots are: e, f, d, g, a, b, c. In this list, the first four nodes

e, f, d, g conflict with each other since they are all children of the base station s. Thus, these four nodes are all added to the set $N(s)$. Among the last three nodes a, b, c in the base station's descendant list, node a does not conflict with node g since a and g do not have any common neighbor, and node c does not conflict with node d since c and d do not have any common neighbor. So nodes a and c are not added to the set $N(s)$. Node b is a child of both nodes e and f, and b also conflicts with d and g since b's parents are neighbors of either d or g. Therefore, node b is added to the set $N(s)$. After considering all the descendants of the base station s, we get $N(s) = \{e, f, d, g, b\}$. The earliest possible transmission slots of the nodes in $N(s)$ are $\{2, 2, 1, 1, 0\}$. Thus, the earliest possible transmission slot of the base station s is calculated as $E(s) = \max\{2+1, 2+2, 1+3, 1+4, 0+5\}$ $= 5$. So, the lower bound estimation on the latency of data collection through the routing structure in Figure 4.4 is 5 time slots.

Note that our lower bound estimation includes only some constraints that are necessary for constructing a valid data collection schedule. Thus, the calculated lower bound is a super lower bound and may not be achievable by any real valid schedule. We shall use the calculated lower bound as a yardstick of the latency of data collection in performance evaluation.

4.4 Performance evaluation

4.4.1 Experimental setup

We conducted simulation experiments to evaluate the proposed scheduling algorithm for data collection. We implemented our proposed scheduling algorithm using the same Prowler simulator as described in Section 3.4 of Chapter 3.

We compared the performance of our scheduling algorithm with the scheduling algorithm proposed by Yu *et al.* [YLL09]. To the best of our knowledge, Yu's algorithm is the state-of-the-art distributed scheduling algorithm for single-path routing structures. Yu's algorithm is selected to compare with our algorithm because Yu's algorithm is also designed for data collection with in-network aggregation. Moreover, as elaborated in the Section 2.6, existing research work on

TDMA scheduling prior to Yu's algorithm are mostly centralized in nature or focus on different problems such as data delivery from one source node to one destination node, or raw data collection. Yu's algorithm consists of two phases: constructing a single-path routing structure, and scheduling sensor nodes for data collection. These two phases are independent. For comparison purpose, we implemented the scheduling process in Yu's algorithm on the multi-path routing structures constructed in our simulated networks. For both our algorithm and Yu's algorithm, communication among sensor nodes in the scheduling process (i.e., during the execution of the scheduling algorithm) is carried out using the default CSMA protocol in Prowler. Simple acknowledgments and retransmissions are used to guarantee message delivery in scheduling process [LW03].

In multi-path routing structures, the parent numbers of sensor nodes directly affect the sizes of sensor nodes' conflicting sets and thus the length of data collection schedules. To construct the multi-path routing structures for scheduling, for each node placement, sensor nodes were first assigned ring indexes using the localized threshold-based ring assignment approach described in Chapter 3. Then, every node randomly selected some neighbors in its next inner ring as its parents, subject to a maximum allowable number of parents, to form a multi-path routing structure. We tested different maximum allowable numbers of parents in forming multi-path routing structures for evaluating the scheduling algorithms under different redundancy levels of routing.

As in Chapter 3, both square sensing fields and rectangular sensing fields were employed in our experiments. Sensor nodes were deployed at random in the field and the base station was placed at the center of the field. In the default settings, 400 sensor nodes were deployed in a square field of 150 m $\times$ 150 m or in a rectangular field of 75 m $\times$ 300 m. Besides the default settings, we also vary the sensing field size and node density over wide ranges in Sections 4.4.3 and 4.4.4 respectively to investigate their impacts on our proposed scheduling algorithm. For each experimental setting, we simulated 40 randomly generated node placements and plot the average results of these simulation runs for performance comparison together with the 99% confidence interval of the results.

4.4.2 Impact of the maximal allowable number of sensor nodes' parents

First, we evaluate the performance of the scheduling algorithms under different redundancy levels of routing by varying the maximum allowable number of parents for each sensor node from 1 to 10 in constructing the multi-path routing structures. Figures 4.5 and 4.6 show the performance results for the default square and rectangular sensing fields, respectively. We also used Algorithm 3 described in Section 4.3 to estimate lower bounds on the latency of data collection for the multi-path routing structures constructed and plot the results together with the actual data collection latency resulting from the scheduling algorithms in Figures 4.5(a) and 4.6(a).

As seen from Figures 4.5(a) and 4.6(a), the latency of data collection resulting from both our scheduling algorithm and Yu's algorithm increases when the maximum allowable number of parents for every sensor node increases from 1 to 10. This is because when sensor nodes have more children, the sizes of their conflicting sets increase. Thus, fewer sensor nodes can transmit their data in parallel, and the length of the data collection schedule produced is increased. Figures 4.5(a) and 4.6(a) also show that the latency of data collection resulting from our algorithm is very close to that of Yu's algorithm across different redundancy levels of routing. In addition, compared with the lower bound latency estimation, the latency of data collection resulting from our algorithm is within a small constant factor of 1.5 times of the lower bound latency when the maximum allowable number of parents for each sensor node is beyond 2. When each sensor node has at most 1 or 2 parents in the routing structure, the latency of data collection resulting from our algorithm is slightly longer than 1.5 times of the lower bound.

Figures 4.5(b) and 4.6(b) show the average number of messages that each node transmits during the scheduling process. As can be seen, the average number of messages that a node transmits during the scheduling process increases with the maximum allowable number of parents for each sensor node. This is because when sensor nodes have more children, the sizes of their conflicting sets increase.

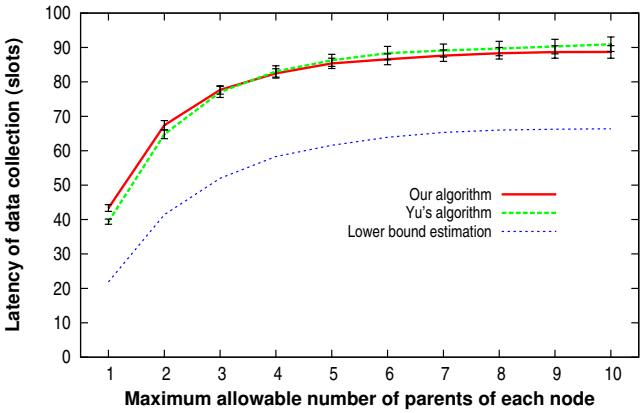

(a) Latency of data collection

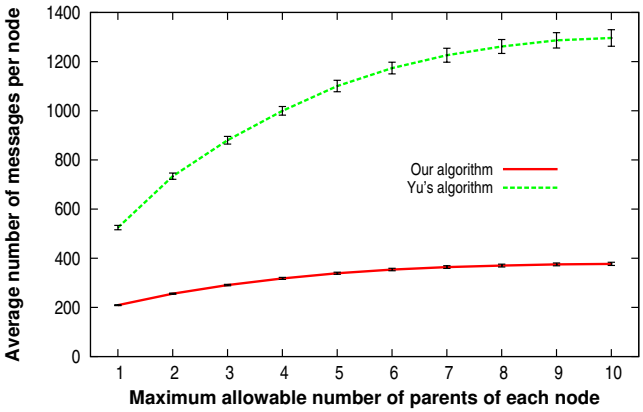

(b) Average number of messages per node

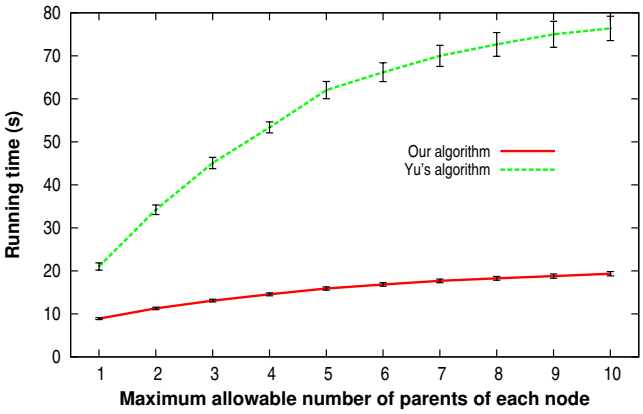

(c) Running times of different scheduling algorithms

Figure 4.5: Performance of different scheduling algorithms in the default square sensing field. Error bars indicate the 99% confidence intervals of the results.

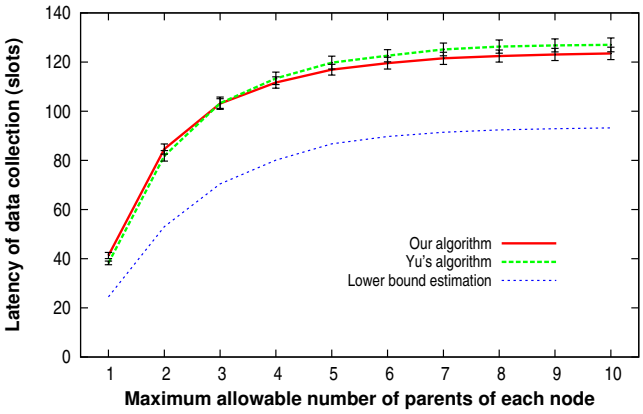

(a) Latency of data collection

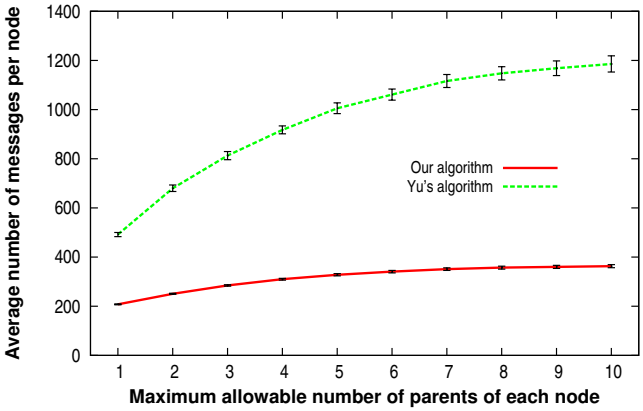

(b) Average number of messages per node

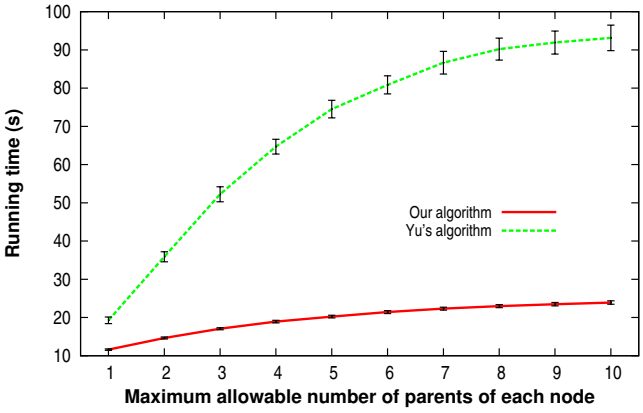

(c) Running times of different scheduling algorithms

Figure 4.6: Performance of different scheduling algorithms in the default rectangular sensing field. Error bars indicate the 99% confidence intervals of the results.

Thus, in general, more messages are transmitted by a node to inform the nodes conflicting with it about its schedule. Comparing the two scheduling algorithms, the number of messages transmitted in Yu's algorithm is about 3 times that of our algorithm. This is because in Yu's scheduling algorithm, each sensor node may need to coordinate with the unscheduled nodes conflicting with it multiple times before it is able to make its schedule.

Figures 4.5(c) and 4.6(c) show the running times of different scheduling algorithms. As can be seen, the running time of our algorithm is normally less than one-third that of Yu's algorithm. This trend is in line with that of message complexity shown in Figures 4.5(b) and 4.6(b) because when more messages are generated in the scheduling process, the time to complete the scheduling process would generally be longer. The results of Figures 4.5 and 4.6 show that our scheduling algorithm is effective in reducing the message complexity and running time of the scheduling process.

4.4.3 Impact of network size

To examine the impact of network size on the performance of the scheduling algorithms, we kept the average node density at 4/225 node per square meter and increased the square sensing field size from 50 m $\times$ 50 m to 500 m $\times$ 500 m, and increased the rectangular sensing field size from 75 m $\times$ 100 m to 75 m $\times$ 1900 m. In these experiments, we kept the maximum allowable number of parents for each sensor node at 5 in constructing the multi-path routing structures. Figures 4.7 and 4.8 show the performance results for square and rectangular sensing fields, respectively.

As seen from Figures 4.7(a) and 4.8(a), the latency of data collection resulting from our scheduling algorithm is consistently very close to that of Yu's algorithm over a wide range of sensing field sizes. In addition, the latency of data collection resulting from our algorithm is within the same constant factor of 1.5 times of the lower bound latency estimation across different sensing field sizes.

Figures 4.7(b) and 4.8(b) show the average number of messages that each node transmits during the scheduling process. As can be seen, the number of messages

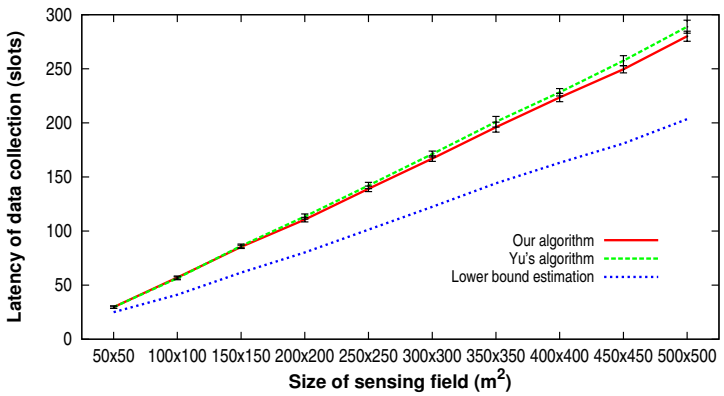

(a) Latency of data collection

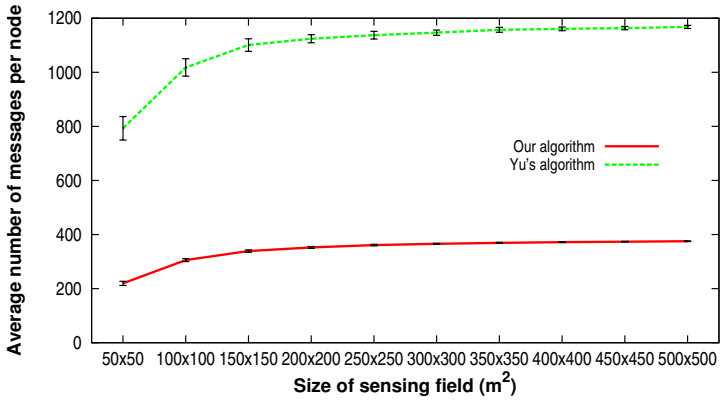

(b) Average number of messages per node

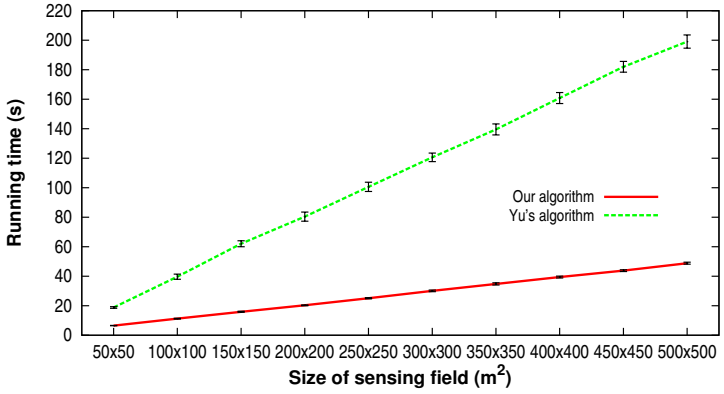

(c) Running times of different scheduling algorithms

Figure 4.7: Performance of different scheduling algorithms for different square sensing fields. Error bars indicate the 99% confidence intervals of the results.

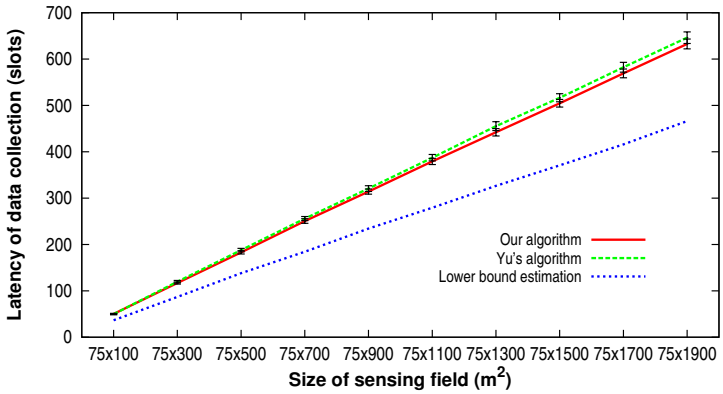

(a) Latency of data collection

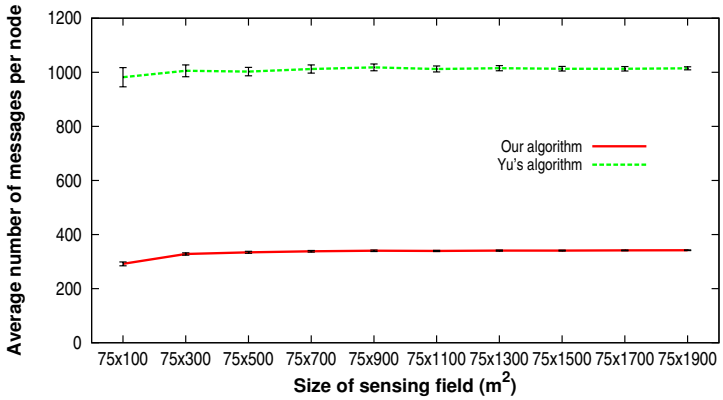

(b) Average number of messages per node

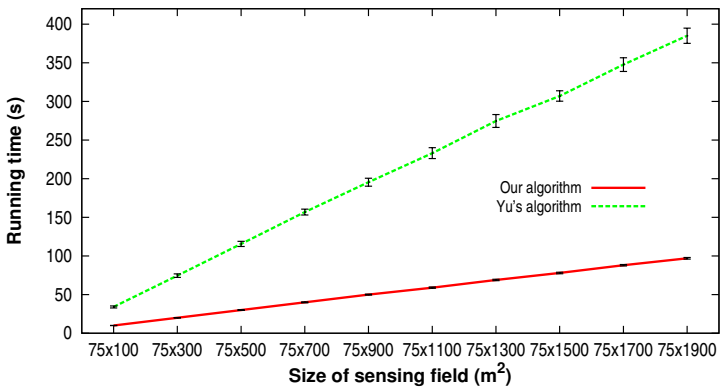

(c) Running times of different scheduling algorithms

Figure 4.8: Performance of different scheduling algorithms for different rectangular sensing fields. Error bars indicate the 99% confidence intervals of the results.

transmitted in Yu's algorithm is 3 to 4 times that of our algorithm. Figures 4.7(c) and 4.8(c) show the running times of different scheduling algorithms. The running time of Yu's algorithm increases very fast with increasing sensing field size. In contrast, the running time of our algorithm increases much slower when the sensing field size increases, and it is consistently shorter than one-third that of Yu's algorithm.

4.4.4 Impact of node density

To examine the impact of node density on the performance of the scheduling algorithms, we varied the number of nodes in the network from 200 to 900 while keeping the square sensing field size at 150 m $\times$ 150 m and the rectangular sensing field size at 75 m $\times$ 300 m. In these experiments, we kept the maximum allowable number of parents for each sensor node at 5 in constructing the multi-path routing structures.

As shown in Figures 4.9(a) and 4.10(a), the latency of data collection resulting from both our scheduling algorithm and Yu's algorithm increases when the node density increases. This is because the sizes of the conflicting sets of sensor nodes generally increase with node density. The results in Figures 4.9(a) and 4.10(a) also show that the latency of data collection resulting from our algorithm is similar to that of Yu's algorithm across different node densities. In addition, the latency of data collection of our scheduling algorithm is normally within 1.5 times of the lower bound latency estimation.

Figures 4.9(b) and 4.10(b) show that the average number of messages that each node transmits during the scheduling process also increases with node density due to larger conflicting sets of sensor nodes. The number of messages transmitted in Yu's algorithm increases very fast with increasing node density and is normally 3 to 4 times that of our algorithm. Figures 4.9(c) and 4.10(c) show the running times of different scheduling algorithms. As can be seen, the running time of our algorithm can be less than one-sixth that of Yu's algorithm at high node densities. These results show again the effectiveness of our scheduling algorithm in reducing the message complexity and running time of the scheduling

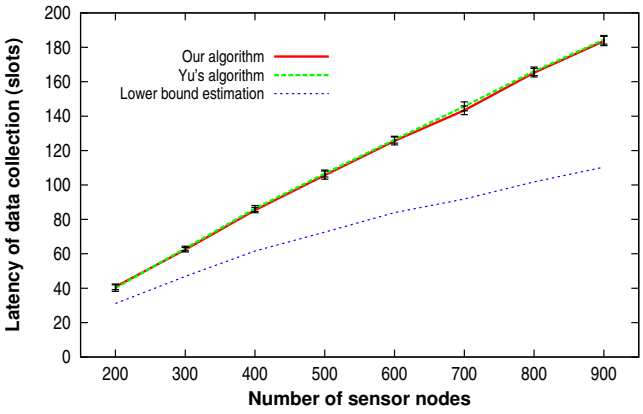

(a) Latency of data collection

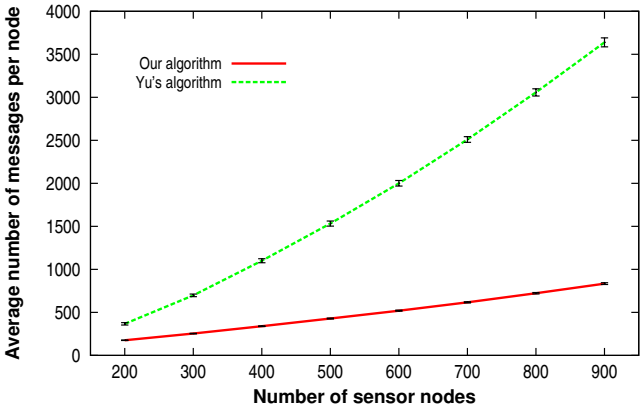

(b) Average number of messages per node

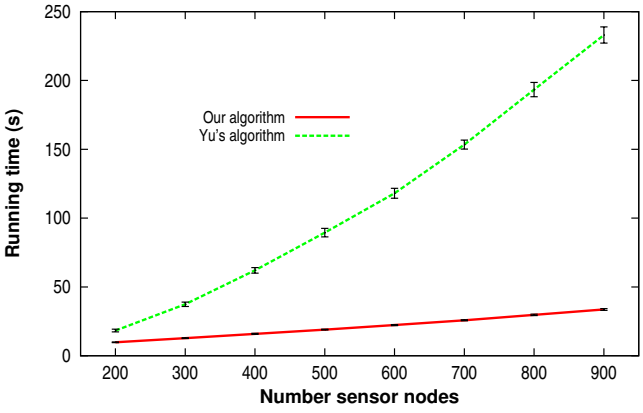

(c) Running times of different scheduling algorithms

Figure 4.9: Performance of different scheduling algorithms with different node densities in the default square sensing field. Error bars indicate the 99% confidence intervals of the results.

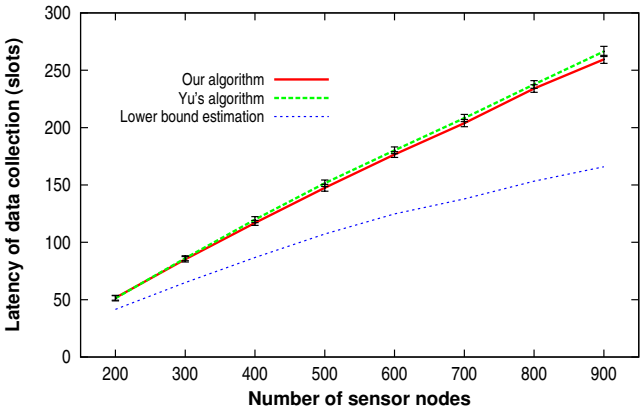

(a) Latency of data collection

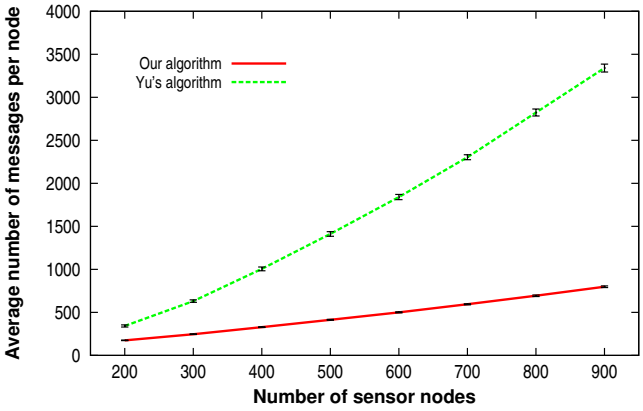

(b) Average number of messages per node

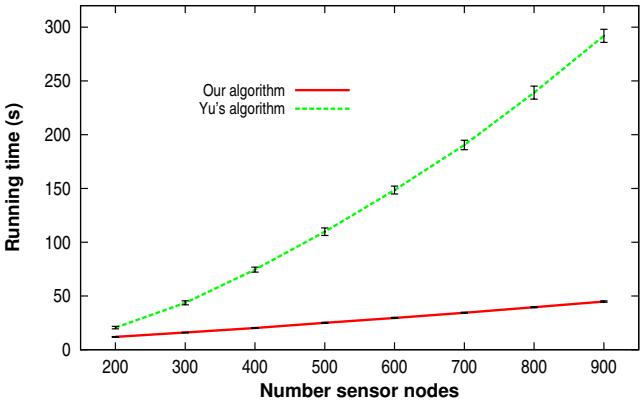

(c) Running times of different scheduling algorithms

Figure 4.10: Performance of different scheduling algorithms with different node densities in the default rectangular sensing field. Error bars indicate the 99% confidence intervals of the results.

process.

4.5 Summary

In this chapter, we have presented a distributed scheduling algorithm for sensor data collection through multi-path routing structures. The scheduling algorithm reduces the coordination overhead among conflicting nodes by resolving their relative scheduling order prior to the scheduling process. We have also developed a method for deriving a lower bound on the shortest possible latency of data collection through a given routing structure. Experimental results show that our proposed scheduling algorithm substantially reduces the number of messages transmitted during the scheduling process and has considerably shorter running time compared to an existing scheduling algorithm. The latency of data collection resulting from our algorithm is very close to that of the existing scheduling algorithm and is normally within a small constant factor of 1.5 times of the lower bound latency estimation across wide ranges of network sizes and node densities.

Chapter 5

An efficient data collection scheme

In Chapter 3, we have focused on improving the robustness of sensor data collection by exploiting the broadcast nature of wireless communication to transport sensor data through multiple propagation paths toward the base station. A distributed scheduling algorithm has been presented in Chapter 4 for constructing TDMA schedules for sensor data collection through multi-path routing structures. TDMA protocols help to improve the energy efficiency and latency of sensor data collection since communication among sensor nodes can proceed without contention, collisions or idle listening [GDP05,MLW+09]. However, there are trade-offs among the robustness, energy efficiency and latency of sensor data collection through multi-path routing structures. On one hand, a higher level of routing redundancy increases the number of data propagation paths and thus improves the robustness of sensor data collection. But on the other hand, a higher level of routing redundancy results in sensor nodes receiving more messages and consuming more energy in data collection. In addition, as have been shown in Section 4.4.2, a higher level of routing redundancy also leads to larger conflicting sets of sensor nodes, thereby increasing the length of data collection schedules.

In this chapter, we design an efficient multi-path data collection scheme that considers the energy efficiency, the latency and the robustness of data collection altogether. First, we propose a distributed method for constructing multi-path

routing structures for sensor data collection. As in the rings overlays in Chapter 3, each sensor node in our proposed multi-path routing structures transmits data only once to all of its parents in a round of data collection by broadcast. To achieve a required level of energy efficiency for communication in data collection, our proposed construction method keeps the number of messages that each sensor node receives in a round of data collection within a given limit. After the routing structure is constructed, the TDMA scheduling algorithm presented in Chapter 4 is used to produce a data collection schedule in which each sensor node is assigned one time slot for transmitting its data to all of its parents in the multi-path routing structure by broadcast. Then, we develop an enhanced scheme for data collection in which sensor nodes have opportunities to overhear data from other neighbors in addition to receiving data from their children in the multi-path routing structure. By following the same transmission schedule as in the original data collection scheme, the enhanced scheme is able to improve the robustness of data collection without sacrificing the latency of data collection and violating the required level of energy efficiency for communication. We analyze the control parameter setting in the enhanced data collection scheme for maximizing its benefits. Experimental results show that our proposed methods achieve significantly better trade-offs among the robustness, latency and energy efficiency of data collection.

The remainder of this chapter is organized as follows. Section 5.1 introduces some preliminaries. Section 5.2 elaborates the distributed method for constructing multi-path routing structures that satisfy a required level of energy efficiency for communication. Section 5.3 presents and analyzes the enhanced scheme for data collection. Experimental evaluation is described in Section 5.4. Finally, Section 5.5 summarizes the chapter. Related work on multi-path routing methods has been discussed in Section 2.2.2.

5.1 Preliminaries

As in Chapters 3 and 4, we consider a wireless sensor network in which an aggregated result of the data acquired by sensor nodes is to be collected at the base

station. To cope with communication failures, a multi-path routing structure rooted at the base station is to be constructed for data collection and aggregation. Conceptually, the multi-path routing structure is a directed acyclic graph in which each node has multiple *parents* and multiple *children*. The nodes within the communication range of a sensor node, including its parents and its children, are called the *neighbors* of the node.

In a round of data collection, each node first receives data from all of its children and aggregates the received data with its own locally acquired data. Then, the node transmits the aggregated data to all of its parents by broadcast. This data propagation and aggregation process starts from the nodes with no children in the multi-path routing structure and proceeds until the base station receives data from all of its children. Communication among sensor nodes in the data collection process is coordinated by a TDMA protocol as described in Chapter 4, where time is divided into slots of equal length and the duration of a time slot allows a sensor node to transmit exactly one message. In a TDMA schedule, each sensor node is assigned one *transmission time slot* for its transmission to its parents by broadcast and a set of *receiving time slots* for receiving data from its children. To avoid collisions, only the nodes that do not conflict with each other are allowed to be scheduled in the same time slot. In addition, to allow for in-network aggregation, the transmission slot of each node must be scheduled after the transmission slots of all of its children.

Since the energy cost of computation is insignificant compared to the energy cost of wireless communication [MFHH02,NGSA04], the energy consumption of a sensor node in data collection is primarily determined by the number of messages it transmits and receives. Note that in a round of data collection, each sensor node transmits only one message to its parents by broadcast, irrespective of its hop-distance to the base station and the routing structure. Therefore, we take the number of messages that sensor nodes receive (or equivalently, the number of their receiving slots in the data collection schedule) as a measure of energy efficiency for communication. To achieve a required level of energy efficiency for communication, sensor nodes must limit their numbers of receiving slots in

the data collection schedule. Since the lifetime of a wireless sensor network is largely determined by the most energy-consuming node [BAS05], we assume a maximum allowable number (denoted by m) of receiving slots for every sensor node in the data collection schedule. Our objective is to construct a multi-path routing structure and its corresponding data collection schedule in which every sensor node receives data from at most m other nodes, such that the latency of data collection is reduced and the robustness of data collection is improved as much as possible.

5.2 Constructing multi-path routing structures

A natural method to construct a multi-path routing structure over a sensor network is to calculate the hop-distance from every sensor node to the base station and let each node transmit its data to the nodes at shorter hop-distances [CLKB04, NGSA04]. In Chapter 3, we have investigated different approaches for organizing sensor nodes into rings around the base station, including a greedy approach and a threshold-based approach. In this chapter, we exploit these ring assignment approaches and use the resultant ring indexes of sensor nodes as their hop-distances to the base station for constructing multi-path routing structures. According to the hop-distances of sensor nodes, a simple method for constructing a multi-path routing structure is for each node to select all of its neighbors that have shorter hop-distances than it as its parents. However, this method does not guarantee that the child number of each sensor node (and hence the number of its receiving slots in the data collection schedule constructed later) is within a given bound m.

To ensure that each sensor node receives data from at most m other nodes, we propose to make parent selections through request-reply interactions between sensor nodes. Specifically, on identifying the neighbors with shorter hop-distances, a node sends parent-selection requests to them one at a time. On receiving such a request, if the neighbor has fewer than m children, it accepts the request by

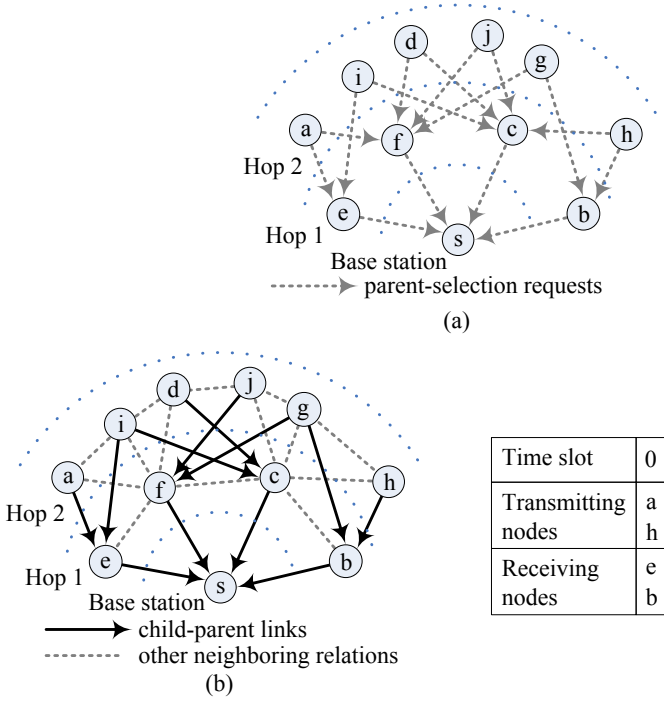

Time slot	0	1	2	3	4	5	6	7	8
Transmitting nodes	a h	d	i	j	g	b	c	e	f
Receiving nodes	e b	c	c e	f	b f	s	s	s	s

(c)

Figure 5.1: An example multi-path routing structure and its data collection schedule.

sending an acceptance response to the requesting node. Otherwise, if the neighbor already has m children, it denies the request by sending a denial response to the requesting node. Unlike sensor nodes, the base station accepts all the parent-selection requests from the nodes at hop-distance 1 because the base station normally has much more powerful energy supply than sensor nodes so that it does not need to limit its number of receiving slots. We shall take the number of parent-selection requests sent by each sensor node as a control parameter in the construction of multi-path routing structures.

Figure 5.1(a) shows a sample network in which nodes a, d, g, h, i, j are at hop-distance 2 and nodes b, c, e, f are at hop-distance 1. Suppose that $m = 2$ and each sensor node at hop-distance 2 sends two parent-selection requests to their neighbors at hop-distance 1 in the following order: $i \to e$, $d \to c$, $g \to f$, $h \to b$, $a \to e$, $i \to c$, $j \to f$, $g \to b$, $a \to f$, $j \to c$, $d \to f$, $h \to c$. Initially, the sensor nodes at hop-distance 1 do not have any children. Thus, the first eight requests $i \to e$, $d \to c$, $g \to f$, $h \to b$, $a \to e$, $i \to c$, $j \to f$, $g \to b$ are all accepted and nodes e, c, f, b each gets two children. After that, the next four requests

$a \to f$, $j \to c$, $d \to f$, $h \to c$ are denied since nodes f and c have already reached the limit of $m = 2$ children. Suppose that each node at hop-distance 1 sends one parent-selection request to the base station. Then, all these parent-selection requests are accepted by the base station. Figure 5.1(b) shows the resultant routing structure, in which solid arrows represent the communication links from children to parents and dotted lines represent other neighboring relations among sensor nodes.

In Chapter 4, we have presented a distributed scheduling algorithm for data collection that greedily assigns to each node the earliest collision-free time slot for its transmission. The scheduling process starts by assigning transmission slots to the sensor nodes that have no children. Subsequently, each remaining node is scheduled after all of its children have been assigned transmission slots. Suppose that the scheduling algorithm assigns transmission slots to the sensor nodes in the multi-path routing structure of Figure 5.1(b) in the following order: $a, h, d, i, j, g, b, c, e, f$. First, node a is assigned slot 0 for its transmission. Since node h does not conflict with a, node h is also assigned slot 0 for its transmission. Node d conflicts with h since d has a parent c that is also a neighbor of h. Thus, the earliest collision-free transmission slot for d is slot 1. Node i conflicts with both a and d since i and a have a common parent e, and i and d have a common parent c. Hence, the earliest collision-free transmission slot for node i is slot 2. Similarly, node j is assigned to slot 3 because it conflicts with nodes a, d and i; node g is assigned to slot 4 because it conflicts with nodes a, d, i and j. Node b must transmit data later than its children g and h, so it is assigned to slot 5. Node c must transmit data later than its children d and i. In addition, node c conflicts with nodes j, g and b. Therefore, the earliest collision-free transmission slot for c is slot 6. Similarly, nodes e and f are assigned to slots 7 and 8, respectively. Figure 5.1(c) shows the resultant schedule for data collection. The length of the schedule is 9 time slots.

5.3 Enhanced data collection scheme

In the above method for constructing routing structures, parent-selection requests are denied when the parent candidates have reached the limit m on their child numbers. As a result, there may exist some sensor nodes having few or even no parents at all in the constructed routing structure (e.g., nodes a, d, h, j in Figure 5.1(b)). The robustness of data collection would be limited when the number of such nodes is significant. On the other hand, there may also exist sensor nodes that receive fewer than m parent-selection requests because they have fewer than m neighbors with longer hop-distances (e.g., all nodes at hop-distance 2 in Figure 5.1(b) do not have any neighbors with longer hop-distances). These nodes would have fewer than m children in the constructed routing structure. Thus, their allowable energy budgets for receiving data are not fully utilized in data collection.

In this section, we propose *an enhanced scheme* for data collection in which sensor nodes are allowed to overhear data from other neighbors in addition to receiving data from their children if their child numbers are below the limit m in the constructed routing structure. Following the original transmission schedule constructed, each sensor node exploits as many additional receiving slots as possible for overhearing data from its neighbors provided that its total number of receiving slots does not exceed the limit m. Overhearing creates additional propagation paths for transporting sensor data to the base station, thereby increasing the robustness of data collection against communication failures. Meanwhile, since the original transmission schedule is followed, these additional propagation paths do not sacrifice the latency of data collection. As opposed to our enhanced scheme, we shall refer to the original scheme in which data are only propagated from children to parents in the constructed routing structure as *the plain scheme* for data collection.

5.3.1 Selecting overhearing slots

Due to interference, a sensor node can overhear data from a neighbor in a time slot only if this neighbor is the only node within its communication range transmitting data in that time slot. In addition, the receiving node can only forward the overheard data to its parents in the same round of data collection if the overhearing time slots are earlier than its own transmission time slot in the schedule. Given a data collection schedule, for each sensor node, we define the transmission slots of its neighbors that satisfy the above two conditions as its *feasible overhearing slots*. To develop the enhanced scheme for data collection, each node first identifies its feasible overhearing slots and then selects as many feasible overhearing slots as possible for receiving data from its neighbors provided that its total number of receiving slots does not exceed the limit m.

For example, in the routing structure and data collection schedule of Figures 5.1(b) and 5.1(c), node i has three neighbors a, d, f and their respective transmission slots are $0, 1, 8$. They are the only neighbors of i transmitting data in their respective transmission time slots. Also note that node i transmits data in slot 2. Thus, i's feasible overhearing slots include slots 0 and 1. Since the limit $m = 2$ and node i has not got any receiving slot in the schedule, node i can select both slots 0 and 1 as its overhearing slots. Similarly, node j has one feasible overhearing slot 1, so it can select slot 1 as its overhearing slot. Node g has two feasible overhearing slots 0 and 3, so both slots can be selected as its overhearing slots. Figures 5.2(a) and 5.2(b) show the data propagation paths in the enhanced data collection scheme and the resultant data collection schedule respectively. In Figure 5.2(a), white arrows represent data propagations due to overhearing and black arrows represent data propagations from children to parents in the original routing structure.

As can be seen, in the original data collection schedule of Figure 5.1, nodes a, d, j and h each has only a single propagation path to the base station. In contrast, in the enhanced scheme, as shown in Figure 5.2, the numbers of propagation paths from nodes a, d, j and h to the base station are increased substantially due to overhearing. Thus, the robustness of data collection would be improved

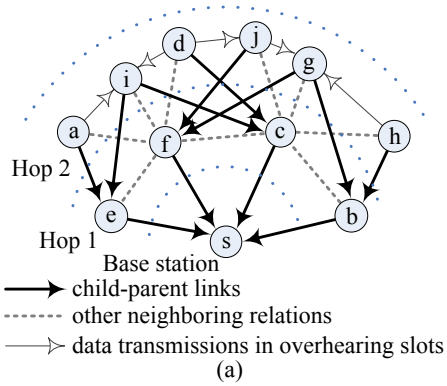

(a)

Time slot	0	1	2	3	4	5	6	7	8
Transmitting nodes	a h	d	i	j	g	b	c	e	f
Receiving nodes	e b i g	c i j	c e	f g	b f	s	s	s	s

(b)

Figure 5.2: An example schedule in the enhanced data collection scheme.

considerably. Since the original assignment of transmission time slots to sensor nodes and the limit m are kept unchanged, the improvement in robustness of the enhanced scheme is achieved without sacrificing the length of the data collection schedule (i.e., latency) or violating the limit on the number of receiving slots for each node (i.e., energy efficiency for communication).

When the feasible overhearing slots of a sensor node together with its receiving slots already assigned in the schedule exceed the limit m, the node can choose only a subset of the feasible slots for overhearing. In this case, to improve the robustness of data collection as much as possible, we propose to let sensor nodes overhear transmissions from the neighbors having the least numbers of parents in the original routing structure. This is because neighbors with fewer parents would benefit more significantly from overhearing for improving the robustness of data collection.

To implement the enhanced scheme, two minor modifications need to be made to the scheduling algorithm presented in Chapter 4. First, to locally identify the feasible overhearing slots, each sensor node needs to learn the transmission slots of all its neighbors. Thus, after each node determines its transmission time slot, it must announce its transmission time slot to all of its neighbors. So, in the algorithm of Chapter 4, when a node broadcasts an RT message to announce its transmission slot, all the neighbors of the node should record the transmission slot on receiving the RT message. Second, when a node announces its transmission slot in an RT message, a value representing its number of parents should be included in the RT message. The purpose is for each node to learn the parent numbers of

its neighbors for prioritizing the feasible overhearing slots in selection.

5.3.2 Setting the number of parent-selection requests

It is obvious that the number of feasible overhearing slots in the enhanced data collection scheme depends on the node density because the number of feasible overhearing slots of any node is limited by its number of neighbors. In addition, the number of feasible overhearing slots depends on the parent numbers of sensor nodes in the routing structure constructed, which in turn is affected by the number of parent-selection requests sent by sensor nodes in the construction process. If sensor nodes send more parent-selection requests, they would generally have more parents in the constructed routing structure. So, there would be more conflicting node pairs in scheduling due to interference among sensor nodes. As a result, the data collection schedule built is expected to be longer and there would be fewer nodes transmitting data in each time slot. Thus, the number of feasible overhearing slots of a sensor node would increase. On the other hand, if sensor nodes have more parents in the routing structure constructed, the child numbers of sensor nodes would generally be larger as well. Hence, the numbers of overhearing slots they can choose would be smaller due to the limit m on their total numbers of receiving slots. Therefore, an unnecessarily large number of parent-selection requests would not further increase the total number of receiving slots used by sensor nodes in the enhanced data collection scheme and improve the robustness of data collection. In contrast, it only increases the latency of data collection due to longer schedules. In this section, we develop a mathematical model to analyze the impact of the node density and the number of parent-selection requests on the total number of a node's children and its neighbors that it can overhear.

Analyzing the expected number of parents of a node

Suppose that each sensor node sends parent-selection requests to k randomly selected neighbors with shorter hop-distances to the base station. We start by

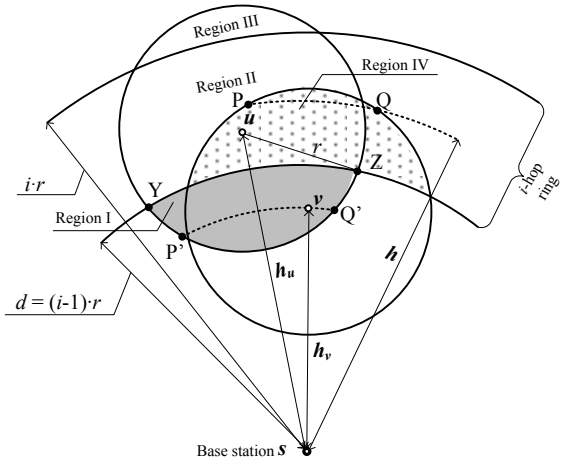

Figure 5.3: Analytical model for estimating the expected number of parents of a sensor node.

calculating the expected number of parents of a sensor node in the routing structure constructed.

Let r be the transmission range of sensor nodes. For simplicity, we approximate the hop-distance of a node by $\lceil \frac{l}{r} \rceil$ hops, where l is the distance from the node to the base station s. That is, the hop-distance of a node is i if the distance from the node to the base station is between $(i-1) \cdot r$ and $i \cdot r$. So, all nodes of hop-distance i are located in the ring-shaped strip centered at the base station s with inner radius $(i-1) \cdot r$ and outer radius $i \cdot r$. We shall refer to this strip as the i-hop ring. Now consider a node u at distance h_u away from the base station s. Assume that u is in the i-hop ring, i.e., $i = \lceil \frac{h_u}{r} \rceil$, and u has a communication range represented by a circular disk of radius r centered at u. As shown in Figure 5.3, the i-hop ring divides u's communication range into three regions: one region closer to the base station than u (region I in Figure 5.3), one region containing node u (region II in Figure 5.3), and one region further away from the base station than u (region III in Figure 5.3). The nodes in region I are u's neighbors that have shorter hop-distances than u and are u's parent candidates. Assuming that sensor nodes are uniformly distributed over the network, the expected number of u's neighbors with shorter hop-distances is then given by the area of region I times the node density.

Note that region I is the intersection between two sectors sYZ and uYZ,

where Y, Z are the intersection points of two circular disks centered at the base station s and node u with radius $d = (i-1) \cdot r$ and r, respectively. Considering triangle $\triangle Ysu$, we have

$$\cos \widehat{Yus} = \frac{r^2 + h_u^2 - d^2}{2rh_u},$$

and

$$\cos \widehat{Ysu} = \frac{d^2 + h_u^2 - r^2}{2dh_u}.$$

Thus,

$$\widehat{YuZ} = 2 \cdot \widehat{Yus} = 2 \cdot \arccos \frac{r^2 + h_u^2 - d^2}{2rh_u},$$

and

$$\widehat{YsZ} = 2 \cdot \widehat{Ysu} = 2 \cdot \arccos \frac{d^2 + h_u^2 - r^2}{2dh_u}.$$

The areas of sectors uYZ and sYZ are given by $\frac{1}{2}r^2 \cdot \widehat{YuZ}$ and $\frac{1}{2}d^2 \cdot \widehat{YsZ}$ respectively, and the areas of triangles $\triangle uYZ$ and $\triangle sYZ$ are $\frac{1}{2}r^2 \cdot \sin \widehat{YuZ}$ and $\frac{1}{2}d^2 \cdot \sin \widehat{YsZ}$ respectively. Therefore, the area of region I can be derived as the following function $A(h_u)$ of the distance h_u from node u to the base station s:

$$\begin{aligned} A(h_u) &= \frac{r^2}{2}\left(\widehat{YuZ} - \sin \widehat{YuZ}\right) + \frac{d^2}{2}\left(\widehat{YsZ} - \sin \widehat{YsZ}\right) \\ &= \frac{r^2}{2}\left(2 \cdot \arccos \frac{r^2 + h_u^2 - d^2}{2rh_u} - \sin\left(2 \cdot \arccos \frac{r^2 + h_u^2 - d^2}{2rh_u}\right)\right) \\ &+ \frac{d^2}{2}\left(2 \cdot \arccos \frac{d^2 + h_u^2 - r^2}{2dh_u} - \sin\left(2 \cdot \arccos \frac{d^2 + h_u^2 - r^2}{2dh_u}\right)\right). \end{aligned}$$

Let ρ be the node density. Then, the number of u's parent candidates is given by $A(h_u) \cdot \rho$. If $A(h_u) \cdot \rho > k$, node u randomly selects k parent candidates and sends parent-select requests to them. If $A(h_u) \cdot \rho \leq k$, node u sends parent-selection requests to all $A(h_u) \cdot \rho$ parent candidates. Denote by $p(h_u)$ the probability that node u sends a parent-selection request to a particular parent

candidate in region I. We have

$$p(h_u) = \begin{cases} \frac{k}{A(h_u)\cdot\rho}, & \text{if } A(h_u)\cdot\rho > k, \\ 1, & \text{if } A(h_u)\cdot\rho \leq k. \end{cases}$$

Now consider a parent candidate v at hop-distance $(i-1)$ in region I. The nodes that may send parent-selection requests to v are those in v's communication range and have longer hop-distances than v, i.e., the nodes located in the portion of v's communication range that is in the i-hop ring (as shown by region IV in Figure 5.3). To calculate the expected number of parent-selection requests that node v receives, let PQ be an arc centered at the base station s that is within region IV (see Figure 5.3). Suppose that the radius of arc PQ is h, i.e., the distance of any point on arc PQ to the base station s is h. Then, all nodes on arc PQ have the same expected number of parent candidates $A(h)\cdot\rho$. Hence, each of them has the same probability $p(h)$ to send a parent-selection request to node v. The number of nodes on arc PQ depends on the length of arc PQ. Note that $\widehat{PsQ} = 2\cdot\widehat{Psv}$. Considering triangle $\triangle Psv$, we have

$$\cos\widehat{Psv} = \frac{h^2 + h_v^2 - r^2}{2hh_v},$$

where h_v is the distance from node v to the base station s. Then, the length of arc PQ is given by

$$\widehat{PsQ}\cdot h = 2\cdot\widehat{Psv}\cdot h = 2h\cdot\arccos\frac{h^2 + {h_v}^2 - r^2}{2hh_v}.$$

Since arc PQ is within region IV, the possible range of its radius h is from $(i-1)\cdot r$ to $(h_v + r)$. Therefore, the expected number of nodes in region IV that send parent-selection requests to v is given by

$$f(h_v) = \int_{(i-1)\cdot r}^{h_v+r} p(h)\cdot\rho\cdot 2h\cdot\arccos\frac{h^2 + {h_v}^2 - r^2}{2hh_v}\,\mathrm{d}h.$$

Due to the limit m on its number of receiving slots, node v can only accept

up to m parent-selection requests. Thus, the expected probability that node v accepts the parent-selection request from a node in region IV is given by

$$q(h_v) = \begin{cases} \frac{m}{f(h_v)}, & \text{if } f(h_v) > m, \\ 1, & \text{if } f(h_v) \leq m. \end{cases}$$

Recall that the probability that node u sends a parent-selection request to node v is $p(h_u)$. Thus, the probability that u sends a parent-selection request to v and v accepts the request (i.e., v becomes a parent of u in the routing structure) is $p(h_u) \cdot q(h_v)$. To calculate the expected number of u's parents, consider the arc $P'Q'$ centered at the base station s with radius h_v that is within region I (see Figure 5.3). All nodes on arc $P'Q'$ have the same probability $p(h_u) \cdot q(h_v)$ to become u's parent. The number of nodes on arc $P'Q'$ depends on the length of arc $P'Q'$. Note that $\widehat{P'sQ'} = 2 \cdot \widehat{P'su}$. Considering triangle $\triangle P'su$, we have

$$\cos \widehat{P'su} = \frac{h_u^2 + h_v^2 - r^2}{2h_u h_v}.$$

Therefore, the length of arc $P'Q'$ is

$$\widehat{P'sQ'} \cdot h_v = 2 \cdot \widehat{P'su} \cdot h_v = 2h_v \cdot \arccos \frac{h_u^2 + h_v^2 - r^2}{2h_u h_v}.$$

Since arc $P'Q'$ is within region I, the possible range of its radius h_v is from $(h_u - r)$ to $(i-1) \cdot r$. Therefore, the expected number of u's parents is given by

$$f_p(h_u) = \int_{h_u - r}^{(i-1)\cdot r} p(h_u) q(h_v) \cdot \rho \cdot 2h_v \cdot \arccos \frac{h_u^2 + h_v^2 - r^2}{2h_u h_v} \, \mathrm{d}h_v.$$

Analyzing the number of a node's children and its neighbors that it can overhear in a valid data collection schedule

Now we analyze the total number of node u's children and u's neighbors that it can overhear in a valid data collections schedule. We focus on the neighbors of u at the same or longer hop-distances than u, i.e., the nodes in regions II and III shown in Figure 5.3.

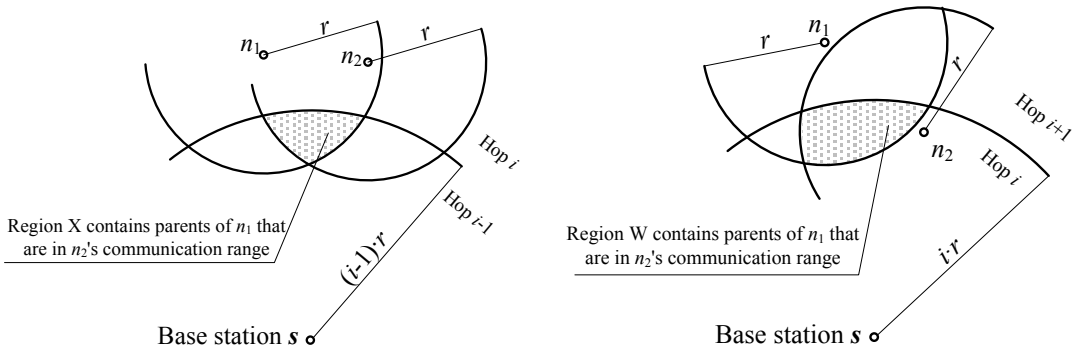

(a) n_1 is at the hop-distance i.

(b) n_1 is at hop-distance $(i+1)$.

Figure 5.4: Analytical model for estimating the number of parents of a sensor node that are within the communication range of another node.

Consider a node n_1 in region II or region III. We first calculate the probability for node n_1 to conflict with other neighbors of u in scheduling. Let n_2 be another neighbor of u, which can be located in region I, II or III. Let h_{n_1} and h_{n_2} be the distances from nodes n_1 and n_2 to the base station s respectively. If n_1 is in region III (i.e., $h_{n_1} \geq i \cdot r$), n_1 is at hop-distance $(i+1)$ and it may be a child of u. Following the earlier analysis, the probability that n_1 is a child of u is given by $p(h_{n_1}) \cdot q(h_u)$. In this case, n_1 certainly conflicts with all other neighbors of u including n_2. Similarly, if n_2 is in region III (i.e., $h_{n_2} \geq i \cdot r$), n_2 has a probability of $p(h_{n_2}) \cdot q(h_u)$ to be a child of u, in which case n_2 conflicts with all other neighbors of u including n_1. If neither node n_1 nor node n_2 is a child of u, whether n_1 conflicts with n_2 depends on whether any parent of n_1 is inside the communication range of n_2 and whether any parent of n_2 is inside the communication range of n_1. If n_1 is in region II (i.e., n_1 is at hop-distance i), as shown in Figure 5.4(a), the parents of n_1 in n_2's communication range are those within region X, which is the intersection area among the communication ranges of n_1, n_2 and the $(i-1)$-hop ring. Since n_1 has a total number of $f_p(h_{n_1})$ parents distributed in a region of area $A(h_{n_1})$, the expected number of n_1's parents within n_2's communication range, denoted by $f_x(n_1, n_2)$, can be approximated by

$$f_x(n_1, n_2) = \frac{S_X}{A(h_{n_1})} \cdot f_p(h_{n_1}),$$

where S_X is the area of region X. Similarly, if n_1 is in region III (i.e., n_1 is at hop-distance $(i+1)$), as shown in Figure 5.4(b), the parents of n_1 in n_2's communication range are those within region W, which is the intersection area among the communication ranges of n_1, n_2 and the i-hop ring. Since n_1 has a total number of $f_p(h_{n_1})$ parents distributed in a region of area $A(h_{n_1})$, $f_x(n_1, n_2)$ can be approximated by

$$f_x(n_1, n_2) = \frac{S_W}{A(h_{n_1})} \cdot f_p(h_{n_1}),$$

where S_W is the area of region W. The expected number of n_2's parents within n_1's communication range, denoted by $f_x(n_2, n_1)$, can be calculated in a similar way. If n_1 or n_2 has at least one parent in the communication range of the other, they must conflict with each other. Otherwise, the probability that they conflict with each other can be approximated by the expected number of parents of one node in the communication range of the other. Therefore, the probability that n_1 conflicts with n_2 is given by

$$p_c(n_1, n_2) = \begin{cases} 1, & \text{if either } n_1 \text{ or } n_2 \text{ is a child of } u, \\ 1, & \text{if } n_1 \text{ and } n_2 \text{ are not } u\text{'s children and} \\ & f_x(n_1, n_2) \geq 1 \text{ or } f_x(n_2, n_1) \geq 1, \\ 1 - (1 - f_x(n_1, n_2)) \cdot (1 - f_x(n_2, n_1)), & \text{otherwise.} \end{cases}$$

We integrate $p_c(n_1, n_2)$ over all possible positions (x_{n_2}, y_{n_2}) of n_2 in the communication range of u to calculate the expected number of u's neighbors that conflict with n_1:

$$C(n_1) = \iint\limits_{u\text{'s communication range}} \rho \cdot p_c(n_1, n_2)\, \mathrm{d}x_{n_2}\, \mathrm{d}y_{n_2}.$$

If n_1 conflicts with an overwhelming number of u's neighbors, n_1 is most likely to be assigned a transmission slot different from all other neighbors of u by the scheduling algorithm. The expected number of u's neighbors is $\rho\pi r^2$. On

computing $C(n_1)$, we compare $\lceil C(n_1) \rceil$ against a threshold value $\rho\pi r^2$. If $\lceil C(n_1) \rceil$ is not less than $\rho\pi r^2$, we consider n_1 to have a transmission slot different from all other neighbors of u. In this case, n_1 can either be a child of u or a neighbor that u can overhear. Integrating the results over all possible positions of n_1 in regions II and III, we obtain the total number of u's children and u's neighbors that it can overhear.

Numerical results

Using the above theoretical analysis, we shall investigate the expected number of a node's children and neighbors that it can overhear in a valid data collection schedule across a wide range of network settings. In the following numerical results, we varied the node density (i.e., $\rho\pi r^2$, the number of a node's neighbors), k (the number of parent-selection requests sent by a node), and m (the maximum allowable number of receiving slots of sensor nodes) across wide ranges of values. Figures 5.5 to 5.8 plot the total number of u's children and u's neighbors that it can overhear as a function of i (the hop-distance of node u) and k for different node densities and m. As expected, the total number of a node's children and neighbors that it can overhear generally increases with k.

The numerical results shown in Figures 5.5 to 5.8 indicate that when k decreases from m down to 3, the total number of a node's children and its neighbors that it can overhear would not be reduced much. When k is smaller than 3, this number decreases sharply with k. Recall that a large k generally leads to more parents for sensor nodes and hence more conflicting node pairs in scheduling and longer data collection schedules. Therefore, to maximize the robustness of data collection without unnecessarily increasing the latency of data collection, we propose to let each node send $k = 3$ parent-selection requests if $m \geq 3$ and send $k = m$ parent-selection requests if $m < 3$ in constructing the multi-path routing structure. This analytical result is used as a design guide line for our enhanced data collection scheme and shall be verified by the experimental results in Section 5.4.

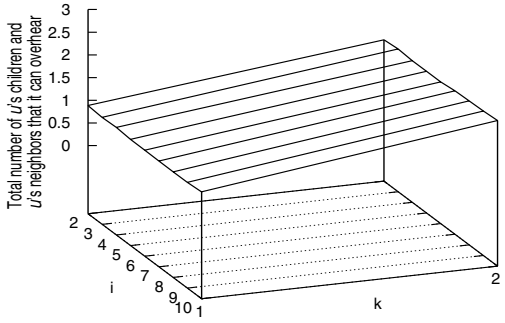

(a) $\rho\pi r^2 = 10$

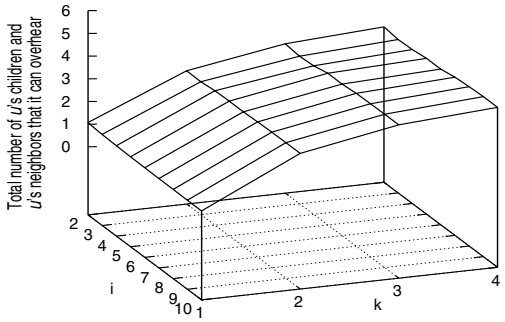

(b) $\rho\pi r^2 = 20$

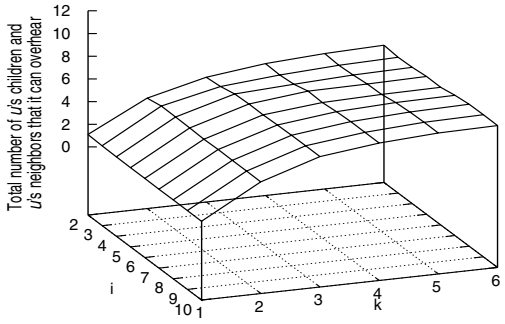

(c) $\rho\pi r^2 = 30$

Figure 5.5: Total number of u's children and u's neighbors that it can overhear. m is set at $0.2\rho\pi r^2$.

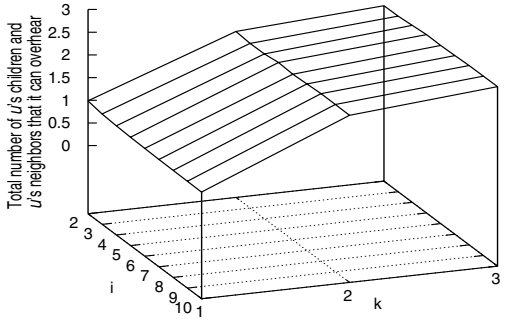

(a) $\rho\pi r^2 = 10$

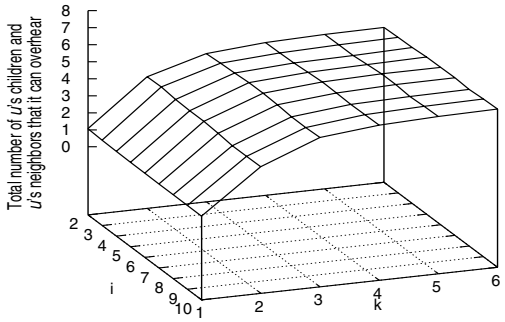

(b) $\rho\pi r^2 = 20$

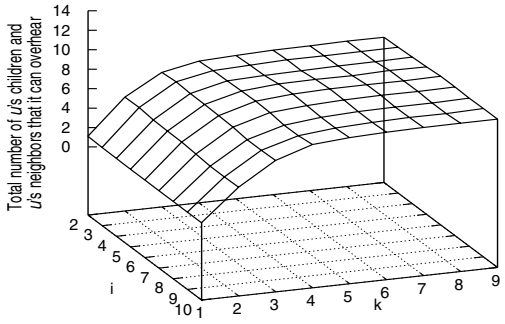

(c) $\rho\pi r^2 = 30$

Figure 5.6: Total number of u's children and u's neighbors that it can overhear. m is set at $0.3\rho\pi r^2$.

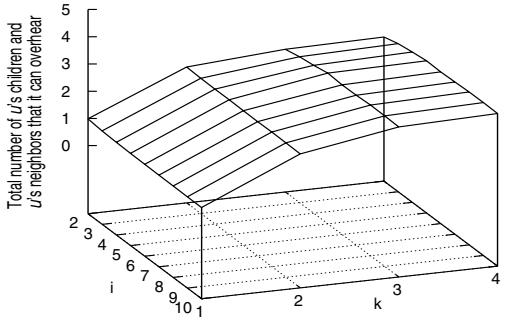

(a) $\rho\pi r^2 = 10$

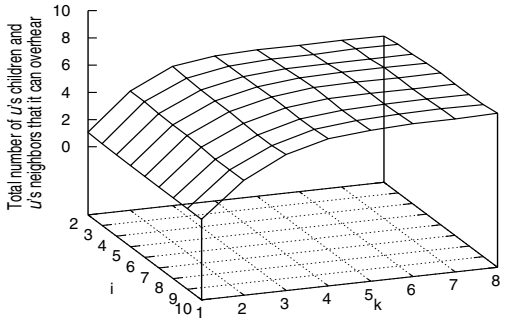

(b) $\rho\pi r^2 = 20$

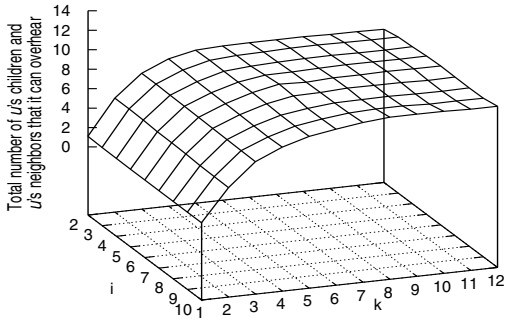

(c) $\rho\pi r^2 = 30$

Figure 5.7: Total number of u's children and u's neighbors that it can overhear. m is set at $0.4\rho\pi r^2$.

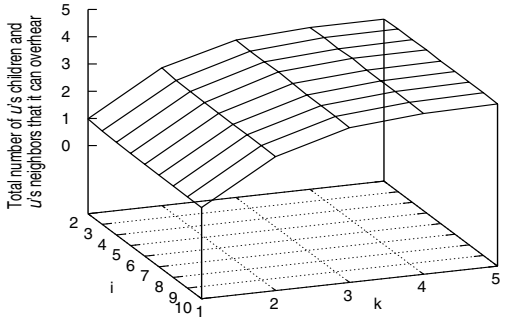

(a) $\rho\pi r^2 = 10$

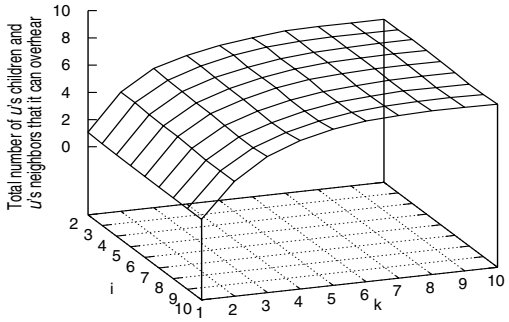

(b) $\rho\pi r^2 = 20$

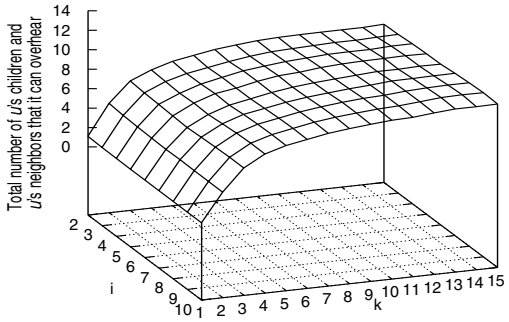

(c) $\rho\pi r^2 = 30$

Figure 5.8: Total number of u's children and u's neighbors that it can overhear. m is set at $0.5\rho\pi r^2$.

5.4 Performance evaluation

5.4.1 Experimental setup

We conducted simulation experiments to evaluate our proposed methods for constructing multi-path routing structures and collecting sensor data. We implemented the proposed methods for constructing multi-path routing structures and collecting sensor data using the same Prowler simulator as described in Section 3.4 of Chapter 3. Communication among sensor nodes in the construction processes of routing structures and data collection schedules is carried out using the default CSMA protocol in Prowler. As in Chapter 4, simple acknowledgments and retransmissions are used to guarantee message delivery in the scheduling process [LW03].

Both square and rectangular sensing fields were employed in our experiments. Sensor nodes were deployed at random in the field and the base station was placed at the center of the field. In the default settings, 400 sensor nodes were deployed in a square field of 150 m$\times$150 m or in a rectangular field of 75 m$\times$300 m. Besides the default settings, we also vary the node density and sensing field size over wide ranges in Sections 5.4.4 and 5.4.5 respectively to investigate their impacts on our proposed methods.

We made use of the distributed scheduling algorithm presented in Chapter 4 for constructing data collection schedules. On constructing the schedule, we simulated 1000 rounds of data collection to evaluate the robustness of data collection. As in Chapter 3, for simplicity, we assumed that the sizes of the aggregated data transmitted by sensor nodes to their parents in a round of data collection fit into one packet by means of digest-based representations [NGSA04,CLKB04]. The robustness of data collection was measured by the mean proportion of nodes whose acquired data reach the base station in a round of data collection. For comparison purpose, we also implemented a baseline scheme for constructing multi-path routing structures and collecting sensor data. In the baseline scheme, there is no limit on the number of receiving slots of sensor nodes (i.e., m is infinite). Each node simply chooses all neighbors that have longer hop-distances than it

as its children. For each experimental setting, we simulated 40 randomly generated node placements and plot the average results of these simulation runs for performance comparison together with the 99% confidence interval of the results.

5.4.2 Performance of the greedy and the threshold-based approaches for assigning hop-distances

Recall that we exploit the ring assignment methods presented in Chapter 3 to determine the hop-distances of sensor nodes for constructing multi-path routing structures. We first compare the localized threshold-based approach and the greedy approach of Chapter 3 for hop-distance assignment. In this experiment, we use the plain data collection scheme in which data are only propagated from children to parents in the constructed routing structure and no overhearing is exploited.

Figure 5.9(a) shows the robustness of data collection resulting from different hop-distance assignment approaches for the default square sensing field of 150 m $\times$ 150 m. Here, Greedy represents the greedy approach and LT represents the localized threshold-based approach for hop-distance assignment. In this experiment, we varied the maximum allowable number of receiving slots m from 1 to 10. As can be seen, the LT approach for hop-distance assignment leads to significantly higher robustness of data collection as compared to the greedy approach, which is consistent with the performance trends of the experimental results in Section 3.4. For example, when the maximum allowable number of receiving slots is 4, the LT approach leads to a robustness of about 67% while the greedy approach results in a robustness of less than 25%. This is because in the LT approach, sensor nodes are less likely to have few neighbors of shorter hop-distances due to the use of a threshold value. So, the LT approach reduces the chance for sensor nodes to have few parents in the constructed routing structure and thus improves the robustness of data collection. Meanwhile, due to the increase in the parent numbers of sensor nodes (see Figure 5.9(b)), the LT approach introduces more conflicting node pairs for scheduling. Therefore, as shown in Figure 5.9(c), the LT approach for hop-distance assignment generally leads to

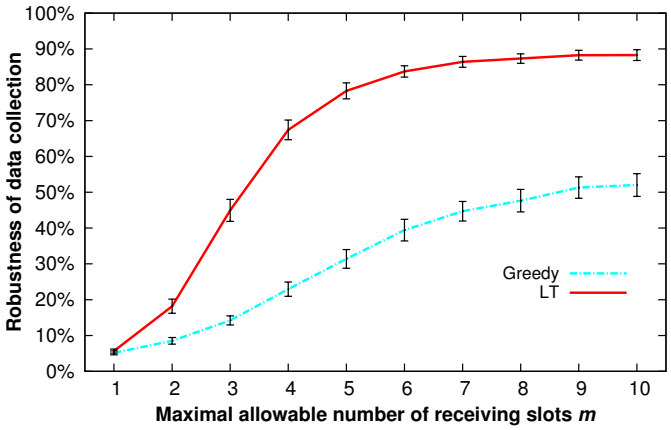

(a) Robustness of data collection

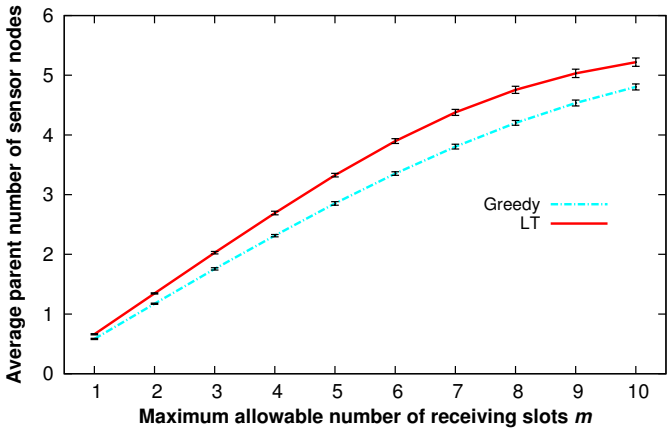

(b) Average parent number of sensor nodes

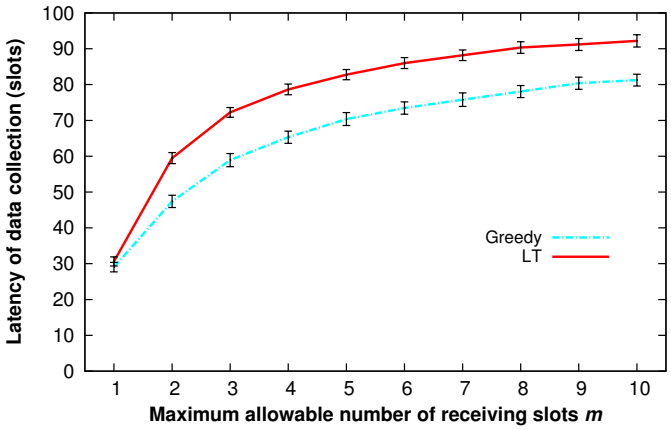

(c) Latency of data collection

Figure 5.9: Performance of different hop-distance assignment approaches for the default square sensing field. Error bars indicate the 99% confidence intervals of the results.

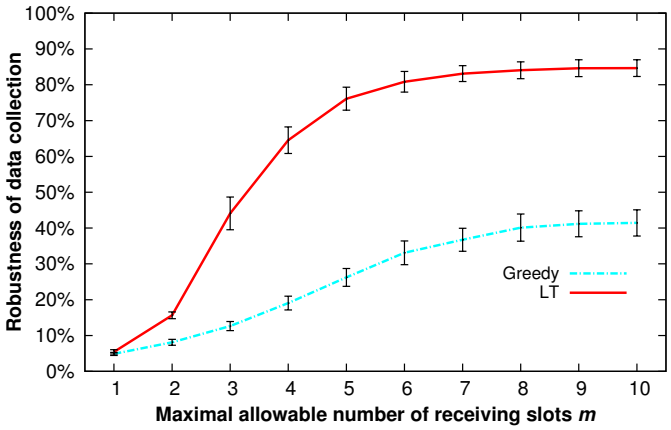

(a) Robustness of data collection

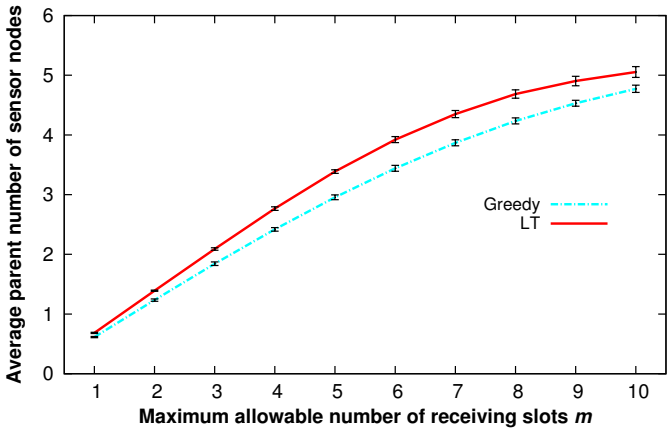

(b) Average parent number of sensor nodes

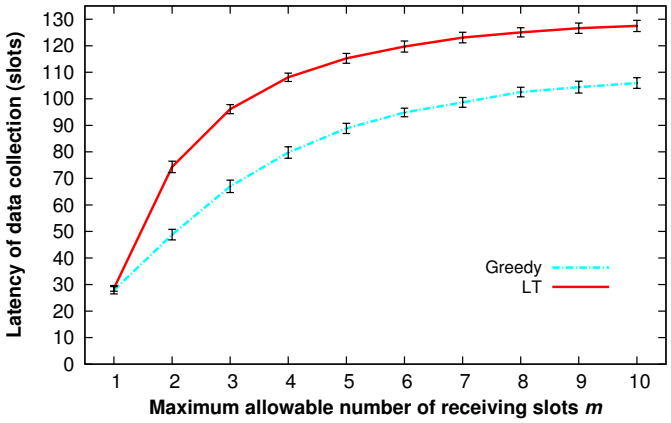

(c) Latency of data collection

Figure 5.10: Performance of different hop-distance assignment approaches for the default rectangular sensing field. Error bars indicate the 99% confidence intervals of the results.

slightly longer latency of data collection as compared to the greedy approach.

The results in Figures 5.9(a) and 5.9(c) show that at similar latency of data collection, the LT approach can significantly improve the robustness as well as the energy efficiency of data collection as compared to the greedy approach for hop-distance assignment. For example, the LT approach with $m = 4$ and the greedy approach with $m = 8$ offer similar latency of data collection (Figure 5.9(c)). The LT approach with $m = 4$ leads to much higher robustness of data collection than the greedy approach with $m = 8$ (Figure 5.9(a)). In addition, a smaller m value implies a higher level of energy efficiency for communication of the data collection process. Thus, the LT approach with $m = 4$ is more energy efficient than the greedy approach with $m = 8$.

Similarly, to achieve a certain level of robustness, the LT approach can offer higher energy efficiency with shorter latency of data collection as compared to the greedy approach. For example, the LT approach with $m = 3$ and the greedy approach with $m = 7$ both achieve a robustness of about 45%. The LT approach with $m = 3$ is more energy efficient than the greedy approach with $m = 7$ and also has slightly shorter latency of data collection than the greedy approach with $m = 7$.

Overall, the LT approach for hop-distance assignment achieves much better trade-offs among the latency, robustness and energy efficiency of data collection compared to the greedy approach. Similar performance trends are also observed from the results for the default rectangular sensing field as shown in Figures 5.10(a), 5.10(b) and 5.10(c). Therefore, in the following experiments, we employ the LT approach for hop-distance assignment in the construction of multi-path routing structures.

5.4.3 Performance of the proposed data collection schemes

Now, we compare our proposed plain and enhanced data collection schemes and the baseline scheme. In this experiment, we varied the maximum allowable number of receiving slots m from 1 to 10 and set k (the number of parent-selection requests sent by each node) equal to m.

Figure 5.11(a) shows the latency of data collection resulting from different data collection schemes for the default square sensing field. As expected, the latency of data collection resulting from the enhanced scheme is identical to that of the plain scheme since the enhanced scheme follows the same transmission schedule as the plain scheme. The plain and enhanced schemes consistently lead to shorter latency of data collection compared to the baseline scheme. This is because in the baseline scheme, sensor nodes do not limit their numbers of children, which would lead to more conflicting node pairs in scheduling. The improvement of our proposed schemes in the latency of data collection is more significant when m is smaller because the child numbers of sensor nodes decerase with m.

Figure 5.11(b) shows the robustness of data collection for different data collection schemes for the default square sensing field. When $m = 1$, each node can have at most one child in the routing structures constructed by our proposed schemes. Each node sends $k = m = 1$ parent-selection request to a parent candidate. If the parent-selection request sent by a node is denied by the parent candidate, this node together with all of its descendants would be disconnected from the base station. Thus, the robustness of data collection resulting from our schemes is low. In addition, when $m = 1$, there is little opportunity for nodes to overhear from their neighbors. Therefore, the plain and enhanced schemes have similar robustness of data collection. When m increases, the robustness of data collection resulting from our schemes increases rapidly. Figure 5.11(b) shows that the enhanced scheme significantly improves the robustness of data collection compared to the plain scheme. This demonstrates that letting sensor nodes overhear data from their neighbors effectively increases the chance for sensor data to be successfully delivered to the base station. When m goes beyond 5, the enhanced scheme even outperforms the baseline scheme in the robustness of data collection.

To achieve the same level of robustness, the enhanced scheme can reduce the latency of data collection. For example, the enhanced scheme at $m = 5$ achieves a similar level of robustness to the baseline scheme and has about 10% lower latency

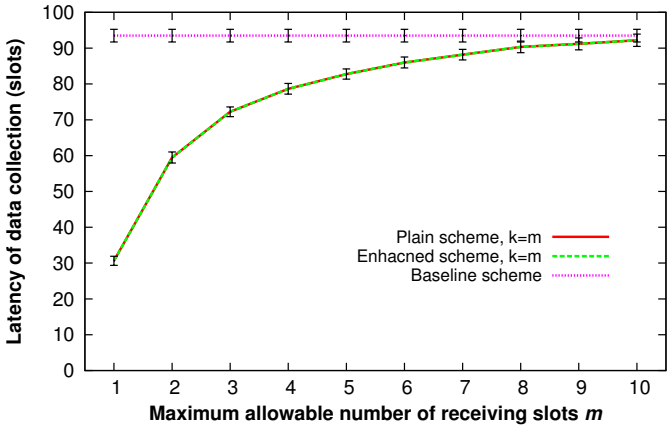

(a) Latency of data collection

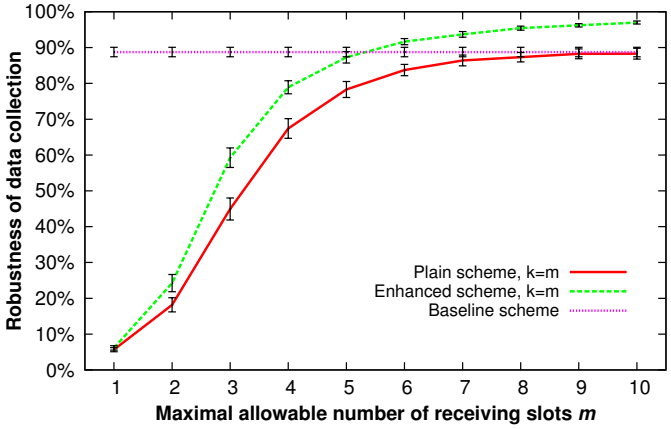

(b) Robustness of data collection

Figure 5.11: Performance of different data collection schemes for the default square sensing field. Error bars indicate the 99% confidence intervals of the results.

of data collection than the baseline scheme. Moreover, the baseline scheme which does not limit the child numbers of sensor nodes leads to a maximum number of about 16 receiving slots for sensor nodes in the data collection schedule. In contrast, in our schemes, the maximum number of receiving slots of sensor nodes is limited by m. Thus, the enhanced scheme at $m = 5$ can reduce the maximum energy consumption of sensor nodes in receiving data by $\frac{(16-5)}{16} = 69\%$. Since each node has only one transmission slot in the schedule, the energy consumption of each node in transmitting data is the same in all the schemes. Therefore, the enhanced scheme at $m = 5$ can substantially reduce the maximum energy

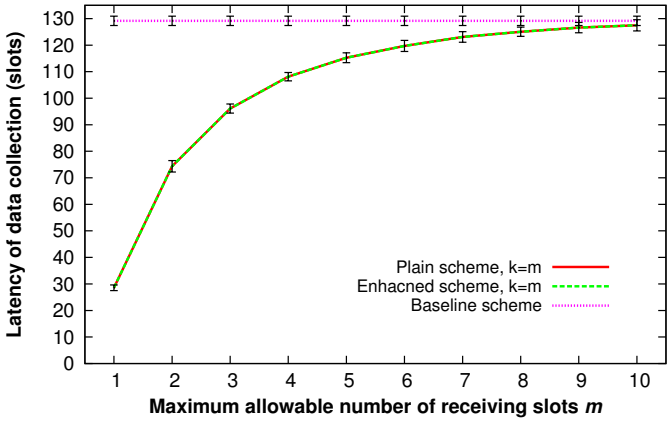

(a) Latency of data collection

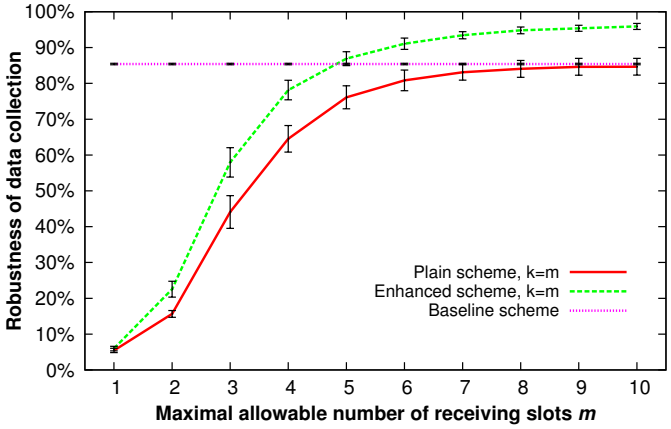

(b) Robustness of data collection

Figure 5.12: Performance of different data collection schemes for the default rectangular sensing field. Error bars indicate the 99% confidence intervals of the results.

consumption of sensor nodes in transmitting and receiving data compared to the baseline scheme. When m increases to 10, our enhanced scheme still reduces the maximum energy consumption of sensor nodes in receiving data by $\frac{(16-10)}{16} = 38\%$ and has similar latency of data collection compared to the baseline scheme. In this case, the enhanced scheme outperforms the baseline scheme by 10% in the robustness of data collection. These results demonstrate that our enhanced scheme with $k = m$ achieves better trade-offs among the robustness, latency and energy efficiency of data collection as compared to the baseline scheme. Similar performance trends are also observed from the results for the default rectangular

sensing field as shown in Figure 5.12.

The results in Figures 5.11 and 5.12 have shown the performance of the enhanced scheme with $k = m$. To evaluate the impact of different k values, we varied k from 1 to m and plotted the performance of the enhanced scheme for different m values in Figures 5.13 and 5.14. The results in Figures 5.13(a) and 5.14(a) show that when k decreases from m to 3, the average number of receiving slots of sensor nodes (including the receiving slots to hear from children and the receiving slots to overhear from neighbors) remain quite stable. When k continues to decrease below 3, the average number of receiving slots decreases remarkably. This performance trend is consistent with the analytical results as shown in Figures 5.5 to 5.8. Since the number of propagation paths from sensor nodes to the base station decreases with decreasing number of receiving slots of sensor nodes, as shown in Figures 5.13(b) and 5.14(b), the robustness of data collection follows the same trend as the average number of receiving slots: the robustness remains almost unchanged when k decreases from m to 3 and drops rapidly when k continues to decrease below 3. Figures 5.13(c) and 5.14(c) show that the latency of data collection generally decreases with decreasing k values. This is because a smaller k value results in fewer parents of sensor nodes in the constructed routing structure and thus fewer conflicting node pairs in scheduling. Overall, setting $k = 3$ in the enhanced scheme is able to produce high robustness without introducing unnecessarily long latency of data collection.

Figures 5.15 and 5.16 compare the performance of the enhanced scheme with k set at 3 if $m \geq 3$ and set at m if $m < 3$ against other schemes. As seen from Figure 5.15(a), when m increases, the latency of data collection resulting from the plain scheme and the enhanced scheme with $k = m$ steadily increases from about 30 to 92 time slots in the default square sensing field. In contrast, when m goes beyond 3, the latency of data collection resulting from the enhanced scheme with $k = \min(m, 3)$ becomes stable at only 78 time slots. Figure 5.15(b) shows that the enhanced scheme with $k = \min(m, 3)$ achieves a similar level of robustness as compared to the enhanced scheme with $k = m$. Under the same m value, the enhanced scheme with $k = \min(m, 3)$ also has the same maximum energy

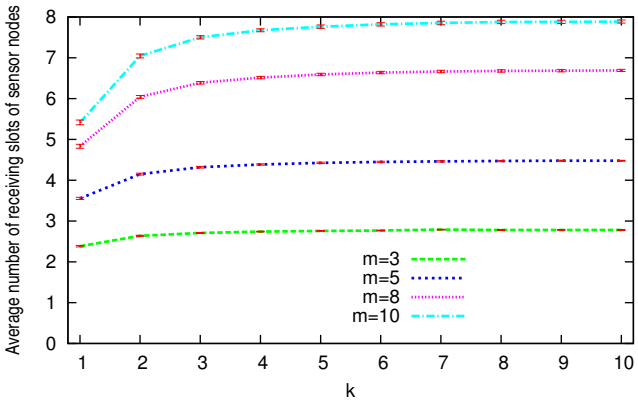

(a) Average number of receiving slots of sensor nodes

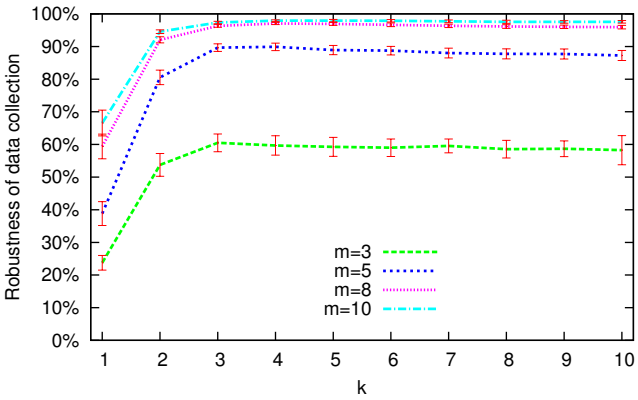

(b) Robustness of data collection

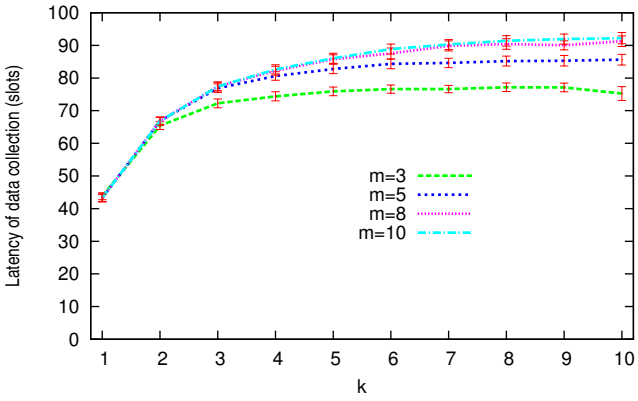

(c) Latency of data collection

Figure 5.13: Performance of the enhanced data collection scheme with different k values for the default square sensing field. Error bars indicate the 99% confidence intervals of the results.

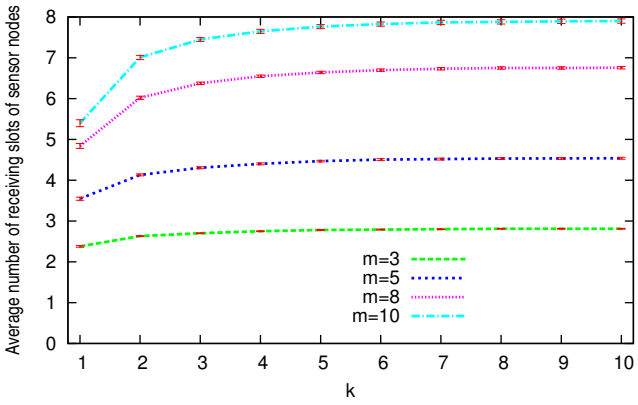

(a) Average number of receiving slots of sensor nodes

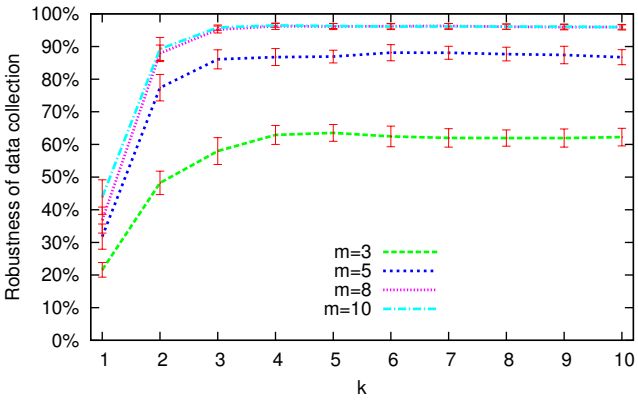

(b) Robustness of data collection

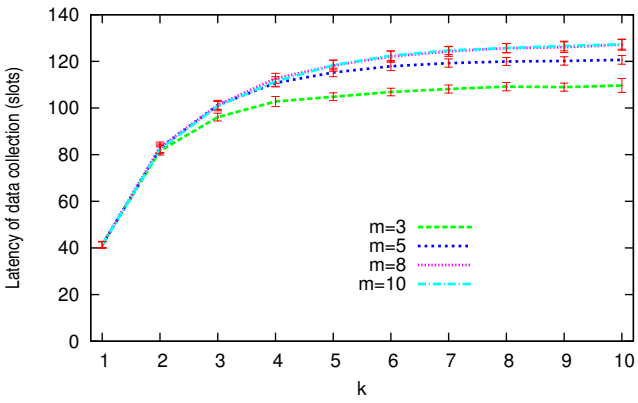

(c) Latency of data collection

Figure 5.14: Performance of the enhanced data collection scheme with different k values for the default rectangular sensing field. Error bars indicate the 99% confidence intervals of the results.

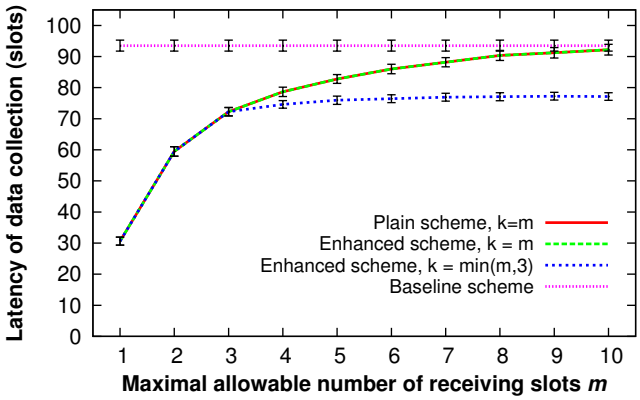

(a) Latency of data collection

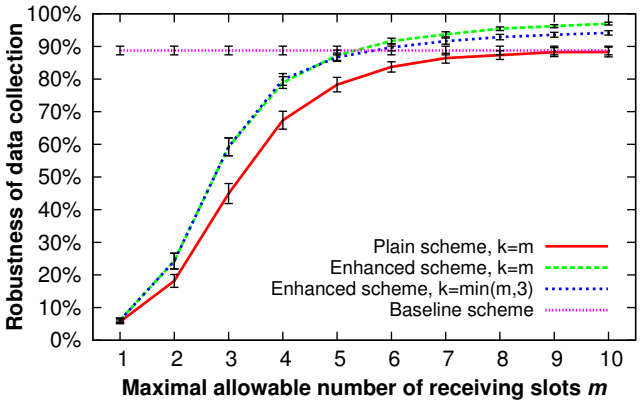

(b) Robustness of data collection

Figure 5.15: Performance of the enhanced data collection scheme with $k = \min(m, 3)$ for the default square sensing field. Error bars indicate the 99% confidence intervals of the results.

consumption of sensor nodes for communication as the enhanced scheme with $k = m$. These results show that the enhanced scheme with $k = \min(m, 3)$ achieves even better trade-offs among the robustness, latency and energy efficiency of data collection compared to the enhanced scheme with $k = m$. Similar performance trends are also observed from the results for the default rectangular sensing field as shown in Figure 5.16.

5.4.4 Impact of node density

To examine the impact of node density, we increased the number of sensor nodes in the network from 200 to 900 while keeping the square sensing field size at

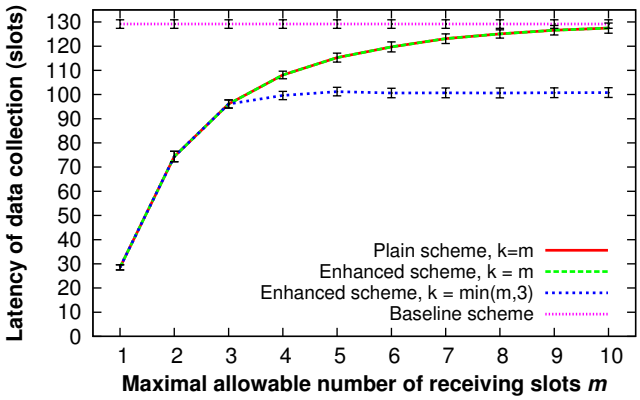

(a) Latency of data collection

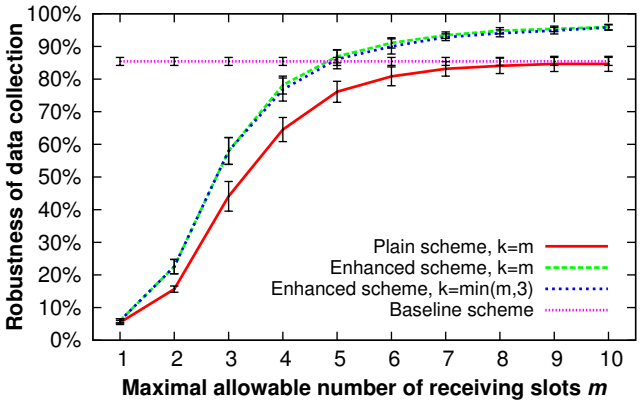

(b) Robustness of data collection

Figure 5.16: Performance of the enhanced data collection scheme with $k = \min(m, 3)$ for the default rectangular sensing field. Error bars indicate the 99% confidence intervals of the results.

150 m × 150 m and the rectangular sensing field size at 75 m × 300 m. In this way, the average node degree increases from 12.7 to 57.7 for the square sensing field, and increases from 12.3 to 55.4 for the rectangular sensing field. In these experiments, m was set at 10. Figures 5.17 and 5.18 compare the performance of the baseline scheme, the plain scheme with $k = m$ and the enhanced scheme with $k = \min(m, 3) = 3$.

As shown in Figures 5.17(a) and 5.18(a), when the node density increases, the latency of data collection resulting from the enhanced scheme with $k = 3$ increases much slower than the other two schemes and is consistently shorter than the other two schemes. On the other hand, the latency performance of the

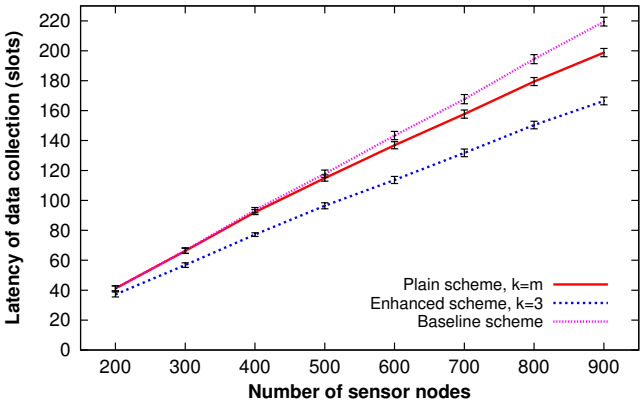

(a) Latency of data collection

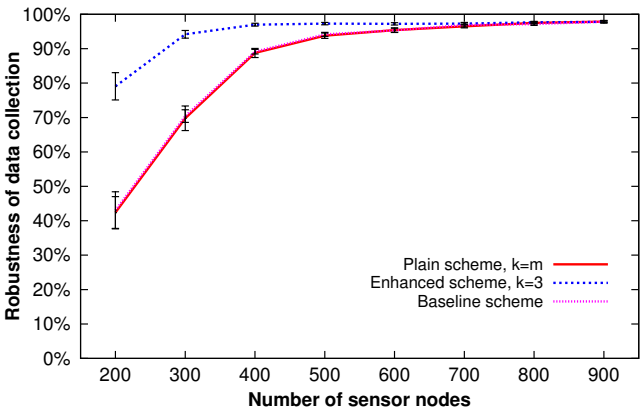

(b) Robustness of data collection

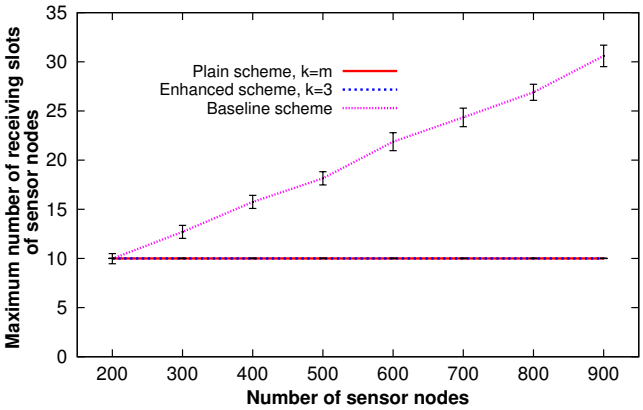

(c) Maximum number of receiving slots of sensor nodes

Figure 5.17: Performance of different data collection schemes at different node densities in the square sensing field. Error bars indicate the 99% confidence intervals of the results.

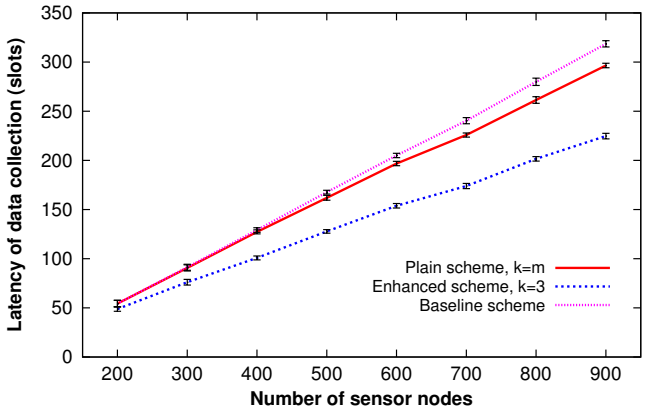

(a) Latency of data collection

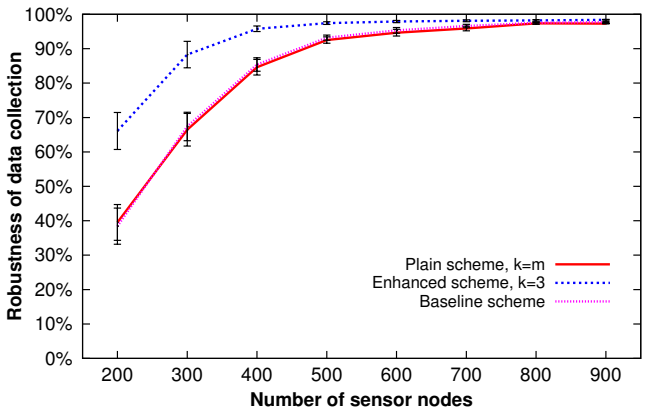

(b) Robustness of data collection

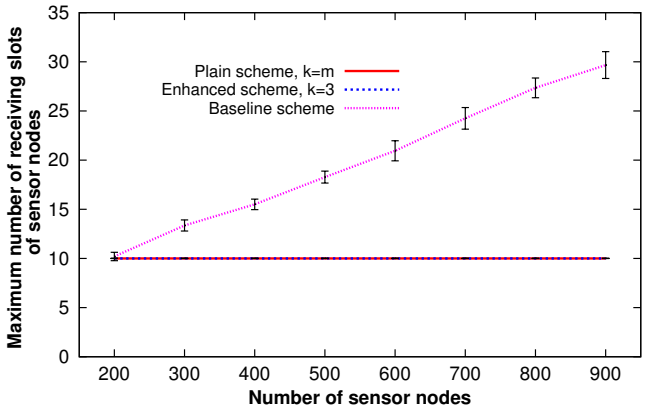

(c) Maximum number of receiving slots of sensor nodes

Figure 5.18: Performance of different data collection schemes at different node densities in the rectangular sensing field. Error bars indicate the 99% confidence intervals of the results.

baseline scheme is always the worst among the three schemes.

Figures 5.17(b) and 5.18(b) show that the robustness of data collection increases with node density for all the three schemes. At low node densities, the enhanced scheme with $k = 3$ significantly improves the robustness of data collection compared to the other two schemes. This again demonstrates the effectiveness of overhearing in the enhanced scheme. At high node densities, the robustness resulting from all the three schemes becomes similar because in either scheme, the sensor nodes have sufficiently large numbers of propagation paths to the base station.

Figures 5.17(c) and 5.18(c) show that in the baseline scheme, the maximum number of receiving slots of sensor nodes increases rapidly with node density. In contrast, the maximum number of receiving slots of sensor nodes in our proposed schemes is kept constant at $m = 10$.

The results in Figures 5.17 and 5.18 demonstrate that our enhanced scheme with $k = 3$ effectively improves the robustness and energy efficiency of data collection and reduces the latency of data collection compared to the baseline scheme across a wide range of node densities.

5.4.5 Impact of network size

To examine the impact of network size, we kept the average node density at 4/225 node per square meter and varied the sensing field size. The square sensing field size was varied from 50 m $\times$ 50 m to 500 m $\times$ 500 m, and the rectangular sensing field size was varied from 75 m $\times$ 100 m to 75 m $\times$ 1900 m. In these experiments, m was set at 10. Figures 5.19 and 5.20 compare the performance of the baseline scheme, the plain scheme with $k = m$ and the enhanced scheme with $k = \min(m, 3) = 3$.

As seen from Figures 5.19(a) and 5.20(a), the latency of data collection increases with network size for all three schemes. The enhance scheme with $k = 3$ consistently results in lower latency of data collection than the other two schemes. Figures 5.19(b) and 5.20(b) show that the robustness resulting from the enhanced scheme is consistently higher than that of the other two schemes, which implies

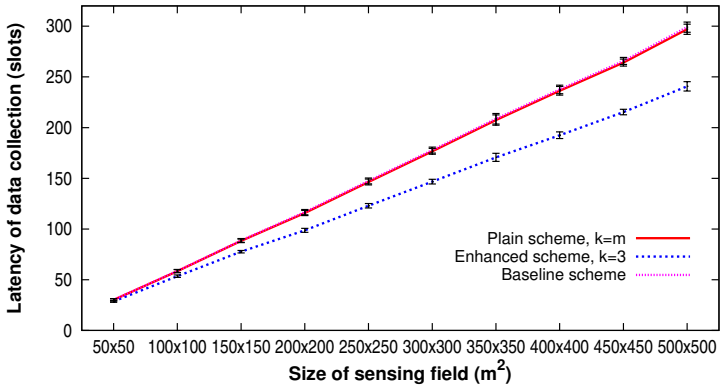

(a) Latency of data collection

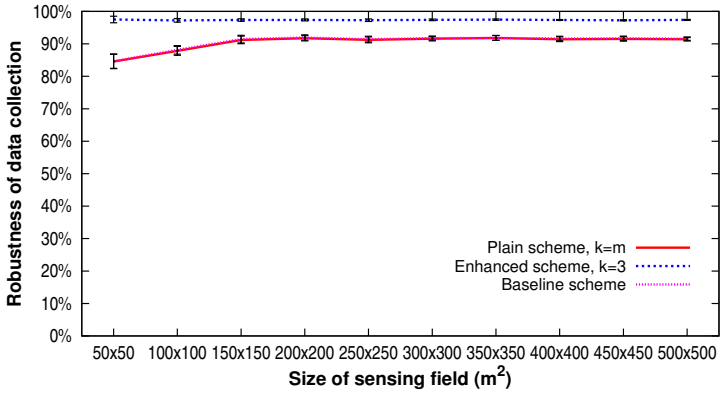

(b) Robustness of data collection

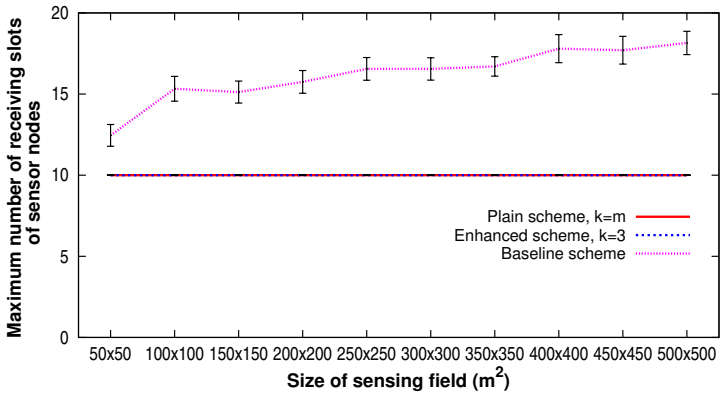

(c) Maximum number of receiving slots of sensor nodes

Figure 5.19: Performance of different data collection schemes for different square field sizes. Error bars indicate the 99% confidence intervals of the results.

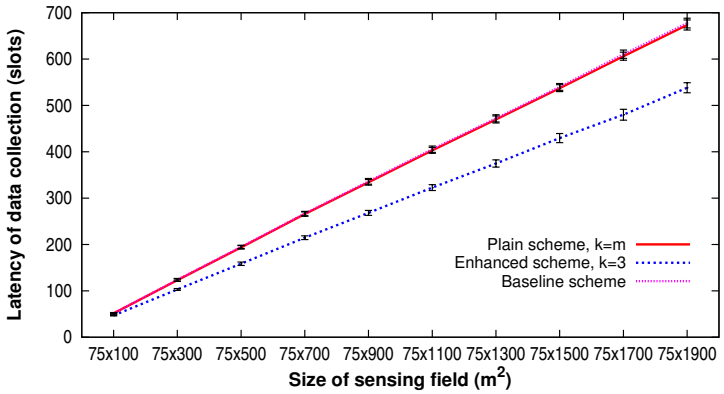

(a) Latency of data collection

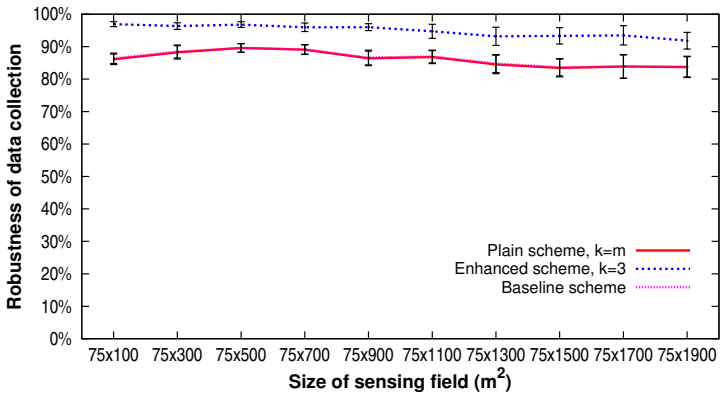

(b) Robustness of data collection

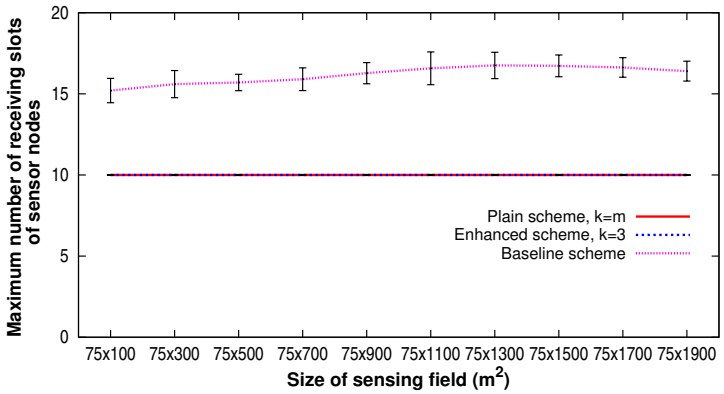

(c) Maximum number of receiving slots of sensor nodes

Figure 5.20: Performance of different data collection schemes for different rectangular field sizes. Error bars indicate the 99% confidence intervals of the results.

the effectiveness of overhearing in the enhanced scheme. Figures 5.19(c) and 5.20(c) show that the maximum number of receiving slots of sensor nodes in the baseline scheme is normally above 15 across different network sizes while the maximum number of receiving slots of sensor nodes in our proposed schemes is only $m = 10$. These results again demonstrate that our proposed enhanced scheme with $k = 3$ can considerably improve the robustness and energy efficiency of data collection and reduce the latency of data collection compared to the baseline scheme across a wide range of network sizes.

5.5 Summary

In this chapter, we have presented a distributed method for constructing multi-path routing structures and developed an enhanced scheme for sensor data collection. The proposed method for constructing multi-path routing structures achieves a required level of energy efficiency for communication by limiting the number of receiving slots of sensor nodes. The enhanced data collection scheme exploits the broadcast nature of wireless communication so that sensor nodes can overhear data from their neighbors in order to improve the robustness of data collection. Experimental results show that our proposed methods achieve better trade-offs among the robustness, latency and energy efficiency of data collection.

Chapter 6

Conclusion

In this thesis, we have focused on collecting data acquired by sensor nodes in wireless sensor networks through multi-path routing structures. Multi-path routing is an important approach for robust sensor data collection against failures in wireless communication among sensor nodes. The robustness of data collection directly affects the accuracy of the collected data. In addition to improving the robustness of sensor data collection, we have also considered two other quality measurements of sensor data collection: energy efficiency and time efficiency. Energy efficiency is critical to many sensor network applications since the energy supplies of sensor nodes are limited. It may not be feasible to replace or recharge the energy supplies of sensor nodes in many situations especially when sensor nodes are deployed in harsh environments beyond the reach of network operators. Time efficiency is also of primary importance to many sensor network applications due to the real-time nature of monitoring applications. These quality measurements of robustness, energy efficiency and time efficiency are inter-related in that improving one quality measurement may affect other quality measurements at the same time.

In this thesis, we have developed several new techniques for improving the robustness, energy efficiency and latency of sensor data collection in error-prone communication environments. In this chapter, we summarize our contributions and discuss some directions for future research.

6.1 Our proposed methods and contributions

Our proposed methods and contributions in this thesis are summarized as follows:

1. To improve the robustness of data collection against communication failures, we have designed a distributed approach for organizing sensor nodes into different rings around the base station to construct a rings overlay. Rings overlay is a class of multi-path routing structures that makes use of the broadcast nature of wireless communication for transporting sensor data through multiple interleaving propagation paths to the base station. The objective of our proposed approach is to assign sensor nodes to appropriate rings to prevent sensor nodes from having only few propagation paths to the base station and let as many nodes benefit from multi-path routing as possible. The proposed ring assignment approach is fully distributed and does not require sensor nodes to have global knowledge about the entire network. We have also designed and analyzed an enhanced scheme for relaying data to the base station from the sensor nodes that are one hop away from the base station. The goal is to improve the resilience of these nodes to communication failures without requiring them to transmit their data multiple times. Experimental results show that compared with a baseline greedy construction approach and the original relay scheme, the proposed techniques of overlay construction and relay enhancement significantly improve the robustness and accuracy of sensor data collection through the rings overlay.

2. We have proposed a multi-path sensor data collection scheme that considers the energy efficiency for communication, the time efficiency and the robustness of data collection altogether. The proposed scheme consists of a distributed method for constructing multi-path routing structures for TDMA-based sensor data collection and an enhanced data collection scheme. Our proposed method constructs multi-path routing structures in which the number of messages that each node transmits and receives in a round of data collection is kept within a given limit in order to achieve a required

level of energy consumption for communication. In the enhanced data collection scheme, sensor nodes exploit overhearing to receive data from their neighbors other than those in the multi-path routing structures constructed, thereby increasing the numbers of data propagation paths from sensor nodes to the base station. The goal of the enhanced scheme is to improve the robustness of data collection without sacrificing the latency of data collection and violating the required level of energy efficiency. We have analyzed the control parameter setting in the enhanced data collection scheme for maximizing the benefits of overhearing. Experimental results show that our proposed methods achieve significantly better trade-offs among the robustness, latency and energy efficiency of data collection.

3. We have proposed an efficient distributed scheduling algorithm for TDMA-based sensor data collection through multi-path routing structures. Our proposed scheduling algorithm is designed to reduce the message complexity and the running time of the scheduling process as much as possible. We have also developed a method for deriving a lower bound on the shortest possible latency of data collection through a given routing structure. The lower bound latency estimation offers a practical method to evaluate the time efficiency of data collection schedules produced by scheduling algorithms. Experimental results show that our proposed scheduling algorithm greatly reduces the number of messages transmitted in the scheduling process and has much shorter running time as compared to an existing algorithm. The length of the data collection schedule produced by our algorithm is normally within 1.5 times of the lower bound estimate across a wide range of network settings.

6.2 Future research directions

Efficient sensor data collection in error-prone communication environments has increasingly become an important issue in wireless sensor networks. There are opportunities for more research on improving various quality measurements of

data collection in large-scale sensor networks. In this section, we discuss some interesting directions for future research.

1. Various aggregation techniques [NGSA04, SBAS04] have been developed for reducing network traffic and improving the energy efficiency of sensor data collection. However, most of these techniques are able to support only simple aggregates such as average or median and simple types of data such as single numerical values. Designing and analyzing new aggregation techniques to support more complex types of aggregates and new types of data such as multi-dimensional location information would be an interesting research direction.

2. Time efficiency is an important quality measurement of data collection due to the real-time nature of monitoring applications. As shown in Sections 4.4 and 5.4, the latency of data collection increases rapidly with the size of the network. In order to meet a strict latency requirement of sensor data collection in large-scale networks, the networks may have to be partitioned into smaller parts and multiple base stations would need to be deployed to collect data from different parts of the networks. However, due to many constraints relating to the costs of deploying and maintaining a base station, the number of base stations deployed in a sensor network should be minimized. There has not been much work on sensor network partitioning for guaranteeing a required time latency of data collection. In addition, the locations of base stations must be carefully selected since they also strongly affect the time efficiency of sensor data collection.

3. In addition to coping with communication failures, sensor network applications would also need to deal with hardware failures of sensor nodes. When node failures occur in TDMA-based data collection, both the multi-path routing structure and the schedules of sensor nodes would need to be adjusted together. In addition, security services would have to be designed to alert network operators when node failures occur at some critical parts of the network. These are both important and practical requirements of many

sensor network applications. More research on these issues would be very useful.

4. Beside the periodic data collection scenario discussed in our thesis, there exists another data collection scenario in which different sensor nodes can report data at different rates to the base station. For example, in an approximate data collection, a sensor node would report data to the base station in a round of data collection only if its acquired data is significantly different from the data it acquired in the previous round. Thus, the data reporting rates of different sensor nodes may be different. To support this data collection scenario, we would need to design flexible data collection schedules that support different traffic requirements. This is an interesting research direction that deserves more work in the future.

5. In Chapter 5, we separate the scheduling and overhearing slot assignment processes from the construction of routing structures in order to make the scheduling algorithm and the enhanced data collection scheme independent of the underlying routing structures. As a result, our proposed data collection scheduling algorithm and enhanced data collection scheme can be applied to any existing multi-path or single-path routing structures. On the other hand, a joint optimization on the construction of routing structures together with the scheduling and overhearing slot assignment processes might further improve the performance of the resultant data collection scheme. It would be an interesting future direction to investigate the possible benefit and cost of such joint optimization.

Appendix A

List of publications

During the thesis research, I have published the following articles:

1. H. V. Luu and X. Tang. "On the Construction of Rings Overlay for Robust Data Collection in Wireless Sensor Networks." In Proceedings of the 2010 IEEE Wireless Communications and Networking Conference (WCNC), 6 pages, Sydney, Australia, April 2010.

2. H. V. Luu and X. Tang. "An Enhanced Relay Scheme for Robust Data Collection through Rings Overlay in Wireless Sensor Networks." In Proceedings of the 2010 IEEE Wireless Communications and Networking Conference (WCNC), 6 pages, Sydney, Australia, April 2010.

3. H. V. Luu and X. Tang. "An Efficient Scheduling Algorithm for Data Collection through Multi-path Routing Structures in Wireless Sensor Networks." In Proceedings of the 6th International Conference on Mobile Ad-hoc and Sensor Networks (MSN), pp. 68-73, Hangzhou, China, December 2010.

4. H. V. Luu and X. Tang. "An Efficient Multi-Path Data Collection Scheme in Wireless Sensor Networks." In Proceedings of the 31st IEEE International Conference on Distributed Computing Systems (ICDCS) Workshops, pp. 198-207, Minneapolis, MN, USA, June 2011.

5. H. V. Luu and X. Tang. "An Efficient Data Collection Scheme through Multi-path Routing Structures in Wireless Sensor Networks." Accepted to appear in International Journal of Sensor Networks.

Bibliography

[AS72] M. Abramowitz and I. A. Stegun. *Elliptic Integrals. Ch. 17*, pages 587–607. Dover, New York, 1972. 40

[ASSC02] I. F. Akyildiz, W. Su, Y. Sankarasubramaniam, and E. Cayirci. Wireless sensor networks: a survey. *Computer Networks*, 38(4):393–422, 2002. 11, 43

[AYY02] K. Arisha, M. Youssef, and M. Younis. Energy-aware tdma-based mac for sensor networks. In *Proceedings of IEEE Workshop on Integrated Management of Power Aware Communications, Computing and Networking, 2002*, pages 21–40. IEEE, 2002. 24

[BAS05] C. Buragohain, D. Agrawal, and S. Suri. Power aware routing for sensor databases. In *Proceedings of the 24th Annual Joint Conference of the IEEE Computer and Communications Societies (INFOCOM), 2005*, volume 3. IEEE, 2005. 103

[BCL03] A. Boukerche, X. Cheng, and J. Linus. Energy-aware data-centric routing in microsensor networks. In *Proceedings of the 6th ACM International Workshop on Modeling Analysis and Simulation of Wireless and Mobile Systems (MSWiM), 2003*, pages 42–49. ACM, 2003. 19

[BM04] S. Biswas and R. Morris. Opportunistic routing in multi-hop wireless networks. *ACM SIGCOMM Computer Communication Review*, 34(1):69–74, 2004. 13

[BTn07] BTnode. Btnode rev3 platform. `http://www.btnode.ethz.ch/Main/Overview`, 2007. 25

[CDHH06] D. Chu, A. Deshpande, J.M. Hellerstein, and W. Hong. Approximate data collection in sensor networks using probabilistic models. In *Proceedings of the 22nd International Conference on Data Engineering, 2006. ICDE'06.*, pages 48–48. IEEE, 2006. 18

[CDNS06] I. Chatzigiannakis, T. Dimitriou, S. Nikoletseas, and P. Spirakis. A probabilistic algorithm for efficient and robust data propagation in wireless sensor networks. *Ad Hoc Networks*, 4(5):621–635, 2006. 16

[CHF+06] Q. Cao, T. He, L. Fang, T. Abdelzaher, J. Stankovic, and S. Son. Efficiency centric communication model for wireless sensor networks. In *Proceedings of the 25th IEEE International Conference on Computer Communications (INFOCOM), 2006*, volume 6. IEEE, 2006. 12, 43

[CHZ05] X. Chen, X. Hu, and J. Zhu. Minimum data aggregation time problem in wireless sensor networks. In *Proceedings of 1st International Conference on Mobile Ad-hoc and Sensor Networks (MSN), 2005*, pages 133–142. Springer, 2005. 27, 79

[CLJ06] H. Cheng, Q. Liu, and X. Jia. Heuristic algorithms for real-time data aggregation in wireless sensor networks. In *Proceedings of the International Conference on Wireless Communications and Mobile Computing, 2006*, pages 1123–1128. ACM, 2006. 14

[CLKB04] J. Considine, F. Li, G. Kollios, and J. Byers. Approximate aggregation techniques for sensor databases. In *Proceedings of the 20th International Conference on Data Engineering (ICDE), 2004*, pages 449–460. IEEE, 2004. ii, 4, 19, 29, 32, 33, 56, 57, 76, 103, 121

[CLL+06] J.Y. Choi, J.W. Lee, K. Lee, S. Choi, W.H. Kwon, and H.S. Park. Aggregation time control algorithm for time constrained data delivery in wireless sensor networks. In *Proceedings of the 63rd IEEE Vehicular Technology Conference (VTC), 2006*, volume 2, pages 563–567. IEEE, 2006. 15

[Cro09a] Crossbow. Crossbows micaz mote. `http://bullseye.xbow.com:81/Products/productdetails.aspx?sid=191`, 2009. 25

[Cro09b] Crossbow. Crossbows telosb mote. `http://bullseye.xbow.com:81/Products/productdetails.aspx?sid=252`, 2009. 24

[CY07] M. Cheng and L. Yin. Transmission Scheduling in Sensor Networks via Directed Edge Coloring. In *Proceedings of IEEE International Conference on Communications (ICC), 2007*, pages 3710–3715, 2007. 25

[DCX03] M. Ding, X. Cheng, and G. Xue. Aggregation tree construction in sensor networks. In *Proceedings of the 58th IEEE Vehicular Technology Conference (VTC), 2003*, volume 4, pages 2168–2172. IEEE, 2003. 14

[DEA06] I. Demirkol, C. Ersoy, and F. Alagoz. MAC protocols for wireless sensor networks: a survey. *IEEE Communications Magazine*, 44(4):115–121, 2006. 3, 5, 21, 74

[DEO09] I. Demirkol, C. Ersoy, and E. Onur. Wake-up receivers for wireless sensor networks: benefits and challenges. *Wireless Communications*, 16(4):88–96, 2009. 19

[DGGR04] A. Dobra, M. Garofalakis, J. Gehrke, and R. Rastogi. Sketch-based multi-query processing over data streams. *Advances in Database Technology*, pages 621–622, 2004. 20

[DKN03] K. Dasgupta, K. Kalpakis, and P. Namjoshi. An efficient clustering-based heuristic for data gathering and aggregation in sensor networks. In *Proceedings of IEEE Wireless Communications and Networking Conference (WCNC), 2003*, volume 3, pages 1948–1953. IEEE, 2003. 14

[DSW06] A.G. Dimakis, A.D. Sarwate, and M.J. Wainwright. Geographic gossip: efficient aggregation for sensor networks. In *Proceedings of the 5th International Conference on Information Processing in Sensor Networks (IPSN), 2006*, pages 69–76. ACM, 2006. 13

[EHD04] A. El-Hoiydi and J.D. Decotignie. Wisemac: an ultra low power mac protocol for the downlink of infrastructure wireless sensor networks. In *Proceedings of the 9th International Symposium on Computers and Communications (ISCC), 2004*, volume 1, pages 244–251. IEEE, 2004. 23

[GDP05] S. Gandham, M. Dawande, and R. Prakash. Link scheduling in sensor networks: distributed edge coloring revisited. In *Proceedings of the 24th Annual Joint Conference of the IEEE Computer and Communications Societies (INFOCOM), 2005*, volume 4, 2005. 5, 25, 74, 76, 100

[GGSE01] D. Ganesan, R. Govindan, S. Shenker, and D. Estrin. Highly-resilient, energy-efficient multipath routing in wireless sensor networks. *ACM SIGMOBILE Mobile Computing and Communications Review*, 5(4):11–25, 2001. 16

[GGW+06] T. Gao, D. Greenspan, M. Welsh, R. Juang, and A. Alm. Vital signs monitoring and patient tracking over a wireless network. In *Proceedings of the 27th Annual International Conference of the Engineering in Medicine and Biology Society (EMBS), 2005*, pages 102–105. IEEE, 2006. 1

[GKS03] S. Ganeriwal, R. Kumar, and M.B. Srivastava. Timing-sync protocol for sensor networks. In *Proceedings of the 1st International Conference on Embedded Networked Sensor Systems (SenSys), 2003*, pages 138–149. ACM, 2003. 32

[GKW+02] D. Ganesan, B. Krishnamachari, A. Woo, D. Culler, D. Estrin, and S. Wicker. Complex behavior at scale: An experimental study of low-power wireless sensor networks. Technical Report Technical Report CS TR 02-0013, University of California, Los Angeles, 2002. 3, 8

[GZH06] S. Gandham, Y. Zhang, and Q. Huang. Distributed minimal time convergecast scheduling in wireless sensor networks. In *Proceedings of the 26th IEEE International Conference on Distributed Computing Systems (ICDCS), 2006*, pages 50–50. IEEE, 2006. 76

[GZH08] S. Gandham, Y. Zhang, and Q. Huang. Distributed time-optimal scheduling for convergecast in wireless sensor networks. *Computer Networks*, 52(3):610–629, 2008. 18

[HBC+09] W. Hu, N. Bulusu, C.T. Chou, S. Jha, A. Taylor, and V.N. Tran. Design and evaluation of a hybrid sensor network for cane toad monitoring. *ACM Transactions on Sensor Networks (TOSN)*, 5(1):1–28, 2009. 1

[HC02] J.L. Hill and D.E. Culler. Mica: A wireless platform for deeply embedded networks. *IEEE Micro*, 22(6):12–24, 2002. 1, 8

[HCB00] W.R. Heinzelman, A. Chandrakasan, and H. Balakrishnan. Energy-efficient communication protocol for wireless microsensor networks. In *Proceedings of the 33rd Annual Hawaii International Conference on System Sciences, 2000*, page 10, 2000. 19, 79

[HCB02] W.R. Heinzelman, A. Chandrakasan, and H. Balakrishnan. Energy-efficient communication protocol for wireless microsensor networks. In *Proceedings of the 33rd Annual Hawaii International Conference on System Sciences, 2002*, pages 10–pp. IEEE, 2002. 15

[HKS+04] T. He, S. Krishnamurthy, J.A. Stankovic, T. Abdelzaher, L. Luo, R. Stoleru, T. Yan, L. Gu, J. Hui, and B. Krogh. Energy-efficient surveillance system using wireless sensor networks. In *Proceedings of the 2nd International Conference on Mobile Systems, Applications, and Services (MobiSys), 2004*, pages 270–283. ACM, 2004. 2

[HM06] J.K. Hart and K. Martinez. Environmental Sensor Networks: A revolution in the earth system science? *Earth-Science Reviews*, 78(3-4):177–191, 2006. 2

[HSC06] C.S. Hwang, K. Seong, and J.M. Cioffi. Opportunistic p-persistent csma in wireless networks. In *Proceedings of the IEEE International Conference on Communications (ICC), 2006*, volume 1, pages 183–188. IEEE, 2006. 21

[HSW+00] J. Hill, R. Szewczyk, A. Woo, S. Hollar, D. Culler, and K. Pister. System architecture directions for networked sensors. *ACM Sigplan Notices*, 35(11):104, 2000. 55

[HWV+07] S.C.H. Huang, P.J. Wan, CT Vu, Y. Li, and F. Yao. Nearly constant approximation for data aggregation scheduling in wireless sensor networks. In *Proceedings of the 26th IEEE International Conference on Computer Communications (INFOCOM), 2007*, pages 366–372, 2007. 27, 79

[HYJ06] Y. Hu, N. Yu, and X. Jia. Energy efficient real-time data aggregation in wireless sensor networks. In *Proceedings of the 2006 International Conference on Wireless Communications and Mobile Computing, 2006*, pages 803–808. ACM, 2006. 15

[HZ09] H. Hu and Q. Zhu. Power control based cooperative opportunistic routing in wireless sensor networks. *Journal of Electronics (China)*, 26(1):52–63, 2009. 13

[IfSIS] Vanderbilt University Institute for Software Integrated Systems. Prowler: Probabilistic Wireless Network Simulator. 55

[IGE+03] C. Intanagonwiwat, R. Govindan, D. Estrin, J. Heidemann, and F. Silva. Directed diffusion for wireless sensor networking. *IEEE/ACM Transactions on Networking*, 11(1):2–16, 2003. xi, 13, 14

[JE06] J. Jeong and C.T. Ee. Forward error correction in sensor networks. *University of California, Berkeley*, 2006. 11, 43

[KAH+04] R. Kling, R. Adler, J. Huang, V. Hummel, and L. Nachman. Intel mote: Using Bluetooth in sensor networks. In *Proceedings of the 2nd International Conference on Embedded Networked Sensor Systems (SenSys), 2004*, pages 318–318. ACM, 2004. 1

[KKP00] JM Khan, R.H. Katz, and K.S.J. Pister. Emerging Challenges: Mobile Networking for" Smart Dust". *Journal of Communications and Networks*, 2(3):188–196, 2000. 1

[KW07] H. Karl and A. Willig. *Protocols and architectures for wireless sensor networks*, page 292. Wiley-Interscience, 2007. 12

[LBPJ04] B.H. Liu, N. Bulusu, H. Pham, and S. Jha. Csmac: A novel ds-cdma based mac protocol for wireless sensor networks. In *Proceedings of IEEE Global Telecommunications Conference Workshops (GlobeCom), 2004*, pages 33–38. IEEE, 2004. 24

[LGP10] Y. Li, L. Guo, and S. Prasad. An Energy-Efficient Distributed Algorithm for Minimum-Latency Aggregation Scheduling in Wireless Sensor Networks. In *Proceedings of the 30th IEEE International Conference on Distributed Computing Systems (ICDCS), 2010*, 2010. 27, 75, 76

[LK06] W. Lou and Y. Kwon. H-spread: a hybrid multipath scheme for secure and reliable data collection in wireless sensor networks. *IEEE Transactions on Vehicular Technology*, 55(4):1320–1330, 2006. 16

[LLH02] N. Lee, P. Levis, and J. Hill. Mica high speed radio stack. *TinyOS manual*, 2002. 60

[LR02] S. Lindsey and C.S. Raghavendra. Pegasis: Power-efficient gathering in sensor information systems. In *Proceedings of IEEE Aerospace Conference, 2002*, volume 3, pages 3–1125. IEEE, 2002. 15, 19

[LRC+08] R.P. Liu, Z. Rosberg, I.B. Collings, C. Wilson, A.Y. Dong, and S. Jha. Overcoming radio link asymmetry in wireless sensor networks. In *Proceedings of the 19th IEEE International Symposium on Personal, Indoor and Mobile Radio Communications (PIMRC), 2008*, pages 1–5. IEEE, 2008. 12, 84

[LSB08] Y.S. Lin, D. Sylvester, and D. Blaauw. An ultra low power 1V, 220nW temperature sensor for passive wireless applications. In *Proceedings of IEEE Custom Integrated Circuits Conference (CICC), 2008*, pages 507–510. IEEE, 2008. 1, 8

[LW03] W. Lou and J. Wu. A reliable broadcast algorithm with selected acknowledgements in mobile ad hoc networks. In *Proceedings of the IEEE Global Telecommunications Conference (GLOBECOM), 2003*, volume 6, pages 3536–3541. IEEE, 2003. 12, 43, 89, 121

[LZZ+06] S. Lin, J. Zhang, G. Zhou, L. Gu, J.A. Stankovic, and T. He. ATPC: adaptive transmission power control for wireless sensor networks. In *Proceedings of the 4th International Conference on Embedded Networked Sensor Systems (SenSys), 2006*, pages 223–236. ACM, 2006. 11, 43

[MEB06] M. Miladi, T. Ezzedine, and R. Bouallegue. Latency of energy efficient mac protocols for wireless sensor networks. In *Proceedings of the International Conference on Digital Telecommunications (ICDT), 2006*. IEEE Computer Society, 2006. 24

[MFHH02] S. Madden, M. J. Franklin, J. M. Hellerstein, and W. Hong. TAG: Tiny aggregate queries in ad-hoc sensor networks. In *Proceedings of*

the USENIX Symposium on Operating Systems Design and Implementation, 2002, 2002. 14, 19, 20, 67, 102

[MFHH03] S. Madden, M.J. Franklin, J.M. Hellerstein, and W. Hong. The design of an acquisitional query processor for sensor networks. In *Proceedings of the 2003 ACM SIGMOD International Conference on Management of Data, 2003*, pages 491–502. ACM, 2003. 2, 3

[MFHH05] S.R. Madden, M.J. Franklin, J.M. Hellerstein, and W. Hong. TinyDB: an acquisitional query processing system for sensor networks. *ACM Transactions on Database Systems (TODS)*, 30(1):122–173, 2005. 14, 32

[MLG06] H.G. Myung, J. Lim, and D.J. Goodman. Single carrier fdma for uplink wireless transmission. *IEEE Vehicular Technology Magazine*, 1(3):30–38, 2006. 24

[MLW+09] J. Ma, W. Lou, Y. Wu, X.Y. Li, and G. Chen. Energy Efficient TDMA Sleep Scheduling in Wireless Sensor Networks. In *Proceedings of the 28th Conference on Computer Communications of the Communications Society (INFOCOM), 2009*, 2009. 5, 25, 74, 100

[MNG05] A. Manjhi, S. Nath, and P.B. Gibbons. Tributaries and deltas: efficient and robust aggregation in sensor network streams. In *Proceedings of the 2005 ACM SIGMOD international conference on Management of data*, pages 287–298. ACM, 2005. 17

[NGSA04] S. Nath, P. B. Gibbons, S. Seshan, and Z. R. Anderson. Synopsis diffusion for robust aggregation in sensor networks. In *Proceedings of the 2nd International Conference on Embedded Networked Sensor Systems (SenSys), 2004*, pages 250–262. ACM, 2004. ii, 2, 4, 17, 19, 20, 21, 29, 31, 32, 33, 44, 56, 57, 60, 76, 102, 103, 121, 143

[NKA+05] L. Nachman, R. Kling, R. Adler, J. Huang, and V. Hummel. The Intel® Mote platform: a Bluetooth-based sensor network for industrial monitoring. In *Proceedings of the 4th International Symposium on Information Processing in Sensor Networks (IPSN), 2005*, page 61. IEEE, 2005. 1, 8

[PC01] G. Pei and C. Chien. Low power tdma in large wireless sensor networks. In *Proceedings of IEEE Military Communications Conference (MILCOM), 2001*, volume 1, pages 347–351. IEEE, 2001. 24

[PFKC08] S.N. Pakzad, G.L. Fenves, S. Kim, and D.E. Culler. Design and implementation of scalable wireless sensor network for structural monitoring. *Journal of Infrastructure Systems*, 14:89, 2008. 1

[PH08] L. Paradis and Q. Han. TIGRA: Timely Sensor Data Collection Using Distributed Graph Coloring. In *Proceedings of the 6th Annual IEEE International Conference on Pervasive Computing and Communications (PerCom), 2008*, pages 264–268, 2008. 18, 26

[PHC04] J. Polastre, J. Hill, and D. Culler. Versatile low power media access for wireless sensor networks. In *Proceedings of the 2nd International Conference on Embedded Networked Sensor Systems (SenSys), 2004*, pages 03–05. ACM, 2004. 2, 3, 57

[PKG04] S. Pattem, B. Krishnamachari, and R. Govindan. The impact of spatial correlation on routing with compression in wireless sensor networks. In *Proceedings of the 3rd International Symposium on Information Processing in Sensor Networks (IPSN), 2004*, pages 28–35. ACM, 2004. 16

[PSC05] J. Polastre, R. Szewczyk, and D. Culler. Telos: enabling ultra-low power wireless research. In *Proceedings of the 4th International Symposium on Information Processing in Sensor Networks (IPSN), 2005*, pages 364–369. IEEE, 2005. 1, 8

[ROGLA06] V. Rajendran, K. Obraczka, and J.J. Garcia-Luna-Aceves. Energy-efficient, collision-free medium access control for wireless sensor networks. *Wireless Networks*, 12(1):63–78, 2006. 25

[RP89] R. Ramaswami and K.K. Parhi. Distributed scheduling of broadcasts in a radio network. In *Proceedings of the 8th Annual Joint Conference of the IEEE Computer and Communications Societies. Technology: Emerging or Converging, 1989*, pages 497–504, 1989. 25

[SBAS04] N. Shrivastava, C. Buragohain, D. Agrawal, and S. Suri. Medians and beyond: new aggregation techniques for sensor networks. In *Proceedings of the 2nd International Conference on Embedded Networked Sensor Systems (SenSys), 2004*, pages 239–249. ACM, 2004. 19, 20, 143

[SGW01] L. Schwiebert, S.K.S. Gupta, and J. Weinmann. Research challenges in wireless networks of biomedical sensors. In *Proceedings of the 7th Annual International Conference on Mobile Computing and Networking (MobiCom), 2001*, pages 151–165. ACM, 2001. 1

[SH03] F. Stann and J. Heidemann. RMST: Reliable data transport in sensor networks. In *Proceedings of the 1st IEEE International Workshop on Sensor Network Protocols and Applications (SNPA), 2003*, pages 102–112. IEEE, 2003. 11, 43

[SKH04] D. Son, B. Krishnamachari, and J. Heidemann. Experimental study of the effects of transmission power control and blacklisting in wireless sensor networks. In *Proceedings of the 1st Annual IEEE Communications Society Conference on Sensor and Ad Hoc Communications and Networks (SECON), 2004*, pages 289–298. IEEE, 2004. 11, 43

[SOP+04] R. Szewczyk, E. Osterweil, J. Polastre, M. Hamilton, A. Mainwaring, and D. Estrin. Habitat monitoring with sensor networks. *Communications of the ACM*, 47(6):34–40, 2004. 1

[ST06] W.K.G. Seah and H.P. Tan. Multipath virtual sink architecture for wireless sensor networks in harsh environments. In *Proceedings of the first international conference on Integrated internet ad hoc and sensor networks*, page 19. ACM, 2006. 17

[Sto05] I. Stojmenović. *Handbook of sensor networks: Algorithms and architectures*, volume 49, pages 256–260. Wiley-Blackwell, 2005. 21, 22, 23, 26

[SVML03] G. Simon, P. Volgyesi, M. Maróti, and A. Ledeczi. Simulation-based optimization of communication protocols for large-scale wireless sensor networks. In *Proceedings of the IEEE Aerospace Conference, 2003*, volume 3. IEEE, 2003. 55

[TJB04] YC Tay, K. Jamieson, and H. Balakrishnan. Collision-minimizing csma and its applications to wireless sensor networks. *IEEE Journal on Selected Areas in Communications*, 22(6):1048–1057, 2004. 21

[TW07] N. Tezcan and W. Wang. Art: an asymmetric and reliable transport mechanism for wireless sensor networks. *International Journal of Sensor Networks*, 2(3):188–200, 2007. 84

[WCK02] C.Y. Wan, A.T. Campbell, and L. Krishnamurthy. PSFQ: a reliable transport protocol for wireless sensor networks. In *Proceedings of the 1st ACM International Workshop on Wireless Sensor Networks and Applications (WSNA), 2002*, pages 1–11. ACM, 2002. 11, 43

[WLX06] H. Wu, Q. Luo, and W. Xue. Distributed cross-layer scheduling for in-network sensor query processing. In *Proceedings of the 4th Annual IEEE International Conference on Pervasive Computing and Communications (PerCom), 2006*, page 10, 2006. 26, 76, 79

[WR67] E. T. Whittaker and G. Robinson. The trapezoidal and parabolic rules. *The Calculus of Observations: A Treatise on Numerical Mathematics*, 1967. 40

[WSW+09] P.J. Wan, C.H.H. Scott, L. Wang, Z. Wan, and X. Jia. Minimum-latency aggregation scheduling in multihop wireless networks. In *Proceedings of the 10th ACM International Symposium on Mobile Ad hoc Networking and Computing (Mobihoc), 2009*, pages 185–194. ACM New York, NY, USA, 2009. 27, 79

[WTC03] A. Woo, T. Tong, and D. Culler. Taming the underlying challenges of reliable multihop routing in sensor networks. In *Proceedings of the 1st International Conference on Embedded Networked Sensor Systems (SenSys), 2003*, pages 14–27. ACM, 2003. 3, 8

[XRC+04] N. Xu, S. Rangwala, K.K. Chintalapudi, D. Ganesan, A. Broad, R. Govindan, and D. Estrin. A wireless sensor network for structural monitoring. In *Proceedings of the 2nd International Conference on Embedded Networked Sensor Systems (SenSys), 2004*, pages 13–24. ACM, 2004. 1

[XWM+09] X.H. Xu, S.G. Wang, X.F. Mao, S.J. Tang, P. Xu, and X.Y. Li. Efficient Data Aggregation in Multi-hop WSNs. *Proceedings of the IEEE Global Telecommunications Conference (GLOBECOM), 2009*, pages 1–6, 2009. 27

[YG02] Y. Yao and J. Gehrke. The Cougar Approach to In-Network Query Processing in Sensor Networks. *SIGMOD RECORD*, 31(3):9–18, 2002. 16

[YG03] Y. Yao and J. Gehrke. Query processing in sensor networks. In *Proceedings of the 1st Biennial Conference on Innovative Data Systems Research, 2003*. Citeseer, 2003. 16

[YG10] E. Yanmaz and H. Guclu. Stationary and Mobile Target Detection using Mobile Wireless Sensor Networks. In *Proceedings of IEEE International Conference on Computer Communications (INFOCOM), Workshops, 2010.*, pages 1–5. IEEE, 2010. 2

[YHE02] W. Ye, J. Heidemann, and D. Estrin. An energy-efficient MAC protocol for wireless sensor networks. In *Proceedings of the 21st Annual Joint Conference of the IEEE Computer and Communications Societies (INFOCOM), 2002*, volume 3, pages 1567–1576. IEEE, 2002. 23

[YLL09] B. Yu, J. Li, and Y. Li. Distributed Data Aggregation Scheduling in Wireless Sensor Networks. In *Proceedings of the 28th Conference on Computer Communications (INFOCOM), 2009*, pages 2159–2167. IEEE, 2009. 27, 75, 76, 79, 88

[YS03] H. Yang and B. Sikdar. A protocol for tracking mobile targets using sensor networks. In *Proceedings of the 1st IEEE International Workshop on Sensor Network Protocols and Applications (SNPA), 2003*, pages 71–81. IEEE, 2003. 2

[YZLZ05] F. Ye, G. Zhong, S. Lu, and L. Zhang. Gradient broadcast: A robust data delivery protocol for large scale sensor networks. *Wireless Networks*, 11(3):285–298, 2005. xi, 9, 10, 16

[ZG03] J. Zhao and R. Govindan. Understanding packet delivery performance in dense wireless sensor networks. In *Proceedings of the 1st International Conference on Embedded Networked Sensor Systems (SenSys), 2003*, pages 1–13. ACM, 2003. xi, 3, 8, 9, 10

[ZHKS04] G. Zhou, T. He, S. Krishnamurthy, and J.A. Stankovic. Impact of radio irregularity on wireless sensor networks. In *Proceedings of the 2nd International Conference on Mobile Systems, Applications, and Services (MobiSys), 2004*, pages 125–138. ACM, 2004. 3, 8

[ZK04] M. Zuniga and B. Krishnamachari. Analyzing the transitional region in low power wireless links. In *Proceedings of the 1st Annual IEEE Communications Society Conference on Sensor and Ad Hoc Communications and Networks (SECON), 2004*, pages 517–526. IEEE, 2004. 56